Characterizing the Disintegration Behavior of Distiller's Spent Grain Compacts during Drying in Superheated Steam

by

Praveen Johnson

A Thesis submitted to the Faculty of Graduate Studies of
The University of Manitoba
In partial fulfillment of the requirements of the degree of

DOCTOR OF PHILOSOPHY

Department of Biosystems Engineering
University of Manitoba
Winnipeg

February 2015

ABSTRACT

Biomass such as spent grain is difficult to dry when it is in the slurry form. Proposed industrial solutions are to compact wet biomass first and then dry it. Compaction develops desired granular form and increases surface area for drying but also brings new technical challenges. Superheated steam (SS) drying is advantageous over hot-air drying as it is more energy efficient. A problem associated SS drying is the initial condensation leading to disintegration of biomass compacts. The current research investigates the disintegration characteristics of distiller's spent grain (DSG) compacts while being dried in SS. The study focuses on the DSG flowability, densification characteristics and disintegration behavior of DSG compacts as affected by SS drying conditions, soluble content and particle size distribution (PSD).

DSG fractions with particle sizes from 300 to 850 µm were dried in SS at 150°C and hot-air at 45 and 150°C. Under these drying conditions bulk density and angle of repose (AOR) varied from 0.379 to 0.435 g/cm^3 and 46.0 to 50.4°, respectively. The stress-relaxation data obtained during the compaction of DSG at different levels of compressive pressure (60.3-135.7 MPa), initial moisture content (15, 20 and 25% wet basis- wb) and soluble content (15 and 30%) were normalized and analyzed to determine the asymptotic modulus (E_A) of the compacts. The highest E_A of 174 MPa was obtained for DSG compacts produced with a compressive force of 135.7 MPa, initial moisture of 25% wb and soluble content of 0%.

The percentage increase in volume of DSG compacts during drying in SS at 110 to150°C temperature range was between 78 to 130%. A comparison between the physical properties of SS dried and hot-air dried compacts revealed the role of SS in

accelerating the release of mechanical energy stored in the compacts. An increase of dimensions and a considerable increase in the hardness and E_A of the compacts was obtained by adding up to 70% (w/w) solubles or by decreasing the PSD of wet distiller's spent grain from d(0.9)=1283.6 to 812.8 µm. This study establishes that compaction of wet biomass followed by SS drying can lead to its effective utilization.

ACKNOWLEDGEMENTS

First of all, I would like to express my deep gratitude and respect to my supervisor, Dr. Jitendra Paliwal, for his advice, motivation and help throughout the period of my doctoral study. I would like to gratefully and sincerely thank my co-supervisor, Dr. Stefan Cenkowski, for his guidance, help and assistance through the course of this research. Thanks to both of you for helping me to understand my abilities and being a part of my growth as a student and as a researcher and teaching me many good things beyond an academic degree. Thank you for inspiring me and providing me with the exceptional ideas.

I sincerely thank my Ph.D committee members, Dr. Susan Arntfield and Dr. Tadeusz Kudra, for their encouragement and advice. Your advice and suggestions helped me a lot in advancing my research. I am greatly thankful to Natural Sciences and Engineering Research Council of Canada for their financial support towards this study.

I gratefully acknowledge and appreciate the efforts of Matt McDonald, Dale Bourns and Robert Lavallee. I really appreciate the help and support you have provided me through the course of this research. Thanks Evelyn Fehr and Debby Watson for helping me with the office duties outside the lab work. Thanks to all other academic staffs, administrative staff and technicians of the Department of Biosystems Engineering and the Department of Human Ecology, University of Manitoba, for their support. I deeply acknowledge and thank my lab mates Dr. Magdalena Zielinska, Dr. Hibru Kelemu Mebatsion, Rani P.R. and other friends for their help and support. Many thanks to all my past and present lab mates for providing me a great time while working in the lab.

I would like to thank my father, mother, brother and all other family members who provided me moral support, confidence, and inspired me to succeed in my research. I thank my wife Sumitha Koshy for her encouragement, patience and support. Finally, my extreme gratitude goes to the Almighty God who provided me with the wisdom, protection and ability to carry out my research, and indeed, all through my life.

TABLE OF CONTENTS

LIST OF APPENDICES

LIST OF FIGURES

LIST OF TABLES

NOMENCLATURE

A_0	cross-sectional area of the original specimen (mm^2)
AOR	angle of repose
BSG	brewer's spent grain
c	regression coefficient
CDS	condensed distiller's solubles
D	diameter (m)
D_i	diameter of the i^{th} particle (mm)
D[4,3]	volume mean diameter
D[3,2]	surface area mean diameter
d(0.1)	size of particle below which 10% of the sample lies
d(0.5)	median
d(0.9)	size of particle below which 90% of the sample lies
DDGS	distiller's dry grain with solubles
DSG	distiller's spent grain
E_A or E_A	asymptotic modulus (MPa)
$F_{(t)}$	force at time t (N)
FMC	final moisture content (% wb)
H_0	initial specimen length (mm)
k	number of independent variables
M	initial moisture content (% wb)
MAPE	mean absolute percentage error
MC	moisture content
m, b	model constants
n	sample size
N_i	initial value before drying
N_f	final value after drying
P	compressive pressure (MPa)
P	applied load (N)
PSD	particle size distribution
R	radius (m)
R^2	regression coefficient/ coefficient of determination
S	soluble content (%)
SS	superheated steam
SSE	sum of squares for error
SST	total sum of squares.
T	temperature (°C)
v	velocity (m/s)
V_i	initial volume before drying
V_f	final volume after drying
wb	wet basis
WDG	wet distiller's spent grain
x	independent variables
X_p	predicted value
X_m	measured value

y	dependent variable
$Y(t)$	decaying parameter
ρ	bulk density (kg/m^3)
σ_0	initial stress (MPa)
σ_t	stress at time t (MPa) or stress after time t at relaxation (MPa)
$\sigma_{0(t)}$	true stress (initial) (MPa)
$\sigma_{(t)}$	true stress (MPa)
σ_x	tensile stress (N/m^2)
σ_y	compressive stress (N/m^2)
τ_{xy}	shear stress (N/m^2)
$\varepsilon_{H(t)}$	true strain
$\Delta H_{(t)}$	actual absolute deformation (mm)
$\underline{R^2}$	adjusted R^2

GLOSSARY

Compact: Densified biomass product which is similar to a pellet.

Stress-relaxation: Stress-relaxation provides information on how a material releases stress under a constant strain.

Relaxation of compact or compact relaxation: An increase in dimensions or volume of a compact after its formation.

Warm-up period: Warm-up period is the first stage of dying in superheated steam. The moisture content as well as the mass of the material increases during this period due to the initial steam condensation. Warm-up period is concurrent with the term condensation period or initial condensation period.

Crushing resistance: The maximum crushing load a compact can withstand before cracking or breaking is called the crushing resistance or compressive resistance.

Hardness: Hardness of the compact is defined as the force needed to attain a given deformation.

1. INTRODUCTION

Drying is the process of removing moisture from a substance; it is the most commonly used food preservation technique. Air-drying, freeze-drying and superheated steam (SS) drying are some of the commonly used methods for drying biomaterials. The type of drying method employed has an impact on the nutritive value and physical characteristics of the food materials (Ezhil, 2010). Though the air-drying process is simple and extends shelf-life of a product, the quality of the dried product is a real challenge for the industry due to its nutritional quality deterioration, shrinkage and lengthy drying times (Ratti, 2008). An advanced drying technique, such as freeze-drying produces a final product with excellent quality. But, unfortunately, due to its high operation cost and a longer drying time compared with air-drying, its application is limited to drying bulk quantities of food materials (Ratti, 2001). Pakowski et al. (2007) referred to SS drying as the best solution for drying biomass for large scale production systems due to its energy savings and less emissions.

Superheated steam drying is an environmentally friendly and energy saving drying technology. It utilizes steam under superheated conditions to remove moisture out of the materials. Superheated steam drying is a promising technology that has the potential to remove and/or prevent the off-flavors and aroma in food products (Speckhahn et al., 2010). No oxidative reactions are possible due to the absence of oxygen during SS drying (Mujumdar, 1991). Superheated steam drying has significant benefits over hot-air drying including higher drying rates, better quality of the dried products, and energy savings (Shibata and Mujumdar, 1994; Taechapairoj et al., 2003; Tang and Cenkowski, 2000). In the process of drying, SS provides heat to the product

and to the moisture to be evaporated. The evaporated moisture from the product becomes part of the drying medium. Only the amount of steam that corresponds to the amount of water evaporated is removed from the drying chamber and can be recovered by condensation. Thus, SS is recirculated and reheated in a closed loop. The emissions coming from the condensate are not expelled to the environment, but appear in the condensate, thus, making it an environmentally friendly technology (van Deventer, 2004). For a sustainable economic growth, shifting of industrial activities into green technologies is of a great significance in the current century (Boye and Arcand, 2013). Considering these potential benefits, this study utilizes the advantages of SS drying conditions.

Distiller's spent grain (DSG) is the major by-product of distilleries. As the production of biofuels is increasing globally, the availability of DSG is also increasing at an exponential rate. Corn and wheat are the major crops used for producing ethanol in Canada (NRCAN, 2013). The Global Aid Network reported that ethanol production in Canada has a growth expectation of 2,006 million liters in the year 2014 compared with the expected 1,979 million liters in 2013 (Canadian Biomass, 2014). Due to an increase in ethanol production, there has been greater availability of distiller's grains. After drying, DSG contains about 86–93% dry matter, 26–34% dry basis (db) crude protein and 3–13% db fat (Tjardes and Wright, 2002; Rosentrater and Muthukumarappan, 2006). Currently, livestock industries are the major market for DSG, but alternative markets for DSG are needed due to the recent increase in its production. The marketability of DSG is dependent on its quality which has an influence on the profitability of ethanol production (Singh et al., 2001).

Distiller's spent grain is increasingly transported in big containers by railcars or trucks to greater distances before entering into the market, hence handling and logistics are essential for determining the marketability of DSG (Clementson and Ileleji, 2010; Ganesan et al., 2008a). During shipping and storage, caking and bridging of DSG are the common problems that hinder its flowability (Ganesan et al., 2008a). Increasing the bulk density of DSG by a densification process can aid to overcome the limitations, such as caking and bridging associated with storage, transportation, cost of shipping and handling of DSG (Tumuluru et al., 2010; Shankar et al., 2008).

Knowledge of compaction mechanisms is a significant factor in designing energy-efficient compaction equipment and for quantifying the effects of various process variables on compact quality. The major factors which affect the densification of biomass are its nutrient composition, feed moisture content, compaction pressure, materials used as particle-binders, feed particle size and densification equipment variables (Turner, 1995). Feed moisture content has an effect on the strength and durability of densified products. Moisture content acts as a binding agent and as a lubricant (Obernberger and Thek, 2004; Grover and Mishra, 1996; Lindley and Vossoughi, 1989). Also, during densification, moisture aids in starch gelatinization, fiber solubilization and protein unfolding (Tumuluru et al., 2011).

Particle size of the feed material is a key factor in determining the durability of compacts. Generally, tiny particles absorb more moisture and heat when compared with larger particles and undergo a higher degree of conditioning (Kaliyan and Morey, 2009). A particle size of 0.6–0.8 mm is recommended for making biomass pellets of high durability (Turner, 1995; Franke and Rey, 2006, as cited in Kaliyan and Morey,

2009). Using smaller particle sizes in feed industries increases the cost of grinding. This problem can be solved by using a mixture of different size particles. Such a mixture makes pellets of optimum quality, as they form the inter-particle bonding with nearly no inter-particle spaces (Payne, 1978; Grover and Mishra, 1996).

Distiller's spent grain must be dried to a safe level of moisture to increase its shelf-life during storage and transportation (Mosqueda et al., 2013). Traditionally, rotary or drum dryers with hot-air as the drying medium, at 240 to 550°C, are used in drying of spent grain (Stroem et al., 2009). But during drying, the sticky and slurry nature of the spent grain greatly complicates the drying process. To overcome this problem, the common industrial practice is to recycle the previously dried spent grain by mixing it with the wet material and then introducing this granular form back into the rotary dryer. The disadvantage of this process is that the same material may be dried many times occasionally leading to dryers catching fire. Moreover, it significantly increases the energy consumption due to the back-mixing process. Stroem et al. (2009) reported that SS drying has a potential to reduce the surface moisture content of the spent grain to a level where this material is no longer sticky. Another possible solution to overcome the sticky nature is to compact wet DSG and introduce granulated and wet compacts into a dryer. Compaction of wet biomass develops the desired granular form and needed surface area for drying. Also, replacing air with SS can eliminate a problem of a potential fire hazard during drying at high temperatures.

Despite the advantages of SS drying, the issue related to breaking and disintegrating of biomass compacts while drying in SS is prevalent (van Deventer, 2004; Prachayawarakorn and Soponronnarit, 2010).Till now, no studies have reported

data regarding the characterization of the physical properties of biomass compact while drying it in SS. In the case of fluidized-bed dryers, crumbled compacts and fines may agglomerate and interrupt the drying system (Prachayawarakorn and Soponronnarit, 2010). Thus, the problem remains whether such a compacted product can withstand vigorous movement inside the SS dryer without disintegrating.

The strength of DSG compacts while drying could be determined using the diametral compression test at their brittle stage. The diametral compression test is also known as the diametral tensile test or compact crushing test. Kaliyan and Morey (2009) recommended the use of diametral compression testing for biomass pellets as this test provides a quick measure of pellet quality immediately after the production. Kashaninejad et al. (2010) used diametral compression test to determine the tensile strength of the pellets developed from microwave pretreated and untreated barley straw samples. The study used approximately 2 mm thick pellets cut diametrically into tablets that were compressed at a constant speed of 1 mm/min until failure occurred. Their results showed that untreated barley straw pellets had significantly lower pellet density, fracture load and tensile strength compared to pretreated barley straw pellets.

A change in rheological properties of the compacts while drying in SS could be determined using the stress-relaxation test. Rheological properties of foods such as flour, barley, fruit and vegetables, fruit gels, fish and cheese have been analyzed using the stress-relaxation test in a variety of studies (Bhattacharya, 2010; Herrero et al., 2004; Bargale and Irudayaraj, 1995; Blahovec, 2001; Peleg, 1979; Al-Mashat and Zuritz, 1993; Marquina et al., 2001; Gamero et al., 1993; Peleg and Normand, 1983; Konstance and Holsinger, 1992). Pons and Fiszman (1996) reported that in gel food

systems, deformation levels between 20-50% have commonly been preferred, as at these deformation level gels do not break and it is possible to gain important details on parameters such as hardness (force at a given deformation), springiness and cohesiveness. They also reported that a cross-head speed in the range of 10 to 250 mm/min was commonly used on gel food systems. Studies conducted by Szczesniak and Hall (1975) and Muntoz et al. (1986) recommended a cross-head speed such as 200 mm/min for gel systems, as at higher cross-head speeds a greater agreement between the sensory and mechanical hardness were observed (Pons and Fiszman, 1996).

Food processing modeling is significant for explaining the behavior of a process or product, simplifying an intricate problem into a less complex one, and reducing the expenditure on experimental studies. A stepwise regression method is one of the statistical tools used for selecting suitable variables for developing regression models. Stepwise regression can be used to identify the most suitable independent variables for predicting the strength and E_A of the compact while drying in SS. Cliff et al. (1996) used stepwise multiple regression analysis to develop the prediction model of cherry liking; one from visual and the other from flavor/texture evaluations. The study showed that the statistical model developed for flavor/texture liking had a higher correlation coefficient of 0.85 as compared with the model developed for visual liking which had a correlation coefficient of 0.56. Burkholder and Lieber (1996) compared the ability of polynomial regression, stepwise polynomial regression and quintic spline approximation for fitting noisy data. Results showed that spline approximation and stepwise polynomial regression provided excellent fits to the data.

The characterization of changes in physical and rheological properties of DSG compacts during the course of SS drying will be helpful for analyzing the breaking and disintegrating behavior of the compacts inside the SS dryer. Also, it will be further useful for finding suitable methods for reducing or eliminating the problems associated with the SS compact drying. A systematic and thorough study for the current problem using an industrial SS drying unit requires large amounts of samples and labor. Some of these problems can be analyzed or reduced by simulating the industrial process using a laboratory SS drying unit and carrying out each trial using single DSG compacts. The knowledge obtained from the pilot study could be effectively utilized by the industry in reducing problem with disintegration of compacts.

The main objective of this study was to investigate the disintegration behavior of compacted DSG as affected by drying in superheated steam. The following specific objectives were addressed:

1. Determining the important physical characteristics (i.e., bulk density and angle of repose) before densification and compaction/stress-relaxation characteristics of DSG.
2. Determining the effect of superheated steam drying conditions as well as the effect of solubles and particle size on the disintegration behavior of DSG compacts.
3. Modeling the asymptotic modulus of DSG compacts through the SS drying process.

Thesis Format

This thesis is a compilation of four published journal papers (Johnson et al., 2010; 2013b; 2014b; 2014c) four conference papers (Johnson et al., 2011a; 2011b; 2013a; 2014a) and another journal paper that is under review (Johnson et al., 2014d). The present thesis is prepared in a modified manuscript format. Chapter 1 covers the overall scope of the research work and its relevance to the current developments in the industrial and laboratory context. Chapter 2 describes the fundamental concepts of SS drying, current issues related to physical characterization of biomaterials and recent advances in the studied area. The Materials and Methods section (Chapter 3) gives the detailed description of all procedures that were followed for different experiments. Description of the analysis and relevant equations used in determination of specific characteristics are presented in Chapter 4. The findings of the study are described under Results and Discussions (Chapter 5) in five sections followed by the thesis conclusions in Chapter 6. Recommendations for Future Research are given in Chapter 7. Additionally, detailed information on the results and data analysis is presented in Appendices.

2. LITERATURE REVIEW

2.1 Superheated steam drying

Literature shows that SS drying was first used in Germany in 1908 as an alternative for hot-air drying (Douglas, 1994). Even though its initial application was limited, many industries embraced this technology once its potential was realized. Currently, SS drying is considered as an emergent technology utilized for many applications such as food, coal, wood and fuel (Tang et al., 2005; Chen et al., 2000; Pang and Dakin, 1999; lyota et al., 2008; Dev and Raghavan, 2012). In the SS drying method, material is dried by the direct contact with SS in a drying chamber. Recently, food and pharmaceutical industries are showing more interest in SS drying technology as SS imparts several benefits to dried materials when compared to other conventional drying techniques. These benefits include enhanced color, reduced shrinkage, better rehydration properties, faster drying rates and elimination of microbes (Ezhil, 2010). Other advantages of using the SS drying technology are: lower net energy consumption, safe operation, no fire hazard and limited oxidation of the dried product. Superheated steam has the ability to pasteurize, sterilize and deodorize dried products (Ezhil, 2010; Taechapairoj et al., 2003; Tang and Cenkowski, 2000; Tang et al., 2005; Pakowski et al., 2007). Using a SS drying method, desirable organic compounds can be captured without any losses (Mujumdar and Law, 2010). Strict laws regarding environmental pollution and energy savings in many countries offer another incentive for using SS drying technology (Beeby and Potter, 1985).

Nathakaranakule et al. (2007) investigated the influence of two multi-level drying methods for chicken meat. In the first method, SS drying in the first stage

followed by heat pump drying in the second stage (SSD/HP) was used. In the second method, SS drying in the first stage followed by hot-air drying in the second stage (SSD/AD) was used. The SS drying experiments were conducted at the temperatures of 120, 140 and 160°C. For two-stage drying experiments, initially the meat was dried by SS to moisture contents of either 42.8% or 66.7% db; in the second-stage of the drying process, both the heat pump and hot-air drying experiments were performed at a constant drying temperature of 55°C. Chicken dried in pure SSD had the shortest drying time, and the smallest percent shrinkage compared with other drying methods. Also, it was observed that, chicken dried with high SS temperature (160°C) adsorbed more water than that dried with lower SS temperatures as larger pores developed at the high SS temperature. However, the protein molecules inside the chicken samples were denatured due to the long term exposure to high-temperature SS causing a reduction in water solubility. The study found that SSD/HP is an appropriate method for drying chicken to use it as a constituent in ready-to-eat noodles.

Taechapairoj (2003) used a SS fluidized bed drying system for drying paddy. The experimental conditions for drying were: initial moisture contents of 25–45% db, bed depths of 10–15 cm and SS temperatures of 150–170 ° C at a fixed SS velocity of 3.1 m /s. The study found that the color of white rice became darker when the moisture content of paddy was brought below 18% db. Kozanoglu (2006) carried out drying experiments in a SS vacuum fluidized bed dryer, using coriander and pepper seeds. In their study, lower temperatures between 90 and 110°C were used for the SS drying process. The authors found that with an increase in temperature, the drying rates increased, and the final moisture content along with the drying times decreased for the

seed particles. Cenkowski et al. (2007) conducted a study investigating the effect of SS on decontamination of food products. The study was conducted on wheat contaminated with deoxynivalenol (DON), a *Fusarium* mycotoxin and with *Geobacillus stearothermophilus* spores. The results of the study showed that SS is effective in reducing the contamination in foods products.

Zielinska and Cenkowski (2012) investigated the drying characteristic and moisture diffusivity of distiller's wet grains and condensed distiller's solubles in a SS drying medium. The study was performed at different temperature ranges in the SS equipment. It was observed that for all drying conditions, the overall moisture diffusivity of the spent grain samples increased with a decrease in moisture content. Tang et al. (2005) developed an empirical equation to explain the thin-layer drying of brewer's spent grain (BSG) and DSG in SS. Drying experiments were conducted at SS temperatures of: 110, 115, 120, 130, 145, 160 and 180 °C. The velocity of SS passing through the sample chamber was: 0.25, 0.47, 0.66, 0.86 and 1.08 m/s for BSG drying, and 0.28, 0.49, 0.70, 0.92 and 1.15 m/s for DSG drying. Results of the experiment showed that both SS temperature as well as SS velocity had an influence on the drying rate of BSG and DSG in SS. Superheated steam drying of spent grain did not have a significant effect on the change of nutrients, such as ß-glucan, pentosan and protein content of BSG and DSG samples. Moreover, SS velocity had no significant influence on the nutrient composition of the processed samples. It was found that a high temperature of about 180°C gelatinized the starch content of both BSG and DSG samples.

Stroem et al. (2009) evaluated the drying behavior of BSG in a pilot-scale rotary SS dryer. Product moisture content, measurements of stickiness and energy consumption were evaluated during the study. The experimental conditions selected were; 14 and 23 kg/h for feed rate, 200 and 240°C for SS temperature and 1 and 2.5 m/s for SS velocity. The results of this study showed that the sticking profile varied exponentially along the drum length. A correlation between sticking and product moisture content was developed. The operating conditions which minimize sticking were also determined. Many studies have been carried out by researchers globally on drying of materials such as wood chips, oats, longan, noodles, sludge and pork meat (Head et al., 2010; Johansson et al., 1997; Somjai et al., 2009; Fitzpatrick, 1998; Sa-adchom et al., 2011; Pronyk et al., 2008).

The above mentioned studies show that SS can be effectively used for drying materials such as, chicken meat, paddy, spices and spent grain. Superheated steam drying can also be beneficial for decontamination of food or feed products contaminated with deoxynivalenol (DON), a *Fusarium* mycotoxin and with *Geobacillus stearothermophilus* spores. Even the loss of nutrients during drying while using conventional drying techniques can be minimized by using the SS drying method. Another important issue of sticking of spent grain to the dryer surface during drying can be minimized with the use of SS drying. Research is still underway in many countries to fully explore the potential of SS in drying of biomaterials.

2.1.1 Superheated steam condensation

Condensation of steam during the initial phase of SS drying is a common problem. Steam condenses in the drying chamber of SS equipment during the initial phase of the drying process. The process of condensation on the material surface followed by evaporation of the deposited moisture into SS is called as “reverse process” (Iyota et al., 2001). Tang et al. (2005) reported that at the beginning of SS drying process, the sample mass was increased due to the condensation of SS on the sample surface. Condensation normally takes place when the material is at a lower temperature than the saturated temperature for steam (100°C in the case of SS at atmospheric pressure) (van Deventer, 2004).

Markowski et al. (2003) reported that since the condensation process happens only for a short period of time, i.e., a few seconds, it is difficult to mathematically model the initial steam condensation process. However, due to the quick heating and temporary rising of the moisture content of the material, the condensation phenomenon greatly influences the dried material quality as well as the drying processes (Iyota et al., 2001). Shi et al. (2011) conducted a numerical simulation of drying of rapeseed in SS on a fluidized bed. The researchers numerically showed that steam condensation cannot be ignored as it affects the initial non-uniform distribution of particles in the fluidized space resulting in disparity between simulation and experimental results.

Figure 2.1 shows the change in moisture of the material dried in SS over time, occurring in the initial stage of SS drying. During the initial warm-up period, which is concurrent with the condensation phase, the moisture content as well as the mass of the material increases. At time, t_s, called ‘‘reverse time,’’ the moisture content reaches its

maximum and the condensation reverses to evaporation. At time t_R , termed the restoration time, the actual moisture content returns to its original moisture content. The time from reverse time t_s to restoration time t_R is termed as ‘‘restoration period ’’ (Iyota et al., 2001). The restoration period is followed by the ‘‘drying stage.’’ During the drying stage the moisture content of the material evaporates and the rate of evaporation mainly depends on the rate of heat transfer between SS and the drying material.

Tang et al. (2005) reported a small deposition of steam condensate on the surface of DSG and BSG samples at the beginning of the SS drying process. The study reported a linear change in the condensate deposited with a change in SS temperature or velocity. The study was conducted at SS temperatures of 110, 115, 120, 130, 145, 160 and 180ºC; and SS velocities of 0.25, 0.47, 0.66, 0.86 and 1.08 m/s for BSG drying, and 0.28, 0.49, 0.70, 0.92 and 1.15 m/s for DSG drying. The moisture gained by the sample increased in low temperature or low-velocity SS compared with high-temperature or high-velocity SS. Due to the steam condensation phenomenon, the initial moisture ratio of the sample increased to a value between 1.00 and 1.30 for DSG drying and between1.00 and 1.20 for BSG drying.

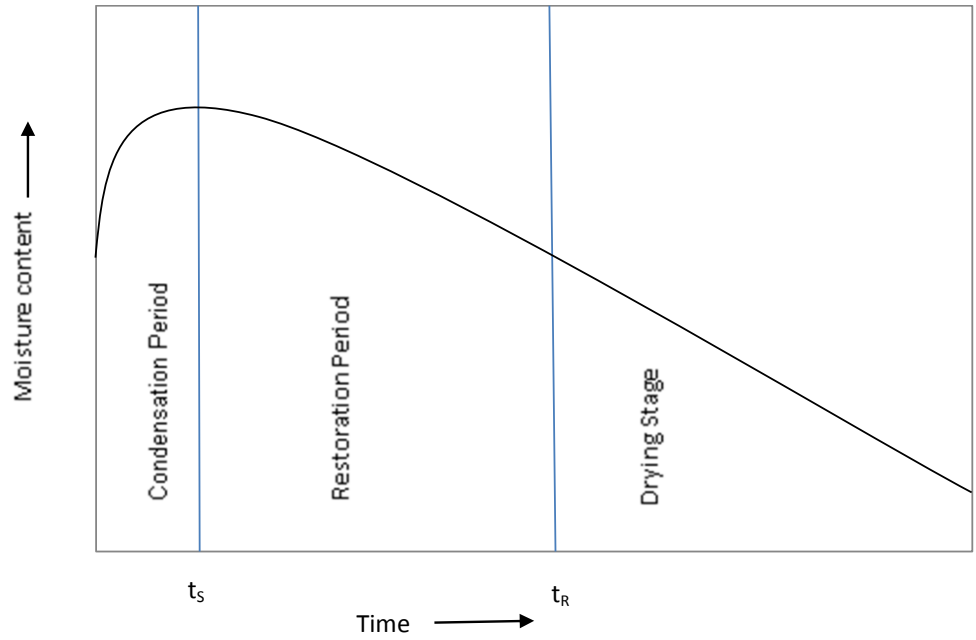

FIG. 2.1. The reverse process model for superheated steam drying. The time t_s and t_R are termed as reverse time and restoration time, respectively (modified from Iyota et al., 2001).

During the SS drying process, the heat required to bring the sample from its ambient temperature to the saturation point of steam (100ºC at the atmospheric pressure) is supplied by the SS. The sensible heat of steam increases with an increase in temperature. When the SS temperature decreases, the sensible heat of steam also decreases, and increased steam condensation takes place for providing heat to raise the temperature of the sample to 100ºC. The influence of SS velocity on the moisture gain in the sample could be described by taking into consideration the heat-transfer characteristics. For low-velocity SS, a higher initial condensation was observed due to the lower heat-transfer coefficient between the SS drying medium and the sample. Due to the lower heat-transfer coefficient, less heat is transferred to the sample by convection (Tang et al., 2005).

2.1.2 Breaking of biomass compacts in superheated steam

Prachayawarakorn and Soponronnarit (2010) reported that there is a 2-3% increase in moisture content of the material initially while drying in SS. This results in an increase in the drying time by approximately 10-15%. Condensation causes the material to be very wet and the materials may break and agglomerate leading to a huge loss for the industries. This problem is more common during the SS fluidized bed drying process and it may interrupt the drying system during operation. One way to avoid this problem is to warm-up the material before feeding it into the dryer. van Deventer (2004) reported that the initial condensation caused the product to heat up quickly by absorbing the heat of condensation. Hence, the product temperature rose quicker during the SS drying compared with hot-air drying process.

2.2 Current and potential applications of distiller's spent grain

The material presented in section 2.2 is the modified reproduction of work published by Johnson et al. (2011b) under the realm of this thesis.

2.2.1 Distiller's spent grain

Distiller's spent grain is a major by-product of distilleries, where starchy materials such as cereal grains are fermented and distilled to yield ethanol. There are two types of ethanol processing methods, i.e., dry milling and wet milling (Belyea et al., 2004). In dry milling process, the starchy grain is first ground into flour (meal) and then processed without separating out the various components of the grain. Whereas in wet milling process, the starchy grain is first soaked in water and dilute sulfurous acid, and

then separated into constituent fractions. Dry milling process is less capital intensive and is more common among ethanol plants (Belyea et al., 2004). During dry milling process three major co-products are produced: ethanol, carbon dioxide and DSG. During the fermentation process starch is converted to alcohol and other fermented products, whereas nutrients such as protein, fiber, fat, vitamins and minerals remains in DSG (Tsen et al., 1983).

Production of ethanol has tripled in the last decade and recent estimates indicate a continued high growth (UNEP, 2009). Due to an increase in ethanol production there has been a greater availability of distiller's grains. Currently, livestock industries are the major market for the distiller's grains, but the alternative markets for DSG are needed due to an increase in its production. Recent research has shown that DSG has the potential to be used as an ingredient in human food products, industrial and agricultural sectors (Liu et al., 2011; Tavasoli et al., 2009). This section discusses the potential applications and the issues associated with the use of DSG in cattle feed, human consumption and industrial applications.

2.2.2 Current uses and concerns

The presence of highly digestible fiber, high protein content, less starch content and fairly high concentration of fat compared with feed grains, makes DSG an excellent replacement for cattle feed. Oba et al. (2010) reported that DSG can replace canola meal or soybean meal in the diets of lactating dairy cows without affecting the production adversely. There are some advantages of using spent grains in cattle feed due to their low starch content. For dairy cows, high-energy diets that are typically high in starch

content can increase the risk of ruminal acidosis (Yang and Beauchemin, 2006). Low starch content in DSG can reduce the chances of acidosis and serves as an excellent replacement for corn (Larson et al., 1993). In addition, the presence of fairly high amounts of fat makes it a high-energy feed for animals (Kleinschmit et al., 2006). There are, however, some practical issues related to the usage of DSG. Due to the high temperature used in drying DSG, damage of protein molecules are common among dried DSG (Kleinschmit et al., 2006). Lysine, tryptophan and arginine present in proteins of DSG are the amino acids that are prone to heat-damage (Schwab, 1995; Nakamura et al., 1994; Nichols et al., 1998; Whitney et al., 2000).

The dark color of DSG is an indication of heat-damaged protein molecules. Powers et al. (1995) observed less milk yield when dairy cows were fed with diets comprising dark colored DSG than when fed with diets containing golden colored DSG. The quality of the cattle feed can be improved by blending DSG diet with other protein supplements that contain more lysine, tryptophan and arginine (Nichols et al., 1998). The mycotoxins present in DSG can be another risk for the cattle. According to Applegate and Adeola (2008), if corn used in fermentation is contaminated with mycotoxins, the resulting DSG will contain three to four times the concentration of mycotoxins as the removal of starch lowers the mass of the product after fermentation. Due to its high phosphorous content and low cost, DSG can also be used for partial replacement of swine diets (Whitney et al., 2001). Phosphorous and calcium are the two most abundant minerals in swine; they are vital in the development and maintenance of the skeletal system, muscle contraction, blood clotting and many other regulatory functions in pigs (Crenshaw, 2001). It is reported that DSG from corn has at least two to

three times greater phosphorous content when compared to corn before fermentation (Parsons et al., 2006; Whitney et al., 2001).

DSG can be a source of nutrient for poultry. Current recommended maximum dietary inclusion levels for corn DSG are 10% for broilers and 15% for chicken layers (Shurson and Noll, 2005). A study conducted by Pettersson et al. (1987) showed that the addition of up to 20% DSG into broiler rations did not significantly affect the growth rate of the birds. Corn DSG contains about 40 ppm of xanthophylls which significantly increases egg yolk color and increases skin color of broilers (Applegate and Adeola, 2008). Skin color, which is associated with feed choices of broilers, plays a significant role in consumer acceptance of broilers especially in United States and Mexico (Bunell and Bauernfeind, 1962). Some of the issues related to the usage of DSG in poultry are: presence of mycotoxins, and variability in factors such as Aminocid content (a mixture of amino acids extracted from vegetative origin with the aid of enzymatic hydrolysis), energy, phosphorous availability, sodium content and particle size (Applegate and Adeola, 2008). If particle size of DSG is overly fine (i.e., 300-400 microns) it will lower the nutrient digestibility in the bird as fine particles of feed pass quickly through the gizzard of the bird (Applegate and Adeola, 2008).

2.2.3 Variability in nutrition

Researchers reported a significant variation in nutrient profile of DSG among various ethanol plants and even within plants (Spiehs et al., 2002; Belyea et al., 2004). This creates a challenge in using DSG as feed for cattle and poultry as information regarding its nutrient profile and amino acid digestibility is not reliable (Shurson and

Noll, 2005). There are substantial differences in nutrient composition between soluble and solid fractions of spent grain. Because the ratio of blending these two fractions to produce distiller's dry grain with solubles (DDGS) varies among plants, the end product may have a different nutrient composition (Reese and Lewis, 1989; Shurson and Noll, 2005). As the solubles have a higher fat content, DDGS has a relatively high fat content because of the added solubles. The solubles are obtained by the evaporative concentration of thin stillage, which is the separated liquid fraction from the spent grain after fermentation. Some ethanol plants partially remove the germ of the corn before fermentation (Singh and Eckhoff, 1996, 1997). As the germ contains high fat content, the DDGS produced from de-germed corn has a lower fat content.

2.2.4 Human foods

There are many indications that the expansion of biofuel industries will lead to food insecurity and a food price hike (FAO, 2011). Studies conducted by the International Food Policy Research Institute (IFPRI) suggested that, for every percentage increase in the real prices of staple foods, the number of food-insecure people in the world will increase by over 16 million (Runge and Senauer, 2007). Many studies have recently been carried out in an effort to use byproducts from either ethanol production plants (DSG) or breweries (brewer's spent grain) as such or their constituents into human food products (Liu et al., 2011; Johnson et al., 2010). However, the utilization of biofuel by-products for human consumption can reduce the existing gap between the biofuels and food insecurity.

Various studies done by researchers prove that DSG has fairly good potential for commercial food uses, especially in baked foods (Bookwalter et al., 1984; Wall et al., 1984; Abbott et al., 1991; Maga et al., 1989; Prentice et al., 1978; Rasco et al., 1987a; Rasco et al., 1989; Reddy et al., 1986). Incorporation of DSG into human foods could add value to the traditional baked food market by imparting a favorable nutritional profile, lower glycemic effect and higher dietary fiber (Liu et al., 2011). Brochetti and Penfield (1989) studied the effect of varying levels of distiller's dried grain (DDG) addition on the sensory characteristics of bakery products. Corn muffins, hush puppies, spiced doughnuts and molasses-raisin cookies were the products selected for the study. It was observed that compared with baked foods made with all-purpose flour, supplementing the flour with DDG increased the absorption of water and oil, increased food acidity, and yielded a darker color for the food products. The study showed that about 10 to 20% DDG can be added to the products without adversely affecting the appearance, flavor and texture of the products.

Rasco et al. (1987a) conducted studies by incorporating, 0, 12.5 or 25% distiller's dried grains with solubles obtained from soft white winter wheat to make baguettes, cinnamon rolls and chocolate chip cookies. Their results showed that the sensory panelists were unable to differentiate cookies containing 12.5% DDGS from control cookies. The cinnamon rolls and chocolate chip cookies obtained from the study were rated as highly acceptable. But the baguettes containing DDGS showed stronger flavor and/or off-flavor and were found to be less acceptable than the control ones. In another study Liu et al. (2011) showed that supplementing corn flour with 20 to 25 g/100 g DDGS produced corn bread of acceptable quality.

It was reported by Bookwalter et al. (1984) that the soluble component in DSG is considered to be the main source of off-flavors for the distiller's products. Morad et al. (1984) removed a significant portion of solubles from DDGS and incorporated 25% DDG obtained from white sorghum into molasses cookies. The cookies obtained were rated higher by a consumer panel than the control (0% DDGS) cookies. DDGS can be used for preparing soft paste mixes for fried foods. DDGS obtained from red wheat, white wheat, or corn was added to soft paste mixes in the amount of 25%. The results showed that all the products were acceptable with the highest sensory rating given to soft paste mixes prepared with corn DDGS (Rasco et al., 1987b).

Studies done by Reddy et al. (1986) showed that DDG can be added up to 10% in wheat muffins without affecting the appearance, texture, flavor, and overall acceptability. It was reported that the incorporation of either raisins or blueberries to wheat muffins allowed to increase the DDG level up to 15%. Brochetti et al. (1991) reported that with the increase in addition of DDG, the loaf volume of the bread decreased. Breads made with wheat distiller's grain had the poorest crumb grain. When the fiber fractions were ground, crumb grain improved in many cases. A decrease in the stability of the dough was observed by replacing 10 and 20% wheat flour with corn DDG in a high-protein bread formula (Tsen et al., 1983). Morad et al. (1984) observed an increased water absorption by the addition of DDG from sorghum in a white-pan bread formula. When the soluble solids were removed from wheat distiller's grain the baking performance decreased (Fiasco et al., 1990).

Brochetti et al. (1991) showed that the quality of breads containing 5, 10 and 15% DDG was similar to that of control bread containing 50% whole-wheat flour.

There were only few differences observed in the mixing and baking properties of wheat distiller's grains irrespective of which drying method was employed, i.e., whether the wheat distiller's grain was dried using steam or drum dryers (Fiasco et al., 1990). Also, DSG can be used in the production of bran. Sodium bicarbonate, amino acids, or mixture of amino acids and potato starch are added to the wheat distiller's grain, and then the residue-additive mix is blended and dried to form a type of nutritious bran (Reddy and Stoker, 1991). This bran can be used on a 50-50 weight basis with wheat flour, and can be used for making noodles or baked foods.

2.2.5 Problems related to inclusion of distiller's spent grain into human foods

Consumer acceptability of food products containing DSG is among the main issues. Therefore, poor flavor, darker color, oxidative rancidity, odor, poor texture and loaf volume of the developed food products are of major concern for their marketability (Tsen et al., 1982; Dresse and Hoseney, 1982; Morad et al., 1984; Prentice and D'Appolonia, 1977; Murphy et al., 2006; Dawson et al., 1984). When utilizing DDGS for human consumption, distilleries must meet food safety standards and good manufacturing practices (Murphy et al., 2006). Contamination of DSG with mycotoxins is another concern (Applegate and Adeola, 2008). After harvesting, food grains must be dried to reduce the moisture content to safe levels of storage. Delay in drying to safe moisture levels may increase the risk of mold growth and mycotoxin production. Faulty storage conditions may also increase the risk of microbial attack and production of mycotoxins (Semple et al., 1989).

2.2.6 Drying

Drying is used for increasing the shelf-life of DSG and for increasing its ease of handling and transportation capabilities. DSG must be dried to about 10% wb moisture content (Woods et al., 1994). Drying also affects the nutritional properties and physical characteristics of DSG. The use of DSG is limited by the presence of off-flavors and a specific aroma. Using appropriate drying technology, its off-flavors and aroma can be reduced to a large extent (Ezhil, 2010). Hot-air drying (240 to 550°C) using rotary or drum dryers are traditionally used to dry spent grain (Stroem et al., 2009), but, issues concerning the sticking of spent grain to dryer surfaces create an additional burden for the processing plants. Stroem et al. (2009) reported that SS drying has a potential to reduce the surface moisture content of the brewer's spent grain to a level where this material is no longer sticky. The advantages and the potential applications of SS drying are discussed in section 2.1.

A study done by Cenkowski et al. (2012) showed that SS drying has the ability to preserve the protein and phenolic contents of DSG as compared with hot-air drying. Another study conducted on SS drying of beef indicated low peroxide values in the product due to the absence of oxygen during SS drying process. Also, off-flavors and off-odors hardly developed during SS drying compared with hot-air drying method (Speckhahn et al., 2010). Stringent laws regarding environmental pollution and energy savings in many countries provide another advantage for using SS drying technology as the steam used in drying can be condensed controlling possible pollutants (van Deventer and Heijmans, 2001; Ezhil, 2010).

Drying technique plays an important role in increasing the marketability of DSG. The selection of a drying technique also depends on the end use of DSG. For example, DSG used for cattle feed can be of low quality, as odor, color and off-flavors are not a problem for animal feeds, but DSG used for human consumption must be of high quality. Thus, drying method plays a key role in improving the quality of DSG as well as for increasing the profitability of distilleries.

2.2.7 Industrial applications

DSG has high fiber content and a favorable molecular structure for enhancing binding. Therefore, it can be used as a filler for plastics (Rosentrater, 2008a), as potential alternative to bio-based fillers such as bamboo, corn stover and soybean hulls (Rosentrater, 2008a), and to produce hydrogen, syngas (H_2+CO) and hydrocarbons by further processing it using methods such as pyrolysis, gasification and catalytic reforming reaction (Tavasoli et al., 2009).

Addition of lower-cost fillers and reinforcements to plastic resins has accelerated rapidly over the past decade. This can reduce production costs and increase the rigidity of the composite material (Julson et al., 2004; Oksman et al., 1998). However, the result of the study conducted by Julson et al. (2004) showed that DSG might not be acceptable as a filler due to its poor mechanical properties. Rosentrater (2008a) prepared a compression-moulded blend of DDGS and phenolic resin (ranging from 0 to 90% DDGS) for use as fillers for plastics. The result of this preliminary study showed that DDGS concentration between 25% and 50% produced excellent fillers for plastics.

Gasification is a technologically advanced and environmentally friendly way for generating energy from biomass resources as conditions in the process are non-oxidative. Tavasoli et al. (2009) studied the production of hydrogen and syngas using gasification of the corn and wheat DDGS. The results showed that corn DDGS gasification produced gas of higher H_2 and CO concentrations (11 and 56.5%) whereas gasification of wheat DDGS produced 10.5 and 51.5% of H_2 and CO concentrations, respectively. Also gasification of corn DDGS gave higher gas yield (0.42 m^3/kg), lower heating value (10.65 MJ/m^3) and carbon conversion efficiency (44.2%) compared with wheat DDGS gasification.

2.2.8 Fractionation

There are a number of nutritionally essential components present in DSG, such as phytosterols, tocols, zein, etc. These components can be extracted and can be used for industrial purposes or can be incorporated into various food items for nutrient enrichment. Screening is considered as a simple procedure for fractionating spent grains. There can be a shift in the nutrient content depending on the particle size. A fine fraction obtained after sieving has a reduced fiber content and elevated protein level (Wu and Stringfellow, 1982). The major benefits for separating fibers from DSG are: (i) to enhance the nutritional characteristics of DDGS, and (ii) to use the separated fibers along with the solubles for energy generation by combustion (Srinivasan et al., 2008).

The economic value of DSG can be enhanced by extracting the lipid compounds from DSG. The oil obtained from corn DSG has similar properties compared with corn

oil and can be used in food industries or as a biofuel (Xu et al., 2007). The lipid portion of DSG mainly constitutes considerable amounts of long-chain fatty acids, fatty aldehydes, fatty alcohols (policosonols), triacylglycerols, phytosterols, tocols and diacylglycerols (Hwang et al., 2002a,b; Singh et al., 2003; Cheryan, 2002; Wang et al., 2008). Valuable lipid compounds such as phytosterols, tocopherol, policosanols and unsaturated fatty acids may have the ability to prevent diseases due to their nutraceutical properties (Singh et al., 2003; Wang et al., 2008).

Distiller's dry grain with solubles also contains zein, one of the major proteins present in corn. Zein is suitable for various industrial applications such as binders needed in paints, films and in binding fibers (Lawton, 2002). Various researchers studied the possibility of using cellulose obtained from DDGS for developing films and fibers (Yamashiki et al., 1992; Zhang et al., 2001). Also, DDGS cellulose can be used in applications such as composites, paper, water absorbents, lubricant and nutritional supplements (Xu et al., 2009). As energy consumption in the world is increasing and fossil fuels are depleting at a fast rate, alternative sources of energy using biomaterials like DDGS will gain more attention in the future. Extraction of bioactive compounds and other nutritionally essential compounds from DDGS and utilizing it for nutraceutical and pharmaceutical industries can increase the value of DDGS.

The reuse of industrial by-products is gaining more importance in the recent years as it's economically beneficial and environmentally friendly. DSG is one such agro-industrial by-product generated in huge quantities from the distilleries globally. But the use of DSG is still limited to feeding cattle despite all the potential uses. More studies should be conducted to develop alternative uses for DSG, economical and

energy efficient drying techniques for bulk quantities of DSG, methods to increase the incorporation of DSG into human food products, and techniques for easy and economical extraction of different nutraceutical components from DSG. Moreover, there is a need for more affordable technologies for increasing the use of DSG as fillers for plastics in industries, as well as for the generation of energy using DSG.

2.3 Flowability characteristics of distiller's spent grain

The material presented in this chapter is the modified reproduction of work published by Johnson et al. (2011a) under the realm of this thesis.

The knowledge of flow characteristics of DSG is essential for the ease of conveying, blending, packaging and for optimizing the designs of storage containers (Kamath et al., 1994). DSG is increasingly being transported in big containers by rail cars or trucks to greater distances before entering into the market, hence handling and logistics are essential for determining the marketability of DSG (Clementson and Ileleji, 2010; Ganesan et al., 2008a). During shipping and storage, caking and bridging of DSG are the common problems that hinder its flowability (Ganesan et al., 2008a). The flowability of DSG is influenced by a number of factors including storage moisture, temperature, relative humidity, particle size, storage time, ageing and pressure (Ganesan et al., 2008b). Small variability in the aforementioned parameters can lead to caking/bridging of the granular materials, which in turn can induce severe damage to shipping and storage containers (Ganesan et al., 2008a). Such damage could result in

unnecessary expenses related to renting extra machinery, labor, unloading charges, and railcar downtime (Schlicher, 2005; Rosentrater, 2006a; Tumuluru et al., 2010).

2.3.1 Particle size

Particle size is a key factor for determining the flow characteristics of bulk solids. Properties such as bulk density, angle of repose, and compressibility of bulk solids are dependent on the particle size of a material (Ganesan et al., 2008a). A small change in particle size can cause significant variations in flowability. Farely and Valentin (1967/68) found that particle size is the most important factor governing the 'structure' of the powder compact, and the inter-particulate forces which govern the strength of the structure. DSG is a heterogeneous material having particles of different size fractions (Ileleji et al., 2007). Particle segregation occurs when different sized particles are lodged, causing the particle size distribution (PSD) of a heterogeneous bulk to change with time during discharge (Shinohara et al., 1968). Therefore, it becomes essential to separate DSG into various particle sizes before studying its physical characteristics.

2.3.2 Bulk density

Bulk density is defined as the mass of particles that occupies a unit volume of the container. It decreases with an increase in particle size, as well as with an increase in equilibrium relative humidity (Yan and Barbosa-Canovas, 1997). Bulk density is an important property for determining the size of transport vehicles and storage vessels for granular solids and powders (Ganesan et al., 2008a). Maintaining a consistent bulk

density can minimize handling and transportation costs of bulk solids (Ileleji and Rosentrater, 2008). It was reported by Ganesan et al. (2008a) that there exists a gap in scientific data on the influence of the bulk density of DSG on its flow characteristics.

2.3.3 Angle of repose

Angle of repose is an indication of the inter-particulate friction between the particles. It can be used to characterize the flow behavior of materials with respect to flowability, avalanching, stratification and segregation (Ileleji and Zhou, 2008; Frette et al., 1996; Zhou et al., 2002). The AOR values can be used as baseline data for designing bulk storage structures (Ileleji and Zhou, 2008). Particle size of material is an important factor affecting its AOR values (Ileleji and Zhou, 2008). Typically, dry materials with a lower AOR value (30–40º) have better flowability than materials with a higher AOR value (50–60º) (Carr, 1965).

2.3.4 Effect of distiller's spent grain solubles

Ganesan et al. (2008b) conducted a study to investigate the effect of addition of solubles to DDGS. It was observed that increased addition of solubles affected the DDGS flow negatively. The compressibility of DDGS was found to increase with increased level of solubles. Also, DSG with 25% solubles had higher strength, and had the greatest ability to support obstructions to flow when compared with DSG with 10% solubles (Ganesan et al., 2008b). Another study done by Ganesan et al. (2008c) showed that, an increase in soluble content and moisture content influenced the physical and

flow properties such as aerated bulk density, packed bulk density, and compressibility of DDGS. Also, addition of solubles had a significant effect on the color of DDGS.

Flowability properties such as bulk density and angle of repose of DSG are important for determining the size of transportation vehicles, designing storage structures and minimizing transportation and storage costs. Studies show that particle size of DSG and addition of solubles has a significant role in the flowability behavior of the material.

2.4 Biomass densification

2.4.1 Densification process and its significance

Biomass has high moisture content and low bulk density, and, therefore, it is very difficult to handle, transport, store, and utilize it in its original form. Densification of biomass is the process of reducing the volume of the biomass. In the densification process biomass is usually shaped into pellets, briquettes or cubes. Densification reduces the costs of transportation, handling, and storage. It also provides better flow properties than the ground feed, reduced ingredient segregation, less feed wastage, improved animal performance and improved palatability (Holley, 1983; Mani et al., 2003; Obernberger and Thek, 2004; McMullen et al., 2005; Franke and Rey, 2006). The major factors which affect the densification process are: starch, protein, fat, moisture, calcium, phosphorous and fiber content of biomass. Other factors such as feed moisture content, pellet binders, feed particle size, and densification equipment variables also affect the densification process (Kaliyan and Morey, 2009; Turner, 1995; Tumuluru et al., 2011).

Densification can be carried out using unit operations such as: pelleting, extruding and briquetting (Pietsch, 2002; Tumuluru et al., 2011; Li and Liu, 2000). Among these, the most popular densification method in fuel and feed industries is pelleting where a pelletizer or a pellet- mill is used for producing the pellets (Tumuluru et al., 2011). In a pelletizer, a perforated die and rollers are rotated to squeeze the feed through the perforations to produce pellets. The diameter and length of pellets may range from 4.8 to 19.0 mm and 12.7 to 25.4 mm, respectively (Kaliyan and Morey, 2009). In an extruder, the compacted products are produced by compressing the material using a screw or a piston through a die of desired cross-section. Briquettes can be produced using mechanical, hydraulic or roller presses. A briquetter can handle feeds having large particle sizes and high moisture contents without the addition of additives or binding agents (Tumuluru et al., 2011).

Before the densification process, if necessary, the material must be ground to an appropriate particle size. The ground material may then be pre-treated using steam and mixed well with additives for improving the strength and durability of the densified products. Due to the frictional heat developed during the densification process, the temperature of the densified products must be brought down to acceptable levels before storage (Thomas and van der Poel, 1996; Kaliyan and Morey, 2009).

2.4.2 Moisture content of feed

Feed moisture content has an effect on the strength and durability of the densified products. Strength and durability of the densified products increase with an increase in moisture content until an optimum is reached. Water acts as a lubricant and

it also helps in briquetting when water-soluble compounds (starch, sugar, sodium phosphate, calcium chloride etc.) are present in the raw material (Obernberger and Thek, 2004; Grover and Mishra, 1996; Lindley and Vossoughi, 1989; Kaliyan and Morey, 2009; Tumuluru et al., 2011). During densification, the moisture in the feed stimulates the van der Waal's forces and increases the bonding between the particles (Mani et al., 2003, 2006). van der Waal's forces are intermolecular attraction forces attributed to hydrogen bonding, dispersion forces and dipole-dipole attractions. Steam conditioning is a method used to apply moisture to the feed before densification (Maier and Gardecki, 1992). Generally, steam conditioning adds about 1.0-6.0% of moisture before pelleting (Young et al., 1963; Pfost, 1964; Maier and Gardecki, 1992, as cited in Kaliyan and Morey, 2009).

For samples containing wheat and corn, moisture content of 11.0-12.0% wb are generally used for making pellets (Thomas et al., 1997). Tumuluru et al. (2010) adjusted the moisture content of DDGS to 13.5% wb by spraying additional amounts of water before pelleting for DDGS with no steam conditioning. For feeds with high fiber content, water rests on the particle surface, as the feed particles are unable to absorb moisture during the process of compression (Winowiski, 1995). This causes excess lubrication between particles while reducing the durability of the pellets produced.

2.4.3 Feed particle size

Particle size of the feed material is a key factor in determining pellet durability (Mani et al., 2006b; Mani et al., 2004). Generally, tiny particles absorb more moisture and heat compared to larger particles and they undergo a higher degree of conditioning

(Kaliyan and Morey, 2009). A particle size of 0.6-0.8 mm is recommended for producing good quality biomass pellets of high durability (Turner, 1995; Franke and Rey, 2006). Rosentrater (2008b) suggested a particle size between 500 and 650 μm for producing high quality pellets using both unmodified and deoiled DSG. The presence of larger particles in pellets can act as predetermined breaking points causing damage to the pellets. Particle size greater than 1.0 mm will adversely affect the durability of the pellets (Franke and Rey, 2006). However, care must be taken to avoid very small particles as it may results in clogging of the pelleting equipment (Tumuluru et al., 2011).

The major issue involved in using small particle sizes in feed industries is the high cost of grinding. Using a mixture of differently sized particles can solve this problem. A mixture of differently sized particles make pellets of optimum quality, as they form the inter-particle bonding with nearly no inter-particle spaces (Payne, 1978; Grover and Mishra, 1996). For briquetting, larger particles sizes (>6 mm) are preferred due to their good bonding capabilities during briquette formation (Tumuluru et al., 2011). Payne (2006) suggested that to produce good quality (durability) pellets, a particle size distribution of the feed mixture should be: feed particle of up to 1% on a 3 mm sieve, up to 5% on a 2 mm sieve, around 20% on a 1 mm sieve, around 30% on a 0.5 mm sieve and around 24% on a 0.25 mm sieve.

Some of the physical properties of three biomass grinds from two different hammer mill screen sizes are given in Table 2.1. Results show that the bulk densities increase with a decrease in hammer mill screen openings. Corresponding to a hammer mill screen size of 3.2 mm, corn stover had the highest bulk density among the three

samples. The highest bulk density (182 kg/m^3) among the biomass samples was for switchgrass obtained from a hammer mill screen size of 0.8 mm.

2.4.4 Feed preheating

Feed preheating is usually done to improve the durability of pellets by activating the binders between the particles (Rosentrater, 2008b). Aqa and Bhattacharya (1992) reported that preheating of feed may significantly reduce the energy required for pelletizing the biomass. An elevated feed temperature can be obtained by either direct or indirect heating methods. Frictional heating, fluidized bed heating, and steam conditioning are considered as direct heating methods; whereas indirect heating includes conduction heating and hot-oil circulation heat exchangers (Kaliyan and Morey, 2009).

Table 2.1. Some physical characteristics of three different biomass grinds (modified from Mani et al., 2004).

Biomass type	Moisture content (before compacting, % wb)	Hammer mill screen size (mm)	Geometric mean particle diameter (mm)	Bulk density (kg/m^3)
Corn stover	6.22	3.2	0.41	131
		0.8	0.19	158
Wheat straw	8.30	3.2	0.64	97
		0.8	0.28	121
Switchgrass	8.00	3.2	0.46	115
		0.8	0.25	182

Steam conditioning helps to add both moisture as well as heat to the feed; it also helps in starch gelatinization and protein denaturation. Liu and Wyman (2005) reported

that steam conditioning creates a favorable condition for lignin bonding during the densification of biomass. The percentage of steam in the vapor phase or steam quality is an important steam property that can affect the pellet durability (Kaliyan and Morey, 2009). Gilpin et al. (2002) reported that a steam quality of 70-80% is preferred for producing pellets with good strength and durability.

For producing good quality pellets, specific conditioning pressures and feed temperatures are recommended. For example, 103.4 kPag (15 psig) and 80-85°C for high starch and low fiber rations is used and 448.2 kPag (65 psig) and 80°C for high protein rations are recommended (Payne, 1978, as cited in Kaliyan and Morey, 2009). For feeds with high starch and protein contents, an increase in temperature in the range of 54-88°C increased the pellet durability, but when processing high fiber feed with steam, the pellet durability decreased as the high fiber feed didn't absorb moisture (Winowiski 1985, as cited in Kaliyan and Morey, 2009**)**. Skoch et al. (1981) reported that steam conditioning, at temperatures of 65 and 80°C, of a poultry layer-diet resulted in increased pellet production rate and pellet durability.

2.4.5 Adding binders or additives and mixing of feed

Binders such as modified cellulose binders, starches, proteins, lignosulfonate and bentonite are commonly used in feed manufacturing plants (Thomas et al., 1997; Payne, 1978; Tabil et al., 1997; Tabil and Sokhansanj, 1996). Binders between 1-3% of the total weight are incorporated into the feed for increasing the strength and durability of the densified products (Tumuluru et al., 2011). Addition of binders followed by addition of heat to the feed by preheating or steam conditioning is necessary for

activating the added binders. Also, thorough mixing of the feed after adding the binders is important for improving the pellet strength and durability; good mixing enables a consistent distribution of heat and moisture throughout the feed mass. To achieve good mixing, retention times between 30 s to 5 min are recommended for DSG (Rosentrater, 2008b).

2.4.6 Feed ingredients

Feed components such as starch, protein, fiber, lignins and fat have an influence on the strength and durability of the densified products (Tumuluru et al., 2011; Kaliyan and Morey, 2009). Starch serves as a binder (Alebiowu and Itiola, 2002; Thomas et al., 1998; Wood, 1987) as gelatinization of starch takes place in the presence of heat and moisture. Whereas, proteins denature under the presence of heat only and act as a binder (Thomas et al., 1998; Sokhansanj et al., 2005). Tumuluru et al. (2011) reported that high protein content biomass (like alfalfa) can be used as a binding agent in feed materials having lower lignin contents.

Among fibers, water-soluble fibers increase the viscosity of the feed and increase the durability of pellets. But water-insoluble fibers may negatively affect the durability of the densified products (Thomas et al., 1998). However, the resilience characteristics of fibers may not always create good interparticle bonding in the pellet (Thomas et al., 1998). Lignin and extractives can soften at elevated temperatures and can positively affect the binding process as well. Fat/oil in feed can produce pellets of lower strength and durability (Briggs et al., 1999; Angulo et al., 1996). Fat is hydrophobic and acts as a lubricant between the feed particles, and between the feed

and the die-hole wall. Also, fat imparts a low friction in the die causing a reduction in the pelleting pressure (Tumuluru et al., 2011).

2.4.7 Pellet equipment variables

In a pellet mill, the raw material is forced through the holes of the die to form a densified product. The die geometry is important as when the feed passes through the die, the heat produced due to friction leads to particle binding. The die geometry includes the number of openings in the die and the length/diameter ratio (L/D); length refers to the die thickness (Rosentrater, 2008b). Increasing the die length or decreasing die diameter up to a certain limit may increase pellet durability due to an increase in the quantity of shear during densification (Kaliyan and Morey, 2009; Tumuluru et al., 2011). A study conducted by Tumuluru et al. (2010) on DDGS showed that a smaller die diameter of 6.4 mm produced more durable pellets as compared to a larger die diameter of 7.2 mm for pellets produced with and without the incorporation of steam. Thomas and van der Poel (1996) reported that a change in pellet-mill die dimensions from 5.0 mm diameter and 25.0 mm length to 5 mm diameter and 35 mm diameter caused a shift in barley-pellet hardness (Instron) from 161 to 175 N, and durability (Holmen) from 91.3 to 94.5% at 80°C feed temperature.

2.4.8 Removing excess heat, moisture and fines

Moisture content of the pellet must be brought to acceptable levels before storage. Ciolkosz (2009) reported that the final moisture content of the pellets must be less than 8% for safe storage. Since the pellets leave the mill at elevated temperatures of

approximately 150°C, they need to be immediately cooled to avoid any cracks that may develop on the pellet surface. Also, cooling aids in recrystallization and increases the particle-particle bonding leading to increased pellet durability (Ciolkosz, 2009; Thomas et al., 1997). After cooling, the fine particles and dust are removed from the pellets by screening before packaging (Rosendahl, 2013).

Studies show that moisture content, particle size and ingredients of feed have a significant effect in the densification of biomass. Feed preheating is necessary for activating the added and inherent binders. The die geometry plays a significant role in determining the pellet quality in terms of strength and durability. Removing excess heat and moisture from the pellets after production helps in preserving the integrity and improving the shelf-life of the pellets.

2.5 Determination of strength and durability of densified products

Damage occurring in the densified products during handling, transportation and storage is a common problem of the densification industry. These damages are a result of compressive, impact, and shear forces induced in the pellet (Kaliyan and Morey, 2009). Bonding or interlocking of the particles during pelletization is significant for producing high quality densified products. Strength and durability are the two parameters used for determining the quality of the bonds developed during the densification process. Hardness and durability are mainly measured for pellets used for feed. Durability provides a measure of the physical strength and resistance to breaking or crushing of the pellets during handling and transportation (Tumuluru et al., 2011).

A selection of a physical property test depends on the kind of stresses induced during the production and handling of the pellets. Since the stress component causing the densified products to fail varies, it is not recommended to compare the results of compressive resistance, durability resistance, and impact resistance tests each other (Pietsch, 2002, as cited in Kaliyan and Morey, 2009). The methods used for determining the compressive resistance, abrasive resistance (durability) and impact resistance of the densified products are explained below.

2.5.1 Compressive resistance test

Compressive resistance is a measure of the maximum amount of compressive load a pellet can resist before it cracks or disintegrates. This test provides a quick and easy measure of the pellet strength immediately after the pellets are made. In compressive resistance test, a single pellet is placed between the upper and lower plates, and an increasing compressive force is applied at a constant rate until the pellet breaks or disintegrates (García-Maraver, 2010; Kaliyan and Morey, 2009; Carone et al., 2011). The compressive force at the point of cracking or disintegration is the compressive strength which can be determined from a recorded force-strain curve.

A compressive resistance test mimics the compressive stress due to the pressure created by the weight of the top pellets on the bottom ones during storage or transportation, breaking of pellets in a conveyor, or crushing of pellets between the animal teeth while chewing (Kaliyan and Morey, 2009). The Kahl shear press, Stokes tablet hardness tester, universal testing machine (Instron), Pendulum hardness tester and

Kramer shear press can be used to measure the compressive strength of the pellets (García-Maraver, 2010; Behnke, 1994; Thomas and van der Poel, 1996).

2.5.2 Durability or abrasive resistance test

Durability of the densified product can be tested using a tumbling can, Holmen tester, Dural tester or Ligno tester (Tabil et al., 1997; Sokhansanj et al., 1991; Kaliyan and Morey, 2009). In the tumbling can method, 500 g of pellets are tumbled inside the tumbling box device for 10 min at a speed of 50 rpm followed by sieving the pellets (ASAE, 2003a). Generally, pellets are subjected to tumbling test after reducing the temperature of pellets to less than 5°C by cooling. The pellet durability is calculated as the percentage of mass of pellets or crumbles after tumbling to the mass of pellets or crumbles before tumbling. This testing method mimics the impact and shearing forces encountered in the pellets during mechanical handling (ASAE, 2003a).

The Holmen durability tester predicts the degradation of pellets during handling and conveyance by providing a more rigorous testing of the pellets (Salas-Bringas, 2007). About a 100 g sample is pneumatically circulated for 0.5-2 min through a square conduit of pipe with right-angled bends. This causes the pellets to collide over and over again on the hard surfaces. During the durability test, the fines are removed from the pellets using the air stream blowing process. The durability is calculated based on the remaining pellets which are collected from the tester and sieved through a sieve size of about 80% of the pellet diameter (Thomas and van der Poel., 1996).

In a Dural tester, Tabil et al. (1997) used a 100 g alfalfa pellet at 1600 rpm for 30 s. A Dural tester has four inclined blades which are used for imparting shear and

impact forces in the pellets. The material in the chamber of the Dural tester is placed on a sieve (mesh size of 5.95 mm) and is shaken before weighing the material left on the sieve (Adapa et al., 2004). Ligno tester is faster than tumbling can and Holmen tester. In a ligno tester, which uses a swirled air stream, the particles are forced to impinge against each other as well as between the perforated walls of the tester. In this method, a 100 g sample of pellets is exposed to an air stream of 70 mbar for 60 s. After the test, the pellets retained in the apparatus chamber are weighed and their durability is calculated as the percentage of mass of pellets retained in the chamber to the initial mass of the pellets (Temmerman et al., 2006).

2.5.3 Impact resistance test

The impact resistance (drop resistance) test mimics the forces experienced by the pellets in situations such as during unloading the pellets from a truck on to the floor or during loading the pellets into the bins from an elevation (Kaliyan and Morey, 2009). In the impact resistance test, the pellets are dropped four times from a 1.83 m height onto a metal plate (Saikia and Baruah, 2013). Pellet durability is calculated as the percentage of mass retained to the initial mass taken (Shrivastava et al., 1989; Saikia and Baruah, 2013; Al-Widyan and Al-Jalil, 2001). The impact resistance test is often called as a drop test; and it can be used to determine the safe height from which pellets can be dropped during their production process (Pietsch, 2002).

Lindley and Vossoughi (1989) measured the drop resistance of briquettes by dropping a single briquette from a height of 1 m onto a concrete surface 10 times repeatedly. The percentage loss of mass as a result of shattering was taken as the impact

resistance. The ASTM (1998) method (D440-86) of the impact resistance test for coal may also be used to test the impact resistance of the biomass material. Saikia and Baruah, (2013) calculated the impact resistance of densified biomass made from rice straw, banana leaves and teak leaves after dropping the pellets onto a concrete floor from a height of 1.83 m. The impact resistance index (IRI) was calculated using the formula (Saikia and Baruah, 2013):

$$IRI = (100 \times N)/n \quad (2.1)$$

where N is the number of drops, and n is the total number of pieces after N drops.

From the above sections (Section 2.5.1, 2.5.2 and 2.5.3) it is clear that, though there are different tests used for testing the physical quality of pellets, the choice of a test depends on the type of stresses occurring in the pellet during handling or processing. For the current study, compressive resistance test was selected for checking the physical strength of the pellet due to its relevance and advantages as described in section 2.5.1. A diametrical compression test, which is a type of compressive resistance test, chosen for the present study is discussed below in section 2.5.4.

2.5.4 Diametral compression test

The diametral compression test is widely used to test the tensile strength of materials such as concrete, biomass pellets and pharmaceutical tablets (Wright, 1955; Kashaninejad et al., 2010; Fell and Newton, 1970). A diametral compression test provides a quick measure of the pellet quality immediately after its production; hence, it

helps in modifying the pelleting process for producing better quality pellets (Kaliyan and Morey, 2009; Fahad, 1996). During the diametral compression testing the fracture line occurs along the diametral plane. Hence, it is assumed that the fracture is initiated by tensile stresses caused by the applied load.

Al-Widyan et al. (2002) studied the physical durability and post-compression expansion (stability) of olive cake briquettes of 25 mm diameter as influenced by the compaction variables. The stability of the briquettes was expressed in terms of their relaxed density or the final density after sufficient time period for their dimensions to stabilize. Results showed that highly durable olive cake briquettes were obtained with a density of 1100 to 1300 kg/m3 after relaxation (increase in volume). Garcia-Maraver et al. (2010) determined the crushing resistance and tensile strength of pellets from olive grove residual biomass pellets using diametral compression testing using a Kahl tester. The study showed that the use of different types of raw materials from olive grove residues produced pellets of different physical and chemical properties. Pellets made from olive tree leaves had lower bulk density (481.56 kg/m^3) and crushing resistance (4.00 kg) as compared with pellets made from olive tree branches (bulk density= 582.53 kg/m^3; crushing resistance = 22.50 kg).

Zamorano et al. (2011) used diametral compression testing for determining the crushing resistance (which was defined as the maximum crushing load a pellet can withstand before cracking or breaking), and tensile strength of five different types of pellets produced from leaves of olive trees, olive trees (branches of different size), almond trees, black poplar and holm oak trees. The study showed that pellets produced from the lopping waste from the holm oak possessed the highest crushing resistance

(23.33 kg), whereas pellets produced from the leaves of olive tree had the lowest crushing resistance (4.00 kg). Ahmad et al. (2012) compared the tableting properties of Assam Bora rice starch with the commercially available direct compression excipient, Starch 1500. A diametral compression test was used for determining the tensile strength of tablets. The tensile strength of Assam Bora rice starch varied between 1 and 4 kg/cm^2 and Starch 1500 varied between 0 and 3 kg/cm^2 when the compression pressure for pellet making varied between 10 to 250 MPa. Results showed that Assam Bora rice starch tablet has high tensile strength and is beneficial for the development of tablets with good compaction and mechanical properties.

The studies show that diametral compression test is used in a variety of studies to test the crushing resistance and tensile strength of pellets used for feed, food and energy applications. This test is commonly used due to its significance and simplicity. Another advantage of using diametral compression test is that it provides a quick measure of the pellet strength immediately after the pellet production; which in turn helps in adjusting or making modifications to the pelleting process without causing much delay to the production process.

2.5.5 Stress-relaxation test

In the stress-relaxation test, the sample is deformed to a preset value and the deformation is kept constant for a specific time period. During the holding stage, the changes in stress are measured as a function of time. The stress-relaxation test has a number of advantages such as being non-destructive, quick, simple and robust (Herrero et al., 2004). The stress-relaxation test has been used in characterizing rheological

properties of food materials such as: fruit gels (Gamero et al., 1993), fruits and vegetables (Peleg 1979; Marquina et al., 2001) and fish (Herrero et al., 2004).

Herrero et al. (2004) evaluated the possibility of using the stress-relaxation test to analyze the post-mortem textural changes of ice-stored codfish. The fish was compressed to a 5% deformation and the deformation was kept constant for 60 s. The data obtained from the stress-relaxation test during the 60 s period was fitted to linear and nonlinear regression models. The study showed that stress-relaxation test can be used to differentiate the post mortem textural changes of cod during its ice-stored preservation. Bhattacharya (2010) studied the effects of thermal treatment (raw and roasted) on the viscoelastic properties of moth bean flour dough at different moisture levels. Two strain levels, low (0.05) and high (0.50) were used to characterize the relation to extrusion and dough flattening. An increase in moisture content of moth bean flour dough markedly reduced the initial and residual stresses in the dough. Thermal treatment of the flour improved the post-extrusion or post-flattening shape retention of the product. Marquina et al. (2001) used compression test, penetration test and compression-relaxation test to study the mechanical parameters of Burlat sweet cherries. Results showed that compression-relaxation test is the most suitable test for characterizing the Burlat cherries in terms of the five degrees of ripeness. However, the penetration test did not correctly differentiate the five degrees of ripeness analyzed.

Ahmed and Fluck (1972) conducted stress-relaxation studies on irradiated peaches. The study aimed to determine the significance of gamma radiation and storage on the creep deformation and stress-relaxation behavior of peach fruits. Results showed that irradiation, degree of ripening and stress-strain history of the peaches affected the

creep deformation and stress-relaxation behavior of the fruits. Kingsly et al. (2013) studied the effect of moisture content, conditioning temperature and compression loads on the stress-relaxation behavior of DDGS bulk solids. Stress-relaxation test was used to evaluate the caking potential and flowability of DDGS in terms of cohesiveness between the particles. The cohesiveness was observed to increase with an increase in moisture and environmental temperature. The study showed that moisture content, temperature, and compressive load significantly influenced the caking and flowability of DDGS. The cohesiveness of DDGS increased with an increase in moisture content and environmental temperature. The solidity values of DDGS decreased with an increase in moisture content, and the bulk density increased with an increase in compressive force.

The studies show that stress-relaxation test has been employed in a number of studies to characterize the materials such as fish, bean flour, peaches and DDGS. Stress-relaxation studies can even be used to differentiate fruits based on their ripeness. For DDGS, stress-relaxation test was effectively used to evaluate the flowability properties in terms of cohesiveness between the particles. This test provides a simple procedure for determining the rheological properties of bio-materials.

2.6 Stepwise regression method

Stepwise regression method is used for selecting appropriate variables for a multiple linear regression equation from a list of available variables. Thus, stepwise regression models avoid using non-significant variables in the regression models as

compared with multiple linear regression models. A few studies conducted using stepwise multiple regression method are reviewed below.

Ghani and Ahmad (2010) used stepwise multiple regression method to forecast the marine fish landing. This study showed that marine fish landing can be effectively predicted using two controlled variables – fishermen and fishing gears licensed. Burkholder and Lieber (1996) evaluated the significance of polynominal regression, stepwise polynomial regression and quintic spline approximation for fitting noisy data. Though spline approximation provided the most accurate results, comparable accuracy can be obtained more quickly and simply using stepwise polynomial regression method. A polynomial regression method was found to be more accurate for relatively smooth data. Aishima and Nobuhara (1977) used a stepwise regression method for analyzing the GLC profiles of soy sauce flavor. Regression models for sensory test panel acceptability were developed for each step and the models were later evaluated by substituting the gas chromatographic data. Good accuracy was obtained for the estimation of sensory quality using stepwise regression method.

Guillen -Casla et al. (2011) studied the effect of E-beam irradiation on food compositional parameters (protein, fat, moisture, nitrate and nitrite content), free amino acids and some of their decomposition products. Principal component analysis (PCA) and stepwise multiple linear regression were used to evaluate the results obtained during the study. Results showed that high radiation doses (6 and 8 kGy) alter food chemical composition and low doses (1 or 2 kGy) do not have an adverse effect on the food chemical composition. The PCA and stepwise regression models developed may be used to determine the appropriate radiation dose and level of food safety after

irradiation. Nielsen et al. (1997) conducted a study for the prediction of shelf-life of medium-heat whole milk powders using stepwise multiple regression and principal component analysis techniques. From a list of 35 independent variables, linear regression equations were developed with 6 or 7 variables using stepwise multiple regression and principal component analysis methods.

Studies show that stepwise regression method is widely used and it offers a great way for developing regression models by choosing only significant independent variables. This method is highly suitable when there are a large number of independent variables involved in the model; whereas, the use of multiple linear regression method alone in such cases results in lengthy equations. In addition, removing the non-significant parameters from the equations improves the quality and validity of the developed models.

The review of literature shows that the knowledge of the physical properties of DSG is significant for determining the size of transportation vehicles, designing storage structures and minimizing transportation and storage costs. The densification of DSG has many advantages e.g., it reduces the cost of transportation, handling, and storage; produces less feed wastage, and develops desired granular form and needed surface area for drying. However, the knowledge of the physical and rheological properties of DSG during its densification is limited. This knowledge is important for improving the strength of densified DSG.

Literature shows that the problem of the disintegration of DSG compacts during drying in SS is prevalent for a longer period of time. Characterization of the physical and rheological properties of DSG compacts during drying in SS will be helpful for

analyzing the breaking and disintegrating behavior of the compacts inside dryers. This characterization will also be useful for finding suitable methods for reducing or eliminating the problems associated with the SS drying of DSG compacts.

3. MATERIALS AND METHODS

The material presented in this chapter is the modified reproduction of work published by Johnson et al. (2011 a,b; 2013 a,b; 2014 a,b,c) under the realm of this thesis**.** This chapter provides the detailed description of the materials and methods used for this study.

3.1 Preparation of raw material

Stillage used for this study was obtained from a local distillery (Mohawk Canada Ltd., a division of Husky Oil Ltd.) in Minnedosa, MB. The raw material, a non-fermentable residue from starch-to-ethanol fermentation process, was a mixture of corn and wheat in the ratio 9:1.

The DSG was centrifuged in a Sorvall General Purpose, RC-3 centrifuge (Thermo Scientific Co., Asheville, NC) to separate the raw material into different fractions. The centrifuge was operated at a speed of 2200 rpm on a radius of 0.146 m for 10 min, with a 1000 mL sample container. After centrifugation, the supernatant liquid fraction (thin stillage) was discarded; the remaining part contained the semi-solid fractions (condensed distiller's soluble-CDS) and the coarse fractions (wet distiller's grain-WDG). The CDS and WDG fractions were bagged in separate airtight containers and placed in a freezer. Before each set of experiments, the required amount of samples was thawed at room temperature for 3 hours before it was used in drying experiments involving SS or hot air.

3.2 Superheated steam drying system

A full description of the drying equipment can be obtained from Pronyk et al. (2010). The SS drying system used in this study mainly consists of a steam generator

(boiler), a superheater, drying chamber, conveying pipelines, valves, instrumentation and a control and data acquisition system (Fig 3.1).

The function of the boiler (#1) is to generate and supply saturated steam for the system. The system consists of an electric boiler (ES18, Sussman-Automatic Corp. Long Island City, NY, and U.S.A.) with a steam capacity of 24.6 kg/h (54.2 lb/h). The boiler has a maximum working pressure of 621 kPa (90 psi). The boiler operates on regular tap water as distilled, deionised, or reverse osmosis water can easily corrode its carbon steel design. The system is designed with schedule 40, 316 stainless steel piping with a diameter of 12.7 mm (1/2 in).

The saturated steam, upon leaving the boiler, passes through a pressure reducer (#5) and is directed through a superheater (#7) where steam is superheated to a desired temperature. The superheater used here is an electric element that operates as an inline heater. It requires single phase, 240 V power supply. Next, SS flows through a 1/2 inch pipe where temperature (#11) and flow (#9) of SS is measured, passes through a 3-way solenoid valve (#12) controlled by an actuator, and finally enters the SS drying chamber (#13) where a sample is processed. The SS that passed through the sample is diverted from the drying chamber through a heat exchanger (#24) where it is condensed and diverted to an outlet drain (#27) or back to a reservoir (#17) through a sparge tube (#18).

(i) Drying chamber: Drying chamber is designed with 12.7 mm (1/2 in) thick square tubing made of cold rolled steel that is coated with Teflon® PFA thermoplastic to protect against corrosion. The drying chamber has two compartments (Fig. 3.1); in the lower chamber, SS enters through the system piping, fills it and then is uniformly

funneled through an 89 mm (3.5 in) stainless steel pipe that connects the two chambers. The upper chamber mainly consists of the sample placement area. The upper and lower chambers are separated by a 6.3 mm (1/4 in) coated steel plate with an industrial gasket to prevent SS from bypassing the sample area. The drying chamber consists of the suitable thermocouple assemblies, various valves and pressure gauges (Pronyk et al., 2010). The drying chamber is surrounded by 20 electric strip heaters (2 each on top and bottom and 4 each on the other four sides), each with a power rating of 250 W. Strip heaters help in preheating the chamber and ensure that the chamber walls operate at the same temperature as the SS. By the initial preheating of the chamber, the strip heaters help to reduce the initial SS condensation during the operation.

(ii) Solenoid valve: A 3-way valve (#12) is actuated by a solenoid and is used to control the flow of steam. When the coil is energized using an electric current, a magnetic field is created causing the plunger to either open or close the valve. The SS system is designed with a steam bypass that serves to divert the steam from the drying chamber during the warm-up phase or a sample loading phase (Zielinska et al., 2009). The highest operating temperature for the 3-way solenoid valve is 173.3°C; hence, the SS temperature must be maintained below this level before entering the solenoid valve.

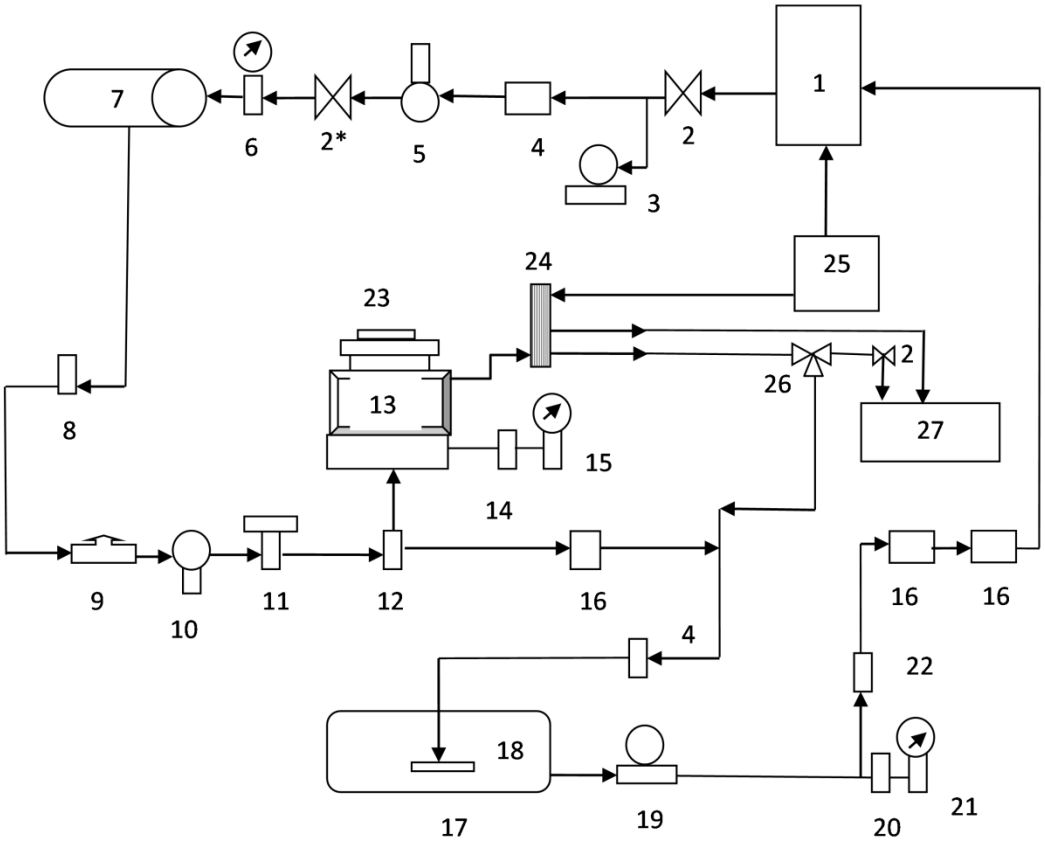

1	steam generator/ boiler	14	steam relief valve (103 kPa)
2	globe valve	15	pressure gauge (100 kPa)
2*	globe valve- steam flow rate control valve	16	check valve
3	steam trap	17	water tank
4	vacuum breaker	18	sparge tube
5	pressure reducing valve	19	pump (1/3HP- impeller type)
6	pressure gauge (415 kPa)	20	truck valve
7	Superheater	21	pressure gauge (1100kPa)
8	steam relief valve (414 kPa)	22	ball valve
9	vortex meter	23	mass balance (accessory)
10	pressure transducer	24	heat exchanger
11	thermoelectric probe	25	water supply inlet
12	3-way solenoid	26	3 way valve for diverting condensed superheated steam
13	drying chamber	27	outlet drain

FIG. 3.1. Schematic diagram of the superheated steam drying system.

3.3 Superheated steam flow measurement

Steam flow rate is adjusted manually using the steam flow rate control valve (2*) to achieve the desired steam velocity. Steam velocity can also be calculated based on the volumetric flow rate and cross-sectional area of SS flow from the bottom section through the drying chamber. Volumetric flow rate of the steam is calculated by measuring the amount of condensate exiting the SS dryer in 3 min, and correlating it to the tabularized values (Irvine and Liley, 1984) of specific volume for the processing temperature and pressure.

3.4 Processing WDG in bulk under different drying conditions and with different concentration of solubles

3.4.1 Thin-layer drying of WDG and a mixture of WDG and CDS

After thawing, initial moisture content of the WDG fraction was measured based on the air-oven drying method (AACC, 2000) using a laboratory hot-air oven (Thermo Electron Corporation, Waltham, MA). In this method, 2 g of samples were placed in the oven at 135°C for 2 hours. In this set of experiments, the measured initial moisture of WDG was determined to be 74.6% wet basis (wb) and 80.1% wb for CDS. Three types of drying experiments of WDG were performed in loose bulk: (i) thin-layer drying in SS at 150°C, (ii) thin-layer air-drying at 150°C, and (iii) thin-layer air-drying at 45°C. Thin-layer air-drying at 45°C was done to mimic the open air-drying of the samples. Hot-air oven was preferred in place of open air-drying so as to prevent the chances of developing molds on the samples by the prolonged exposure of samples in air.

(i) Superheated steam drying experiments were carried out in the SS drying unit. The SS temperature at the inlet of the drying chamber was maintained at 150°C and the velocity of steam passing through the chamber was set to 1.5 m/s. Drying experiments were conducted under or near atmospheric pressure. Each drying experiment was conducted in a thin-layer with a sample size of 30 g placed on a perforated screen. (ii) Thin-layer high-temperature drying at 150°C air temperature was carried out using a convection oven (Thermo Electron Corporation, Waltham, MA) set to 150°C. Samples of 30 g each were dried in aluminum dishes in a thin layer. (iii) Thin-layer low-temperature drying at 45°C air was done in the same convection oven following the same drying methodology as described for high-temperature air-drying.

All air-oven drying and SS drying experiments were carried out until the samples were fully dried or until the samples reached a constant weight, which was confirmed by conducting separate experiments for specific amount of samples for finding the approximate time to reach the dry weight. If the dry weight was not achieved in the specific time, then the mass of the samples was measured at specific intervals during drying until a constant weight was achieved. For SS experiments, after reaching the established time, mass was measured at specific intervals by hanging the sample inside the drying chamber after diverting the SS from the drying chamber using the solenoid valve.

The same set of drying experiments was conducted with WDG samples which had CDS added in quantities of 10, 20 and 30%. Each set of samples was mixed using a laboratory mixer (KitchenAid Classic, KitchenAid, St Joseph, MI), and was manually spread uniformly in thin layers on the aluminum dishes and perforated screens (SS

drying) using spatulas. After drying in SS and high- or low-temperature air, the samples were crushed gently using a lab scale mortar and pestle to separate the agglomerated particles. The ground DSG fractions were sieved using a nest of sieves (US sieve numbers 4, 6, 8, 12, 16, 20, 30, 40, 50, 70, 100 and a bottom pan) in a horizontal sieve shaker (Retsch Inc., Germany) following the method proposed by American National Standard (ASAE, 2008) at 300 RPM for 10-15 min. The drying and sieving processes were continued until enough sample mass was obtained on each sieve for carrying out further experiments. Each fraction size 300, 425, 600 and 850 µm was stored separately in airtight containers.

3.4.2 Measurement of bulk density and angle of repose

Dried WDG obtained at different drying and three blending ratios with CDS were used in measuring bulk density and angle of repose. Bulk density was determined for particle sizes of 300, 425, 600 and 850 µm using a standard Carney funnel setup with hopper, funnel, and leveling rod (ASTM, 2006). Bulk density was calculated from the weight and volume of materials filled in a cup of known volume (25 cm^3). The mass measurements were done using an electronic balance with an accuracy of 0.001 g (Model Adventurer Pro AV313, Ohaus Corporation, Pine Brook, NJ).

Fixed-base piling angle of repose values were found out experimentally (Ileleji and Zhou, 2008) for particle sizes of 300, 425 and 850 µm. The apparatus consisted of a metallic funnel (Carney funnel), a stand, and a cylinder of 30 mm diameter. The cylinder was placed on a rotating base so that it could be imaged from different angles. Prior to measuring angle of repose, the material drop height was determined using

granular sugar particles and DSG so as to form a conical heap with minimum disturbance. The drop height was found to be 55 mm from the base of the cylinder. The bottom of the funnel was positioned right above the center of the base before each experiment.

A digital camera (Rebel XT, Canon Inc., Japan) was used to take the pictures of each heap of the raw material for measuring angle of repose. The images were taken from four different angles at 90º intervals for each conical heap. The images thus obtained were analyzed using Matlab (Version 7, Mathworks Inc., Natick, MA).

3.5 Preparation of single compacts from DSG and measurements of their stress-relaxation characteristics

3.5.1 Sample preparation

In this set of experiments, the initial moisture content of the WDG and CDS fractions were 69% and 79.4% wb, respectively, which were determined using the methods described in section 3.4.1. After separating the WDG and CDS, for ensuring the uniformity of separated fractions, each fraction was blended separately using a laboratory mixer. After blending, 1.8 to 2 g of DSG with solubles were prepared by manually mixing different proportions of WDG with 15 or 30% CDS. Also, oven-drying at 135°C was used to reduce the initial moisture content of samples to 15, 20 and 25 ±1% wb.

A single compaction unit was used for producing compacts for the study (Fig. 3.2). The compaction unit was attached to an Instron universal testing machine (UTM) (Model 3366 Universal Testing Systems, Instron Corp., Norwood, MA). Loading for

the sample was made possible by a 6.4 mm plunger attached to the Instron UTM equipped with a 10 kN load cell. The preset load for the test was set at 2000, 3000, 4000 and 4500 N, corresponding to pressures of 60.3, 90.5, 120.6 and 135.7 MPa, respectively, at a cross-head speed of 50 mm/min. After reducing the moisture content of the sample to required levels, a 0.5 g sample was fed into the die, compressed to a preset load, and held at constant deformation for a specified time of 180 s to arrest the spring-back effect. The compact formed was about 13 mm in height and was removed by freely moving the plunger through the die followed by gentle tapping of the compacted biomass (Tumuluru et al., 2010; Mani et al., 2003).

3.5.2 Stress-relaxation test during compact production

Stress-relaxation data was acquired during the compact production stage, i.e., when the compact was held under constant deformation for a time of 180 s in the compaction unit. The data thus obtained from the stress-relaxation test were normalized and analyzed to determine the asymptotic modulus (E_A) of the compacts.

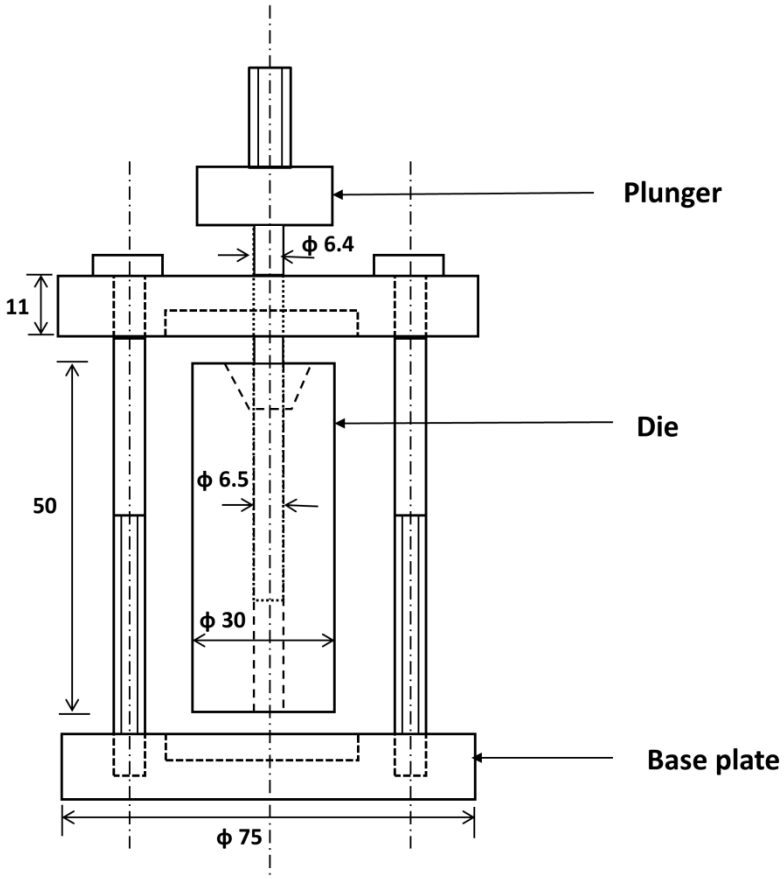

FIG. 3.2. Compaction unit for producing single distiller's spent grain compacts. All dimensions are in mm.

3.5.3 Moisture content, compact density and compact temperature measurements

The moisture content of the compacts was determined using ASAE S358.2 method (ASAE, 2003b), in which single compacts were dried in the convection oven at 103°C for 24 hours. The mass measurements of each compact were done using an electronic balance with an accuracy of 0.001 g (Model Adventurer Pro AV313, Ohaus Corporation, Pine Brook, NJ). For compact density determination, mass and volume of the compact was measured immediately after ejecting the compact from the die after

densification. The volume of the compact was calculated by measuring its length and diameter using a Vernier caliper (Tumuluru et al., 2010; Shankar et al., 2008). The temperature of the compact was measured immediately after densification (no compression holding time) using a T-type needle thermocouple (Omega Technologies Company, Stamford, CT) to determine the extent of temperature rise of the compact due to frictional heating.

3.6 Measurements of disintegration of WDG compacts as affected by drying in SS

3.6.1 Compacting distiller's spent grain

Due to the presence of larger than 1 mm particles in centrifuged spent grain, the particle size of the WDG fractions that came out of centrifuge was reduced using a laboratory grinder. This preparation step increased the uniformity in mechanical strength of samples. Particle size distribution analysis of WDG after grinding is shown in Appendices A.2 and B.1. In this set of experiments, the initial moisture content of the WDG fraction was 69.0% wb which was measured based on AACC (2000) method as described in section 3.4.1 (135°C for 2 h). Samples were compressed in the compaction unit (Fig. 3.2) at a crosshead speed of 50 mm/min and the preset load for the test was set at 4000 N corresponding to a pressure of 120.6 MPa. The preliminary experiments indicated that the initial moisture of about 25% wb was best suited for producing compacts without clogging the compaction unit. Therefore, oven-drying was used to reduce the initial moisture content of WDG to the required level. Then, at ambient temperature, a 0.4 g sample at approximately 25% wb was fed into the die, compressed

to the preset load, and held under compression for 180 s to arrest the spring-back effect. The compact obtained had approximately a 10 mm length.

3.6.2 Moisture content and density of the compacts

As some of the moisture could escape during compaction and handing, moisture content of compacts was measured again after the compaction following the ASAE S358.2 method (ASAE, 2003b) as described in section 3.5.3. The compacts used in this section of experiments had a moisture content of 23.0% wb.

Density of compacts was determined based on mass and volume of the compact that was measured immediately after removing the compact from the die. The volume of the compact was calculated by measuring its length and diameter using a Vernier caliper (Tumuluru et al., 2010). The mass measurements of each compact were done using an electronic balance with an accuracy of 0.001 g (Model Adventurer Pro AV313, Ohaus Corporation, Pine Brook, NJ). The compacts produced for this set of experiments had a density of 1100 kg/m^3.

3.6.3 Superheated steam drying conditions

Experiments were carried out under SS temperatures of 110, 130 and 150 ± 1°C. For each temperature, three different steam velocities of 0.9, 1.1, 1.4 ± 0.01 m/s were used (see section 3.3 for the method). Drying was carried out at chamber pressure of 100 – 102 kPa. The drying chamber was pre-heated for few minutes before experiments to avoid possible steam condensation on the inner walls of the chamber. Each sample was exposed to SS for 5, 120, 300 and 600 s under different drying conditions.

3.6.4 Mass and temperature change measurements

As during drying in SS, mass changes of compacts were recorded and the compacts were placed on an aluminum tray with a plastic bottom mesh (Fig. 3.3). The sample holder was suspended on a thin wire inside a hollow pipe, 85 mm in diameter, attached to the steam entrance. The thin wire was attached to an electronic balance (Model TR-403, Denver Instrument Co., Arvada, CO) located on the top of the drying chamber. The mass changes were measured with an accuracy of 0.001 g.

The empty sample holder was placed in the drying chamber for ~10-15 min before the experiments. This facilitated bringing the temperature of the sample holder to the temperature of the drying medium and eliminated the possibility of condensation on the surface of the sample holder during drying. To adjust for the lifting force acting upon the sample (compact) and the sample tray, the mass was intermittently measured (Kemp et al., 2001) at specific time intervals (5, 120, 300 and 600 s) immediately after redirecting the SS flow and bypassing the drying chamber. Moisture content of the compacts was determined based on their mass changes.

To measure temperature changes of the compacts during a 600 s drying period, separate drying experiments were conducted in SS. A single thermocouple tip was carefully inserted into the center of the compact to measure its temperature during drying. The temperature changes were recorded every 5 s by data logger connected to a computer. The temperature was measured with an accuracy of 1°C.

3.6.5 Percentage increase in volume and density variation

Dimensions of the compacts subjected to drying were determined experimentally using an imaging technique constituting a digital camera (Canon PowerShot G9, Canon Inc., Japan) and a personal computer. The images obtained were processed with a software package Image Tool 3.00 (The University of Texas Health Science Center, Houston, TX). The volume of the samples was calculated for each image using the dimensions of the compacts obtained from the digitized images. Density of the compacts was determined using the calculated volume and its measured mass. The percentage increase in volume and density was determined for each sample from the generalized Eq. 3.1.

$$\text{Percentage change} = \frac{N_f - N_i}{N_i} \times 100 \qquad (3.1)$$

where, N_i – initial value before drying, N_f – final value after drying

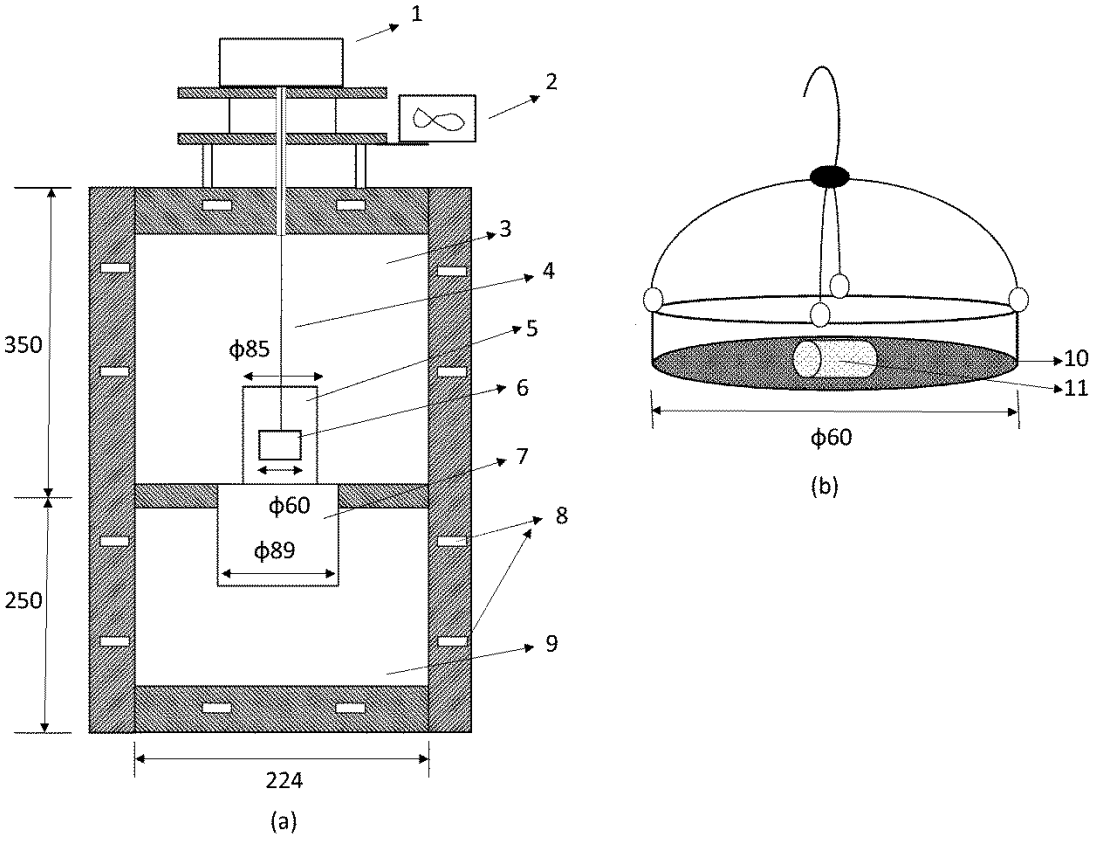

FIG. 3.3. (a) Diagram showing SS drying chamber equipped with accessories for mass measurements: 1: balance; 2: fan; 3: upper drying chamber; 4: sample hanging copper wire; 5: hollow pipe; 6: sample holder; 7: superheated steam inlet; 8: strip heaters; 9: lower drying chamber. (b) Sample holder with compacted WDG for mass measurements: 10: perforated mesh; 11: compacted wet distiller's spent grain. The sample is placed in the upper drying chamber. All dimensions are in mm.

3.6.6 Diametral compression test and crushing resistance

The diametral compression test was used to determine the crushing resistance as well as tensile strength of the compacts. The basic assumption behind the analysis of the diametral compression test was that the stresses and strains in the cylindrical specimen could be derived from a linear elastic solution satisfying the generalized Hooke's law (ASTM, 2011; SHRP Protocol P07, 1993).

In this test, after exposing the compacts to SS for specific time periods, a small piece of the single compact of approximately 4.0 mm thickness was cut and placed between two flat, parallel plates of the Instron machine (Fig. 4.1(a)). An increasing compressive load was applied at a constant rate until the compact failed because of cracking or breaking. The cracking or breaking of the compact was initiated by the tensile forces distributed over a significant portion of the diametral plane resulting from the applied compressive load or stress (Garcia-Maraver et al., 2010).

The maximum crushing load a compact can withstand before cracking or breaking is called the crushing resistance or compressive resistance (Kaliyan and Morey, 2009). The compressive resistance test mimics the compressive stress due to weight of the upper compacts on the lower compacts during storage in containers, or crushing of compacts in a screw conveyor (Zamorano et al., 2011; Kaliyan and Morey, 2009). Crushing resistance of the compact was measured on the assumption that it simulates the vigorous impact forces or stresses acting upon compacts during SS drying in a spouted or fluidized bed dryer. For the current study, compressive load at fracture was obtained from a recorded force-deformation curve by the Instron machine.

3.7 Measurements of disintegration of DSG compacts during SS drying as affected by addition of solubles.

3.7.1 Densification of distiller's spent grain

For this study compacts were produced using a single compaction unit with a 12.1 mm diameter die and 12.0 mm plunger. The compaction unit was attached to the same Instron machine as described before. The initial moisture content of the WDG

fraction was 69.0% wb and solubles 79.4% wb and was determined as described in section 3.4.1. The particle size distribution analysis of WDG and CDS are provided in Table 5.8. Particle size distribution for CDS is provided in Appendix A.1. DSG with 0, 10, 30, 50 and 70% solubles (w/w) were prepared by blending required proportions of WDG with CDS manually as well as using a laboratory mixer.

The initial moisture content of the WDG and WDG-solubles blend was brought down to 51% wb by drying it in a convection oven at 135°C (Thermo Electron Corporation, Waltham, MA) for predetermined amount of time that was established based on drying characteristics in preliminary tests. A 0.6 g sample blend was fed into the die and compressed to a pre-set load of 4000 N corresponding to a pressure of 35.4 MPa, and held at constant deformation for a specified time of 300 s to arrest the spring-back effect. The compact obtained had a moisture content of 50% wb, height of 4-6 mm, and density of 833.3 to 1040.3 kg/m^3, depending on the ratio of solubles to WDG fraction. Procedures for moisture determination of single compacts and their density determination were described in section 3.5.3. The experiment showed that approximately 1% of the moisture was lost due to compaction of biomass.

3.7.2 Superheated steam drying conditions and moisture change measurements

Experiments were carried out at a SS temperature of 150°C, velocity of 0.9 m/s and SS pressure of 100–102 kPa. The sample holder was pre-heated for 10-15 min before each experiment to avoid a possible steam condensation on the holder. The compacted samples at 50% wb moisture were exposed to SS for 5 s initially and after measuring the physical and rheological properties the samples were discarded. These

steps were repeated for each compact after reaching 40, 30 and 20% wb moisture content in SS drying. Also, the same physical and rheological measurements were done for unprocessed (non-dried in SS) compacts and served as reference. When drying in SS to 10% wb final moisture content, the compacts became brittle, hence measurements were taken only for compacts reaching 40, 30 and 20% wb moisture.

An aluminum tray with a plastic mesh at the bottom was used as the sample holder for mass change measurements. The procedure for mass measurement is described in section 3.6.4. During the experiments for determining the drying characteristics of compacts in 150°C SS, the sample mass was weighed intermittently at 3 min intervals after diverting the SS flow from the drying chamber using the solenoid valve. Drying time intervals needed to reach specific moisture contents of 40, 30 and 20% wb was later determined by interpolating the data and were 3-5, 7-9 and 11-13 min, respectively.

3.7.3 Compact dimensions as affected by SS

Dimensions of the unprocessed compacts and compacts subjected to drying were measured with an electronic calliper (Tumuluru et al., 2010; Shankar et al., 2008). Volume of the compacts was calculated using the dimensions of the samples. Percentage change in length, diameter and volume was calculated from the generalized Eq. 3.1 described in section 3.6.5.

3.7.4 Stress-relaxation and hardness tests for compacts

A stress-relaxation test was performed on the DSG compacts before and after exposing the compacts to SS. The test was performed using the Instron machine. The sample was compressed between the upper and the base plates lubricated with a thin layer of petroleum jelly. The upper and base plates had a diameter of 50 and 150 mm, respectively. Each compact was deformed to 40% of its length at a cross-head speed of 200 mm/min. When the desired deformation was attained, the deformation was kept constant and the compact was allowed to relax for 600 s.

Hardness of the compact is defined as the force needed to attain a given deformation (Szczesniak, 1963; Pons and Fiszman, 1996). As in these stress-relaxation experiments each compact was deformed to 40% of its original length, hardness was measured from the applied stress to corresponding 40% applied deformation.

3.7.5 Chemical composition analysis

The analysis of chemical composition of both WDG and CDS was done by the Feeds Innovation Institute at the University of Saskatchewan, SK, Canada. The components analyzed and the methods used for each analysis are provided in Table 5.9.

3.8 Effect of particle size on the disintegration of distiller's spent grain compacts while drying in superheated steam dryer

3.8.1 Particle size measurements

Particle size distribution of the samples was measured using Malvern Mastersizer (Malvern Instruments Ltd., UK). The Mastersizer measures the size of the

particles or the distribution of different sizes within a sample using the principle of Mie theory. Each particle has its own characteristic light scattering pattern; Mastersizer uses the detector array within the optical unit to record the actual scattering pattern from a field of particles (Malvern Instruments, 1997). Then, using the Mie theory, it calculates the size of particles that created that pattern (Torres et al., 2010; Mingard, 2009).

While adding sample to the Mastersizer, the system measures the quantity of sample added by recording the "obscuration" of the beam as a result of the sample being added. The obscuration is referred as the fraction of light lost from the analyzer beam either by scattering or absorption while the sample is introduced (Malvern Instruments, 1997). Once the sample is properly dispersed, the obscuration stabilizes and the measurement is made. The interface between the sample dispersion system and the optical unit is called a cell. The cell has a pair of windows that permits the laser beam to pass through the sample. Two types of cells are available to the Mastersizer for measurements, i.e., a wet cell used on the Hydro 2000G/S/M and a dry cell used on the Scirocco 2000. Since the samples used for the current study were wet, a wet cell was used for the PSD analysis.

Wet samples must be well-dispersed in a liquid dispersant before measurements. An inappropriate dispersant can cause the sample to stick together and float on the surface or even dissolve the samples (Malvern Instruments, 1997). It is possible to examine whether a sample dissolves or not by analyzing it visually or by measuring the obscuration figure of the sample. A decreasing obscuration figure indicates that the sample is probably dissolving. The dispersant used for the current analysis was distilled water.

For PSD measurements, a small quantity of the WDG was used. During the measurement, the sample in the cell was mixed with a magnetic stirring bar without affecting the optical path. Measurements were made in triplicate for each sample and the distributions were prepared based on the average value obtained. After each experiment, the sample area was cleaned well using distilled water and employing ultrasonic action before introducing new set of samples.

3.8.2 Distiller's spent grain

The WDG fraction used for the current experiments had a moisture content of 69.0% wb. The particle size distribution order of WDG was represented in terms of d(0.9) values, which is the size of particle below which 90% of the sample lies. The d(0.9) of WDG after separation, before grinding, was 1283.6 µm. Grinding of the samples had been performed to obtain d(0.9) of 1069.3 and 812.8 µm. Grinding operation was performed in a coffee grinder at 5 s intervals; after 5 s, the samples sticking to the grinder walls were mixed properly using a spatula before continuing the grinding. Approximately 30 g of wet sample was ground each time in the coffee grinder. Particle size distribution order of d(0.9)= 812.8 µm was obtained by increasing grinding time as compared with d(0.9)= 1069.3 µm. After finishing the grinding operation each set of samples was mixed well using a laboratory mixer. The blended samples were stored in separate airtight bags in the freezer and appropriate amount of samples were thawed at room temperature before experiments. In this section, experiments were conducted only for PSD of d(0.9)=1069.3 and 812.8 µm; for d(0.9)=

1283.6 µm, the corresponding values were taken from the previous experiment, WDG with 0% solubles (Section 3.7).

3.8.3 Densification of WDG compacts of different particle size distribution

Samples of various particle size distributions (d(0.9)=1069.3 and 812.8 µm) were compacted using the apparatus and method described in section 3.7.1. Before the compaction of WDG, its moisture content was reduced from 69 to 51% wb by drying it in a convection oven at 135°C air temperature.

Depending on particle size, the compact produced had a height of ~ 4-7 mm**,** moisture content of 50% wb and density of 833.3 to 873 kg/m^3. The difference in moisture content between the sample and the compact (1% wb) was due to expression of water from the biomass during the compaction process. Approximately similar loss in moisture was recorded for the other two samples, d(0.9)= 1069.3 µm and d(0.9)= 812.8 µm, tested. Moisture content determination procedure was described in section 3.5.3.

3.8.4 Moisture change determination

Procedure for mass measurements of WDG compacts, for determining the time taken to reach moisture levels of 40, 30 and 20% wb in SS at 150°C is described in section 3.7.2. The time taken to reach moisture levels of 40, 30 and 20% wb were 3-5, 7-9 and 11-13 min, respectively.

3.8.5 Superheated steam drying and stress-relaxation test for WDG compacts

Experiments were carried out at one SS temperature of 150°C and steam velocity of 0.9 m/s. Drying in SS was carried out until compacts reached their final moisture of 40, 30 and 20% wb. The SS drying procedure was described in section 3.7.2. The description of SS velocity measurements was given in section 3.3. After attaining specific moisture levels, the compacts were removed from the SS dryer and their mass and dimensions were measured. Percentage change in volume of the WDG compact over the course of SS drying was calculated from the generalized Eq. 3.1 described in section 3.6.5.

Next, the compact was exposed to a 40% deformation in a parallel compression tests. The procedure for conducting stress-relaxation test and for determining hardness is described in section 3.7.4. As noted in section 3.7.2, compacts dried to 10% wb moisture were brittle; therefore, stress-relaxation experiments were conducted with compacts of moisture higher than 20% wb.

4. ANALYZES OF DATA

The material presented in this chapter is the modified reproduction of work published by Johnson et al. (2011 a,b; 2013 a,b; 2014 a,b,c) under the realm of this thesis**.** This chapter provides the detailed data analysis techniques of the experimental data obtained.

4.1 Jones model

Experiments described in section 3.5 (Preparation of single compacts from DSG and measurements of their stress-relaxation characteristics) were analyzed using Jones model. Jones (1960) expressed the density-pressure data of compacted powder in the form of Eq. 4.1.

$$\ln(\rho) = m \ln(P) + b \qquad (4.1)$$

where ρ is the bulk density of the compact powder mixture, kg/m^3, P is the applied compressive pressure, MPa; m and b are model constants that are determined from the slope and intercept, respectively, of the extrapolated linear region of the plot of $\ln(\rho)$ vs. $\ln(P)$ (Adapa, 2011; Adapa et al., 2009). The constant m can provide valuable information about the onset of plastic deformation of the ground biomass samples. York and Pilpel (1973) have shown the constant m to be equal to the reciprocal of the mean yield pressure required to induce plastic deformation.

4.2 Stress-relaxation analysis

The stress-relaxation data obtained from the compaction experiments were analyzed by the method given by Peleg (1980) for powdered materials (Peleg, 1979;

Peleg and Moreyra, 1979). The experimental stress-relaxation curve, as recorded by the Instron testing machine was normalized using Eq. 4.2.

$$Y(t) = \frac{\sigma_0 - \sigma_t}{\sigma_0} \qquad (4.2)$$

where $Y(t)$ represents the decay of the stress and is called the decaying parameter. σ_t is the stress at any time t, σ_0 is the initial stress, t is compression holding time**.** The characteristic shape of the function $Y(t)$ vs. t suggests the simplified mathematical form given by Mickley et al. (1957).

$$Y(t) = \frac{t}{k_1 + k_2\, t} \qquad (4.3)$$

where k_1 and k_2 are the empirical constants (Bhattacharya, 2010). The linear form of Eq. 4.3 can be represented by Eq. 4.4. Linear form simplifies the verification of the appropriateness of the formula and calculation of its constants. Peleg and Pollak (1982) stated that besides the mathematical simplicity of Eq. 4.4, its applicability can be verified by testing the fit of data into a linear relationship.

$$\frac{t}{Y(t)} = k_1 + k_2\, t \qquad (4.4)$$

The constants k_1 and k_2 are independent of the test duration and calculation procedure. The reciprocal of k_1 represents the initial decay rate; hence small values of the line intercepts indicate fast relaxation at initial stages. The slope of the straight line,

k_2, is called the solidity index of the material and it can be considered as an index of how "solid" the compacted specimen is on a short time scale.

When time t tends to infinity, the reciprocal of k_2 reaches the asymptotic level of $Y(t) = Y(\infty)$. Since the equilibrium conditions of biological materials are difficult to determine, $1/k_2$ can be used as the representative of the equilibrium condition. The value of $1/k_2$ becomes zero for ideal elastic solids and one for ideal liquids. Therefore, $0 < 1/k_2 < 1$ represents the asymptotic residual values of $Y(\infty)$. Hence, $\sigma_0(1\text{-}1/k_2)$ represents the portion of the stress that would have remained unrelaxed at equilibrium. Therefore, when long term experiments become theoretically difficult, the asymptotic value can be used to calculate a residual modulus that is representative of the short term rheological characteristics. The residual (unrelaxed) modulus is given by Eq. 4.5.

$$E_A = \frac{\sigma_0}{\varepsilon}\left(1 - \frac{1}{k_2}\right) \qquad (4.5)$$

where E_A is the asymptotic modulus (MPa) and ε is the strain (dimensionless). Asymptotic modulus is an indication of an empirical index of solidity of the compacts; the higher the value of E_A, the more solid the compact is (Mani et al., 2006).

The asymptotic modulus for the study described in section 3.5 (Preparation of single compacts from DSG and measurements of their stress-relaxation characteristics) was calculated using Eq. 4.5. But for the studies mentioned in section 3.7 and section 3.8, E_A of the compact was calculated using the modified Eq. 4.6.

$$E_A = \frac{\sigma_{0(t)}}{\varepsilon_{H(t)}} \times \left(1 - \frac{1}{k_2}\right) \qquad (4.6)$$

where E_A is the asymptotic modulus (MPa), $\varepsilon_{H(t)}$ is the true strain (dimensionless) and $\sigma_{0(t)}$ is the true stress (initial).

Since the cross-sectional area of the specimen is expanded considerably during the compression process, it cannot be approximated by the original area of the sample. Hence the use of true stress ($\sigma_{(t)}$) Eq. 4.7 and true strain (also called Hencky's strain) Eq. 4.8 is appropriate for large deformations encountered in food applications (Calzada and Peleg, 1978; Peleg, 1987; Mammarella et al., 2002; Pons and Fiszman, 1996).

$$\sigma_{(t)} = \frac{F_{(t)}\,(H_0 - \Delta H_{(t)})}{A_0 H_0} \qquad (4.7)$$

$$\varepsilon_{H(t)} = \ln \frac{H_0}{H_0 - \Delta H_{(t)}} \qquad (4.8)$$

where $F_{(t)}$ is the force (N) at time t, H_0 is the initial specimen length (mm), $\Delta H_{(t)}$ is the actual absolute deformation that is determined during the test and A_0 is the cross-sectional area (mm^2) of the original specimen.

4.3 Stress analysis for diametral compression

The diametral compression test and measurements of crushing resistance were described in section 3.6.6. The analysis of the data was done as follows. A schematic diagram showing the arrangement of compression plates with respect to the sample in the diametral compression test is given in Fig 4.1(a). The direction of a compressive, tensile and shear stress in the uniaxial diametral compression is shown in Fig. 4.1(b).

Since σ_y is parallel to the direction of the applied load on the diameter of the disk, it is the compressive stress, whereas σ_x is the tensile stress. The value of the compressive stress is at its minimum at the center of the load diameter and infinitely high immediately under the load points. Since the shear stress τ_{xy} is zero along the diameter plane, σ_x and σ_y are the principal stresses on the plane.

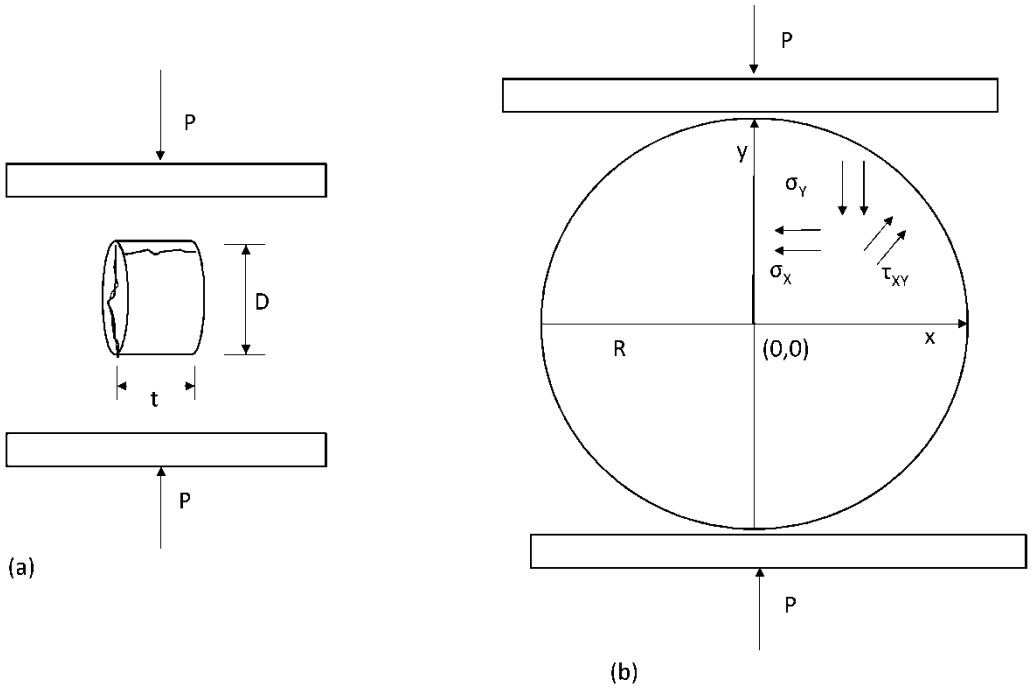

FIG. 4.1. (a) Uni-axial diametral compression testing of the compact and (b) stress distribution of the compact during a diametral compression testing (where, P is the applied load, R is the radius of the disc, σ_x and σ_y are normal stresses in the directions perpendicular and parallel, respectively, to the loaded diameter, and τ_{xy} is the shear stress).

A theoretical basis for the stress analysis of a cylindrical disc has been proposed by Timoshenko and Goodier (1970) and by Frocht (1947). Frocht (1947) showed that the tensile stress (σ_x) on a disc in the x direction for x between 0 and the disk radius R can be calculated by using the general equation:

$$\sigma_x = \frac{2P}{\pi D t} - \frac{2P}{\pi t}\left\{\frac{x^2(R-y)}{\left[x^2+(R-y)^2\right]^2} + \frac{x^2(R+y)}{\left[x^2+(R+y)^2\right]^2}\right\} \qquad (4.9)$$

where σ_x is the normal stress in the direction perpendicular to the loaded diameter, P is the applied load, D is the diameter of the disc, R is the radius of the disc, t is the thickness of the disc and x, y are intercepts. Eq. 4.9 shows that along the loaded diameter (x = 0), the normal stress (σ_x) is tensile and constant over the entire load diameter and is given by:

$$\sigma_x = \frac{2P}{\pi D t} \qquad (4.10)$$

The above equation was derived based on the assumption of a point load on a thin disc along the axis (Hertz, 1895). But in the actual case the load is distributed over a finite area. Hence, the above equations must be modified to accommodate the finite load distribution (Fahad, 1996). Hondros (1959) modified the equation to include distributed loading conditions. However, the analysis done by both Hertz and Hondros converge to Eq. 4.10 at $x = y = 0$ (Fahad, 1996; Procopio, 2003). For the current study, tensile strength of the compacts was calculated using Eq. 4.10.

4.4 Stepwise regression method

The stepwise forward regression method was used to find suitable explanatory variables for predicting the E_A of the compact for the study mentioned in section 3.7 and 3.8. Stepwise regression method is mainly applicable when the independent

variables contributing to the prediction of the dependent variables are unknown. In this method, the most suitable independent variables for the model are selected by the repeated addition or removal of the independent variables from the equation using the variable picking algorithm. Thus stepwise regression method avoids using extraneous variables or under specifying or over specifying the model as compared with regular multiple linear regression models. The governing equation for stepwise regression method is shown in Eq. (4.11).

$$y = \sum_{i=1}^{i=k} c_i x_i + c_0 \qquad (4.11)$$

where y is the dependent variable, x_i is the independent variable (known or predicted variable), and c_0, c_i are the regression coefficients. As the value of c_i varies, the corresponding value for y either increases or decreases depending on the sign of c_i.

Though there are two methods for the stepwise regression analysis, i.e., forward stepwise regression and backward stepwise regression, forward stepwise regression technique has been used for the present study. In the forward stepwise regression method, the independent variable which has an F value higher than a specified F-to-enter and which produces the best prediction of the dependent variable is entered into the model first, subsequently followed by the most suitable independent variable next and so on. After entering each variable, the F value of each variable already entered into the model is checked, and any variables with small F values, i.e. below a specified F-to-remove value, are removed. This process of adding and removing variables is continued until the adding or removing variables into the model does not significantly boost the prediction of the dependent variable (SigmaStat 3.5, 2006).

After determining suitable variables, multiple linear regression method was used for developing the regression equations. The developed equation was evaluated using the coefficient of determination (R^2) (Eq. 4.12) and the adjusted coefficient of determination ($\underline{R^2}$) values (Eq. 4.13).

$$R^2 = 1 - \frac{SSE}{SST} \qquad (4.12)$$

$$\underline{R^2} = 1 - \left(\frac{SSE}{n-k-1} \div \frac{SST}{n-1}\right) \qquad (4.13)$$

where n represents the sample size and k is the number of independent variables in the model. $SSE = \sum(y_i - y_{predicted})^2$ denotes the sum of squares of deviations of observed data (y_i) from the fitted regression line. Total sum of squares (SST), $SST = \sum(y_i - y_{mean})^2$ represents the sum of squares of the difference between observed data (y_i) and the mean (y_{mean}) of y_i.

The major drawback with R^2 is that it cannot represent the true explanatory power of the regression model as more variables are added to the regression equation. The $\underline{R^2}$ modifies the R^2 by taking into account the number of variables that are included in the model. Thus, $\underline{R^2}$ is related to the number of variables and the number of observations.

4.5 Evaluation of the prediction model

Holdout method of cross-validation was used for the evaluation of the models developed using the stepwise forward regression and multiple linear regression methods. In this method, a subset of the total data set was used for developing the

model and the remaining data was used for testing the performance of the model. In the current study, 70% of the data was used for developing the model and the remaining 30% was used for the validation. This method has an advantage over the residual evaluation techniques, as those techniques do not give an indication of how well the model performs when it is asked to make new predictions for the data they have not already seen. In the present study, for the evaluation of the prediction models mean absolute percentage error (MAPE) (Eq. 4.14) and R^2 (Eq. 4.15) were used.

$$\text{MAPE} = \frac{1}{n}\sum_{i=1}^{n}\frac{|X_p - X_m|}{X_m} \times 100 \qquad (4.14)$$

where X_p is the predicted value, X_m is the measured value, and n is the data number. The results of the MAPE examinations can be classified into four types, which are excellent (MAPE<10), good (MAPE = 10–20), acceptable (MAPE = 20–50), and unacceptable (MAPE>50) (Chang et al., 2007).

Regression model developed for predicting the E_A of the compact for the study mentioned in section 3.7 was evaluated using MAPE and R^2 values. Whereas the model developed for predicting the E_A of the compact for the study mentioned in section 3.8 was evaluated using the R^2 value.

4.6 Particle size distribution analysis

The Mastersizer (described in section 3.8.1) uses the volume of a particle to measure its size and hence the results are volume based. Mie theory assumes that the particles present in the sample are perfect spheres (Torres et al., 2010; Mingard, 2009). Since biomass particles are irregular shaped ones, expressing the particle dimensions in

terms of an imaginary spherical particle provides a single unique number for describing the particles. This method is known as “equivalent spheres”. The parameters used for representing PSD in the current study are described below.

(ii) Span: The span is the most common format to quantify the width of a distribution. The wider the distribution, the larger the span becomes. The span is calculated as:

$$\text{Span} = \frac{d(0.9)-d(0.1)}{d(0.5)} \qquad (4.15)$$

where d(0.1) and d(0.9) are the size of particle below which 10% and 90% of the sample lies, respectively. The d(0.5) is the median for a volume distribution, it is the size at which 50% of the sample is smaller and 50% is larger; d(0.5) is also known as the mass median diameter (MMD).

(ii) Volume mean diameter/ DeBroukere mean: Volume mean diameter D[4,3] is the diameter of the average volume of a particle obtained by dividing the total volume of the sample by the number of particles in the sample (McCabe et al. 1993; Singh et al., 2006). The volume mean diameter (Mingard, 2009) is calculated by the equation:

$$D[4,3] = \frac{\sum_{i=1}^{n} D_i^{\,4}}{\sum_{i=1}^{n} D_i^{\,3}} \qquad (4.16)$$

where D_i is the diameter of the i^{th} particle.

(iii) Surface area mean diameter/ Sauter mean: The surface area mean diameter D[3,2] is obtained by dividing the total volume of the sample by the total surface area of all the particles in the sample. Surface area mean diameter is calculated using the equation:

$$D[3,2] = \frac{\sum_{i=1}^{n} D_i^3}{\sum_{i=1}^{n} D_i^2} \qquad (4.17)$$

(iv) Uniformity and specific surface area: The uniformity of the sample is a measure of the absolute deviation from the median (d(0.5)). The specific surface area is defined as the ratio between total surface area of the particles to its total mass. It is calculated by assuming that the particles are both non-porous and spherical. Specific surface area is important to evaluate the surface activity, adsorption capacity and the extent of particle-to-particle bonding in the compacts.

4.7 Statistical analysis

For the section 3.4 (Processing WDG in bulk under different drying conditions and with different concentration of solubles), experiments for determining bulk density and angle of repose (AOR) were repeated 10 times and average values were used for the data analysis. For the section 3.5 (Preparation of single compacts from DSG and measurements of their stress-relaxation characteristics), a completely randomized design was chosen for the study with three factors: compressive pressure (60.3, 90.5, 120.6 and 135.7 MPa), initial moisture content (15, 20 and 25% wb), and soluble content (15 and 30%). All experiments were conducted in triplicate. The WDG sample with 25% moisture content was chosen as reference.

For all sections, excluding section 3.4, each experiment was conducted in triplicate. For all experiments, statistical significance of the data obtained during the study was determined at $P \leq 0.05$. The significance level of each factor was tested separately using one way analysis of variance (ANOVA). All statistical analysis and

regression modeling were carried out using the software package Sigma Stat 3.5 (Systat Software Inc., Chicago, IL).

5. RESULTS AND DISCUSSION

5.1 Processing WDG in bulk under different drying conditions and with different concentration of solubles

The material presented in this chapter is the modified reproduction of work published by Johnson et al. (2011a) under the realm of this thesis.

5.1.1 Influence of particle sizes on bulk density of DSG

The experimental results of the effect of DSG particle size processed with three different treatments on bulk density of DSG are given in Table 5.1 (methodology for finding bulk density is given in section 3.4.2). Four different particle sizes: 300, 425, 600 and 850 μm were chosen for the analysis. All fractions were maintained at the same moisture content through the entire set of experiments. Increasing the particle size in samples caused a significant ($P \leq 0.05$) increase in their bulk density. This is opposite to what normally is observed for ground samples (Lam et al., 2008). In this experiment the large particles were associated with higher concentration of fiber and lignin which have higher molecular weight and thus increase the bulk density of the samples.

5.1.2 Effect of different drying methods on bulk density

Statistical analysis showed that for the corresponding particle sizes, the bulk densities of WDG dried at 45°C and 150°C in hot air, and SS were significantly different (($P \leq 0.05$) (Table 5.1).This gives a clear indication of the dependency of bulk density on the type of drying technique employed. For SS dried samples, the bulk density was lower when compared with 150°C air drying. This was caused by the

increase in porosity of the material as affected by SS. There was no difference in bulk density between SS dried samples and samples dried at 45°C except for 850 µm particle size. Earlier studies indicate that the porosity of granular material increased during SS drying, as higher SS temperature produced samples with a large number of bigger-sized pores (Ezhil, 2010). This led to less shrinkage and an increased volume of the SS dried material. Also, it was observed that samples dried using air at 150°C had higher bulk density compared with samples dried at 45°C.

Table 5.1. Variation of bulk density with particle size for thin-layer drying at low-air temperature of 45°C, high-air temperature at 150°C and superheated steam drying at150°C. The values of significant differences of the mean values are provided in Appendix B.16.

Particle size (µm)	Bulk Density (g/cm^3)		
	Thin-layer low-temperature drying at 45°C	Thin-layer high-temperature drying at 150°C	Superheated steam drying
300	0.379 (0.003)	0.392 (0.003)	0.379 (0.007)
425	0.386 (0.004)	0.417 (0.004)	0.397 (0.002)
600	0.387 (0.004)	0.433 (0.002)	0.384 (0.004)
850	0.397 (0.002)	0.435 (0.003)	0.384 (0.004)

Values in parenthesis indicate standard deviations (n= 10).

5.1.3 Influence of CDS addition on bulk density of SS dried DSG

This study was done to analyze the effect of SS drying on bulk density of samples containing different percentages of CDS addition, i.e., 10, 20 and 30%. The results are given in Table 5.2. A statistically significant difference ($P \leq 0.05$) in the bulk density was observed among various concentrations of CDS. For each particle sizes

(except for 425 µm), an increase in concentration of CDS from 0 to 30% caused an increase in bulk density (Table 5.2).

For higher concentration of CDS, dried DSG particles became harder and therefore, required more force to separate the agglomerated particles while crushing (however, the force needed was not measured experimentally). The CDS fractions adhered strongly to the DSG particles and acted as a binding agent leading to an increase in bulk density. It was observed that the color of DSG became darker with the increase in addition of CDS.

Table 5.2. Variation of bulk density as affected by the addition of the condensed distiller's solubles (CDS). The values of significant differences of the mean values are provided in Appendix B.17.

Particle Size	Bulk Density (g/cm^3)		
(µm)	10%CDS	20%CDS	30%CDS
300	0.391 (0.004)	0.393 (0.004)	0.425 (0.002)
425	0.395 (0.003)	0.403 (0.004)	0.437 (0.005)
600	0.410 (0.005)	0.412 (0.006)	0.444 (0.007)
850	0.413 (0.006)	0.423 (0.005)	0.421 (0.004)

Values in parenthesis indicate standard deviations (n= 10).

The bulk density values obtained from this study concur with the results obtained by other researchers for similar studies involving different treatment methods. Studies done by Rosentrater (2006b) showed that the bulk density of DDGS produced at six ethanol plants in South Dakota ranged from 0.391 to 0.496 g/cm^3. In another study Bhadra et al. (2009) found ranges of 0.490 to 0.590 $g/cm^3$for DDGS obtained from five plants in South Dakota. Bulk density ranged from 0.365 to 0.561 g/cm^3 in a study

conducted using DDGS obtained from 69 sources (US Grains Council, 2008). Clementson and Ileleji (2010) conducted a study by varying soluble content and found that the bulk density values varied from 0.421 to 0.458 g/cm^3.

5.1.4 Angle of repose

Angle of repose values were measured for three different particle sizes, i.e., 300, 425 and 850 µm, obtained from the three drying techniques (Table 5.3) using the methodology described in section 3.4.2**.** Statistical analyzes of the results indicate that the AOR values were significantly different ($P \leq 0.05$) for different particle sizes. In the majority of cases, the AOR values decreased with an increase in particle size. This is due to the fact that smaller particles have more cohesive and adhesive forces compared with bigger particles; also, for bigger particles gravity plays a dominant role in controlling their flow. There was no statistically significant difference ($P \leq 0.05$) found among AOR values for different treatments. This indicates that, the drying methods or treatments do not have a significant influence over AOR. As per Ileleji and Zhou (2008), AOR values less than 30° are considered as free flowing material, between 30° and 35° as good flowing material, above 35 to 40° as fair flowing, greater than 40 to 50° as poor flowing and greater than 50° as very poor flowing material. The range of AOR values for spent grain from this study indicate that DSG falls mainly under poor flowing category (46-51°).

Table 5.3. Variation of angle of repose with particle size for thin-layer drying at low-air temperature of 45°C, high-air temperature at 150°C and superheated steam drying at150°C. The values of significant differences of the mean values are provided in Appendix B.18.

Particle Size (µm)	Angle of Repose (°)		
	Thin-layer low-temperature drying at 45°C	Thin-layer high-temperature drying at 150°C	Superheated steam drying
300	50.4 (1.7)	49.4 (2.0)	50.0 (2.3)
425	47.1 (1.8)	46.9 (1.9)	47.2 (2.5)
850	46.7 (1.8)	46.0 (2.3)	47.2 (2.1)

Values in parenthesis indicate standard deviations (n= 10).

Among different CDS concentrations from 0 to 30% the AOR values ranged between 46–51°, but there was no statistically significant difference ($P \leq 0.05$) observed in AOR values for different percentages of CDS addition (Table 5.4). Only for 850 µm, the particles showed a statistically significant difference ($P \leq 0.05$) of AOR values among different soluble concentrations.

Table 5.4. Variation of angle of repose as affected by different concentrations of condensed distiller's solubles (CDS). The values of significant differences of the mean values are provided in Appendix B.19.

Particle Size (µm)	Angle of Repose (°)		
	10% CDS	20% CDS	30% CDS
300	49.5 (2.0)	49.8 (1.6)	48.9 (2.4)
425	47.9 (1.7)	47.2 (2.4)	48.0 (2.4)
850	46.5 (2.0)	47.7 (1.8)	46.7 (2.2)

Values in parenthesis indicate standard deviations (n= 10).

5.2 Preparation of single compacts from DSG and measurements of their stress-relaxation characteristics

The material presented in this chapter is the modified reproduction of work published by Johnson et al. (2013b) under the realm of this thesis.

5.2.1 Compression test and compact density

The influence of compressive pressure, moisture content and soluble content on compact density is shown in Figs. 5.1 and 5.2. The methodology for this section is described in section 3.5.1 and section 3.5.3. Statistical analysis showed that the density of compacts increased significantly ($P \leq 0.05$) with the increase of compressive pressure for all treatments. During the compaction process, rearrangement, sliding and stacking of the particles takes place under low pressure to closely pack the raw material. With the increase in compression pressure, elastic and plastic deformation of particles occurs to form strong solid bridges between the particles; this results in higher density and strength of the produced compacts. Hence, high compaction pressures resulted in reduced porosity and increased compact density. Sastry and Fuerstenau (1973) reported that higher compaction pressures resulted in the development of bonding forces such as van der Waal forces providing higher strength to the compacts.

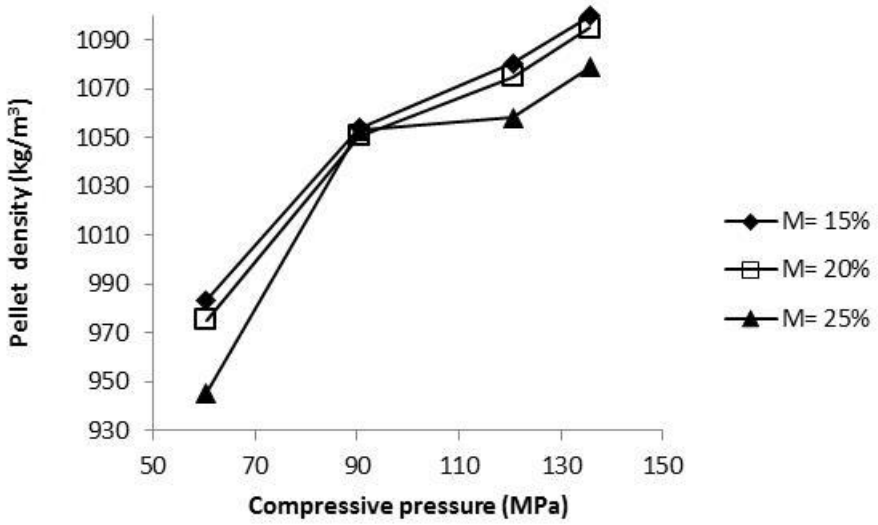

FIG. 5.1. Compact density of wet distiller's spent grain as affected by compressive pressure and initial moisture content (M- initial moisture content, % wb). Values of standard deviation corresponding to each data point in this figure are provided in Appendix B.2.

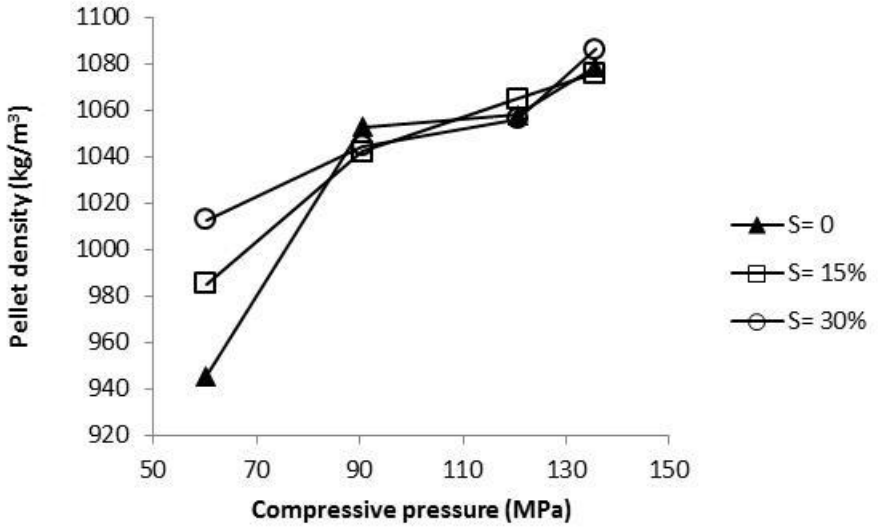

FIG. 5.2. Compact density of wet distiller's spent grain as affected by compressive pressure for samples with and without solubles (initial moisture content of samples is 25% wb; S- soluble content). Values of standard deviation corresponding to each data point in this figure are provided in Appendix B.2.

The major factors which affect the densification of a biomass sample are: its nutrient composition, feed moisture content, compaction pressure, materials used as particle-binders, feed particle size and densification equipment variables (Turner, 1995). Particle size of the feed material is a key factor in determining the compacts' durability. Generally, tiny particles absorb more moisture and heat when compared with larger particles and undergo a higher degree of conditioning (Kaliyan and Morey, 2009). The major issue involved in using small particle sizes in feed industries is the high cost involved in grinding. A mixture of different size particles give pellets maximum strength, as they form the inter-particle bonding with nearly no inter-particle spaces (Payne, 1978; Grover and Mishra, 1996). Nutritional components such as proteins normally denature in the presence of heat and act as a binder during the compaction process (Thomas et al., 1998). Water-soluble fibers increase the viscosity of the feed whereby positively affecting the durability of compacts. But water-insoluble fibers may negatively affect the durability of the densified products. However, due to their resilience characteristics, fibers may not provide good bonding between the particles (Thomas et al., 1998).

Figure 5.1 shows a negative relationship between moisture content and compact density. Though the difference obtained was statistically significant ($P \leq 0.05$) only for 60.6 MPa, a decreasing trend for compact density with increasing moisture content was observed for other compaction pressures too. Increasing the moisture content of samples increases the number of water molecules occupying the void spaces that cannot be expelled during compaction. This, in turn, increases the volume of the compacted mass and at the same time decreases its density.

Compacts of different soluble contents showed differences in compact density which were statistically significant ($P \leq 0.05$) only for the lowest compaction of 60.6 MPa. Compact density increased with an increase in soluble levels (Fig. 5.2) at 60.6 MPa. This may be due to the fact that solubles have smaller particle size and they can effectively occupy the inter-particle void spaces. Previous studies reported by Tabil et al. (2011) showed that compacts with smaller particle sizes have higher density than compacts with larger particle sizes. However, for other compaction pressures this trend was not observed and the differences in the resultant compact density were not statistically significant ($P \leq 0.05$).

The values obtained during temperature measurements of the compacts showed that during compaction the temperature of the compact in the geometrical center increased only up to 4°C. Such a small increase was a result of the slow compaction rate and the cooling effect that decreased frictional heating.

5.2.2 Moisture content of distiller's spent grain compacts

The moisture present in the sample acts as a facilitator for natural binding agents as well as a lubricant. Optimum moisture content is an essential factor for producing high quality compacts. This study showed that samples with higher moisture contents (>25% wb) plugged the compaction unit due to the adhesive forces developed between the sample and the metallic surfaces. An oven-drying temperature of 135°C was chosen to reduce the initial moisture content of the sample. This was based on the studies done by Tang et al. (2005) who demonstrated that in a SS dryer increasing the drying temperature from 110 to 180°C had only a small effect on the change of the nutrients in

spent grain samples. Figure 5.3 and 5.4 show the experimental results of moisture changes in the DSG compacts as a result of the compression level for different initial moisture content of samples and the amount of solubles.

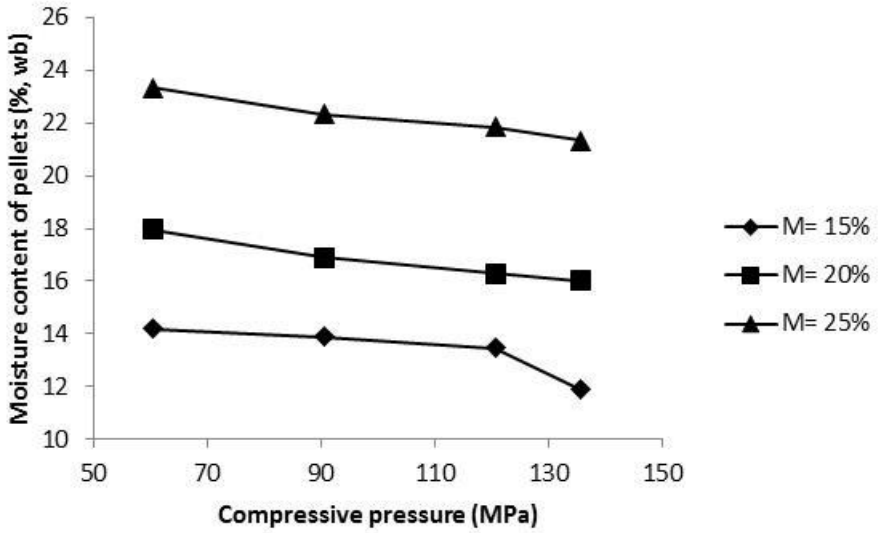

FIG. 5.3. Moisture content of wet distiller's spent grain compacts with different levels of compaction and initial moisture content (M- initial moisture content, % wb). Values of standard deviation corresponding to each data point in this figure are provided in Appendix B.3.

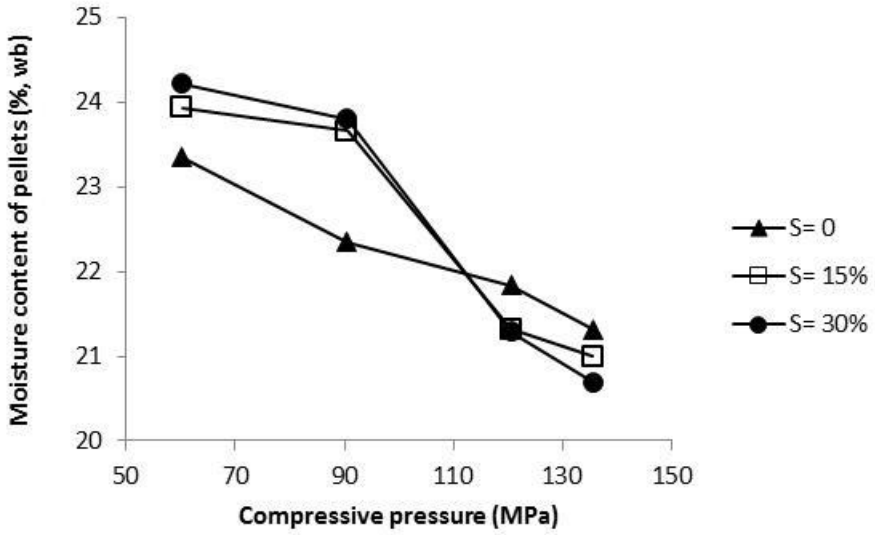

FIG. 5.4. Moisture content of distiller's spent grain compacts as affected by compressive pressure for samples with and without solubles (initial moisture content of samples is 25% wb; S- soluble content). Values of standard deviation corresponding to each data point in this figure are provided in Appendix B.3.

It is evident that there was a difference in moisture content between the initial sample and the compact obtained. Increasing the compressive pressure from 60.3 to 135.7 MPa reduced the moisture after compaction by 1 to 4% wb. The reduction in moisture content was caused by the expulsion of water from inter-particle pore spaces in the process of compaction.

5.2.3 Jones model

The methodology for the Jones model is described in section 4.1. Figure 5.5 shows the logarithmic plot between compressive pressure and compact density for DSG. In this graph the density-pressure data were connected with straight lines instead of showing a regression line for each treatment. However, the analysis of the

relationship between the compact density and compressive pressure was based on the regression line as per Eq. 4.1.

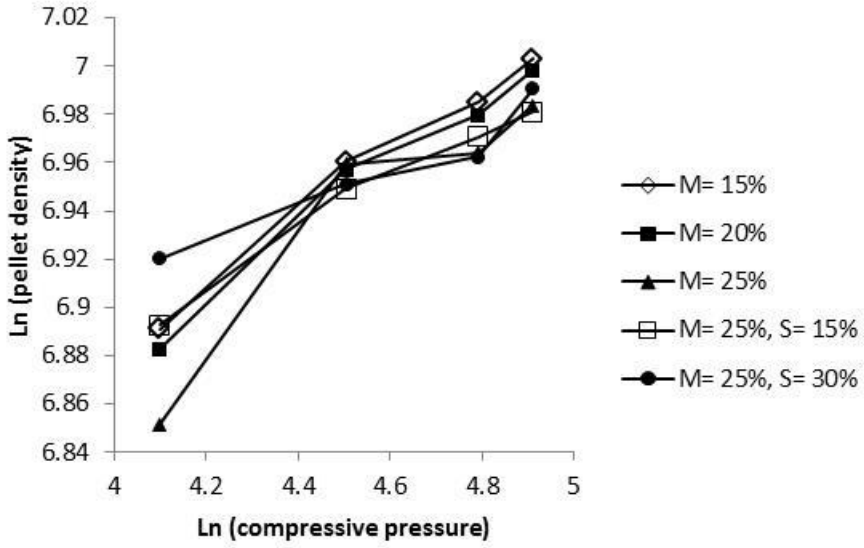

FIG. 5.5. Compact density as affected by compressive pressure in natural log coordinates for distiller's spent grain samples. The symbols S and M denote soluble content and moisture content, respectively.

The constants m and b determined from the slope and intercept of the logarithmic plot are shown in Table 5.5. A large m value (low yield pressure) indicates that the material is more compressible due to the onset of plastic deformation at a relatively low pressure. However, the relatively low compact density obtained at the lowest compressive pressure may have influenced the constants obtained from this study. The results indicate that the increase in compressibility (an increase in coefficient m) with the increase in initial moisture was not statistically significant ($P \leq 0.05$). Weir (1952) reported that compressibility increases markedly for natural polymers having high moisture compared with low moisture polymer, which may be due to the fact that

water exists in hydrogen bonded form at low moisture and as free liquid at high moisture contents.

This study showed that addition of solubles adversely affects the compressibility of samples. A statistically significant decrease ($P \leq 0.05$) in compressibility was observed when the soluble content increased from 0 to 30%. While reducing the moisture content of the DSG samples by oven drying, it was observed that the spent grain particles agglomerated and hardened with the addition of solubles. This hardening may in turn reduce the compressibility of the samples. A statistically significant difference ($P \leq 0.05$) between b values was observed between samples with 30% solubles in comparison to 0% solubles. But for different moisture contents, the b values obtained were not significant ($P \leq 0.05$).

5.2.4 Stress-relaxation analysis and residual modulus

Methodology for stress-relaxation test and analysis is provided in section 3.5.2 and section 4.2, respectively. A typical stress-relaxation curve for the DSG samples is shown in Fig. 5.6. A plot of $\sigma_0 t/(\sigma_0 - \sigma_t)$ vs. time can also be used for testing the fit of a linear relationship (Fig. 5.7). Higher R^2 values (≥ 0.98) were obtained for all treatments when the relaxation data was linearized and presented as a linear function of time. The slope, k_2, ranged between 1.2 to 3.5 for DSG samples. A value of k_2 greater than unity is an indication of the existence of stresses that will eventually remain unrelaxed. Asymptotic modulus was calculated using the slope obtained from the linearized plots. The E_A values indicate the ability of the compressed powder to sustain unrelaxed stresses; the higher the value of E_A the more solid the compact is.

Table 5.5. Compression characteristics of distiller's spent grain samples using Jones Model. The table showing the values of significant differences of the means is provided in Appendix B.20. The symbols m and b are model constants.

Moisture content (%, wb)	Soluble content (%)	*m* (kg/N-m)	*b* (kg/m^3)
15	0	0.135	6.345
20	0	0.138	6.321
25	0	0.155	6.231
25	15	0.108	6.455
25	30	0.078	6.602

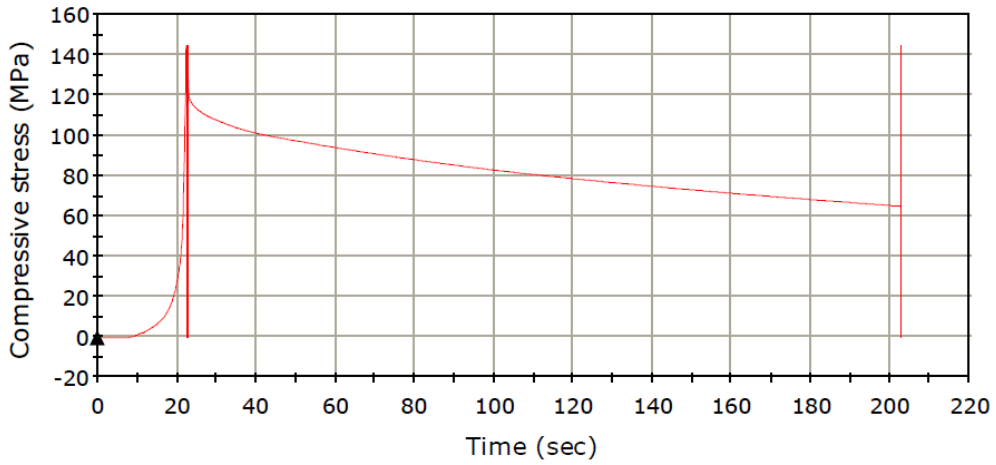

FIG. 5.6. A typical printout from the Instron machine of a stress-relaxation curve for a wet distiller's spent grain at 20% wb initial moisture content, 4000 N (120.6 MPa) compressive force and 180 s compression holding time.

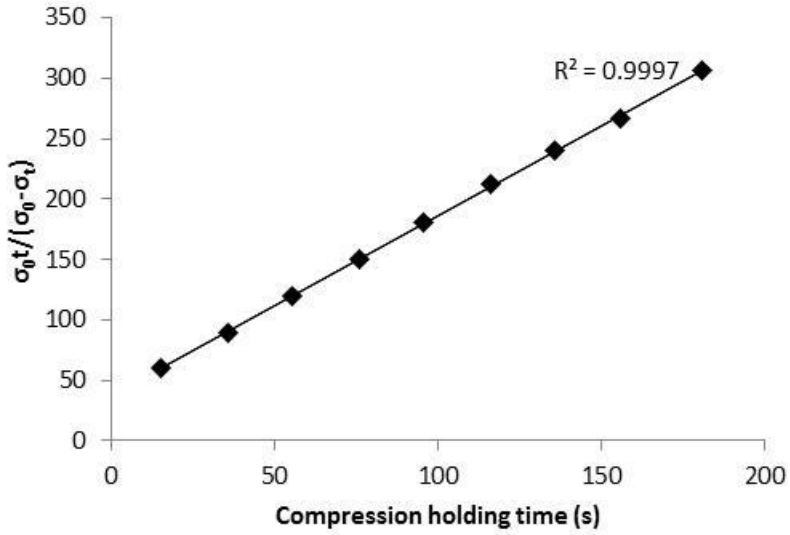

FIG. 5.7. Linearization curve for wet distiller's spent grain at 15% wb initial moisture content, 4500 N (135.7 MPa) compressive force and 180 s compression holding time.

Statistical analysis showed that an increase in compressive pressure from 60.3 to 135.7 MPa significantly increased ($P \leq 0.05$) E_A values for all treatments. Also, increasing the moisture content of samples significantly increased ($P \leq 0.05$) the E_A values; this may be due to the fact that moisture is acting as a binding agent providing more strength to the compacts (Fig. 5.8). Moreyra and Peleg (1980) reported that moisture content modified the stress-relaxation pattern of the compact product due to reorientation of liquid bridges and plasticity of the bed solid matrix. For compacts with different soluble levels, a statistically significant difference ($P \leq 0.05$) in the E_A values was obtained for compacts produced using 60.3, 90.5 and 135.7 MPa (Fig. 5.9).

Results showed that compacts produced using a WDG sample with moisture content of 25% wb, and compressive pressure of 135.7 MPa possessed the highest E_A value. Since E_A values are the indication of rigidity of the compacts, it can be interpreted that those compacts with the highest E_A value have the highest rigidity.

Moreover, results obtained from the study showed that asymptotic modulus can be used to characterize the DSG compacts affected by different compressive pressures and moisture contents. However, E_A was unable to be used to characterize DSG compacts based on soluble levels for specific compressive pressures. A specific relation was not observed for E_A values with respect to different soluble contents for specific compressive pressures. It is anticipated that the results obtained from this study will enable generation of new knowledge for the effective utilization of DSG. Though the study was done for single compacts, the results from the study can be utilized commercially for DSG products such as pellets, briquettes and wafers involving a compaction process.

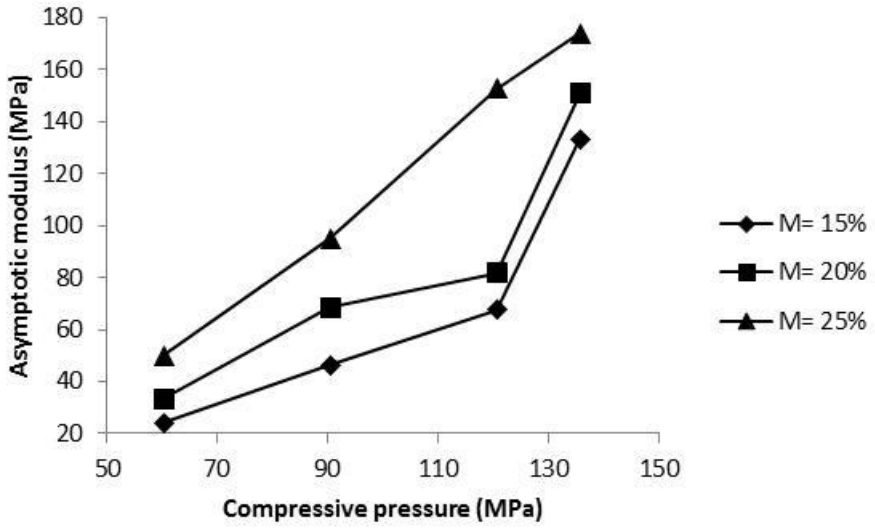

FIG. 5.8. The effect of compressive pressure on asymptotic modulus of wet distiller's spent grain for different levels of initial moisture content (M- initial moisture content, % wb). Values of standard deviation corresponding to each data point in this figure are provided in Appendix B.4.

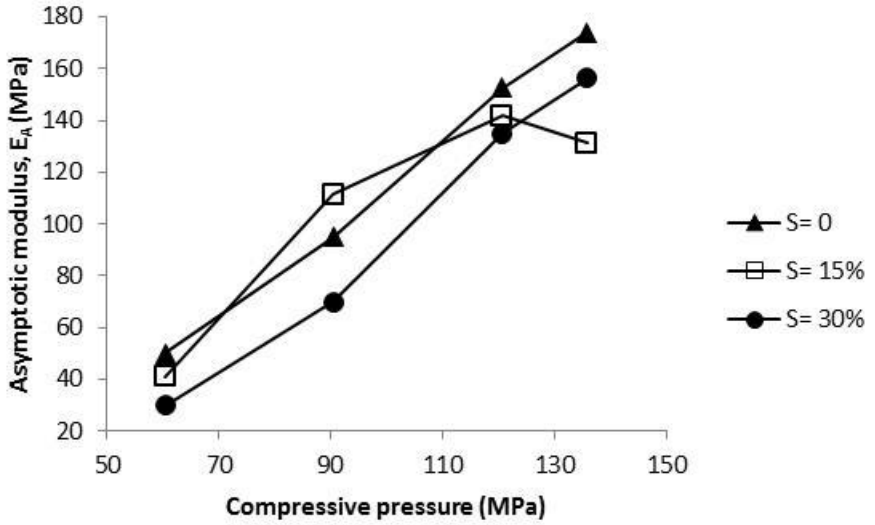

FIG. 5.9. The effect of compressive pressure on asymptotic modulus of distiller's spent grain with and without solubles (initial moisture content is 25% wb; S- soluble content). Values of standard deviation corresponding to each data point in this figure are provided in Appendix B.4.

5.3 Measurements of disintegration of WDG compacts as affected by drying in SS

The material presented in this chapter is the modified reproduction of work published by Johnson et al. (2013a; 2014b) under the realm of this thesis**.** Compact used for this study had approximately 10 mm length, 6.5 mm diameter, and 23% wb moisture content.

5.3.1 Mass change/ moisture content measurements

Methodology for mass and temperature change measurements are described in section 3.6.4. Moisture content of the compacts over drying time for different SS drying conditions is shown in Fig. 5.10. The first stage of drying is referred to as the warm-up period where the sample is heated to the saturation point and only condensation of water vapor is observed with quantities dependent on SS conditions (temperature and velocity) and the surface area of the compact. Condensation normally takes place when the material is at a lower temperature than the saturation temperature of steam (100°C at

atmospheric pressure). During that period, a 5 s exposure to 110 and 130°C shows an increase in mass of the compacts; since in current case the surface area of the compact was small (~2.9 cm^2), it took less than 120 s to evaporate the condensate from the sample surface. For 150°C the amount of initial condensate deposited was not measurable. This was because of the high SS temperature the amount of condensate deposited was too small and a quick evaporation of the condensate had occurred within 5 s which was the first measuring point. For 110ºC, there was a 5.2, 3.1 and 2.3% increase in moisture content after 5 s of SS exposure for 0.9, 1.1 and 1.4 m/s steam velocities, respectively; whereas, for 130ºC, there was a 3.4, 2 and 1.7% increase in moisture content for 0.9, 1.1 and 1.4 m/s steam velocities, respectively.

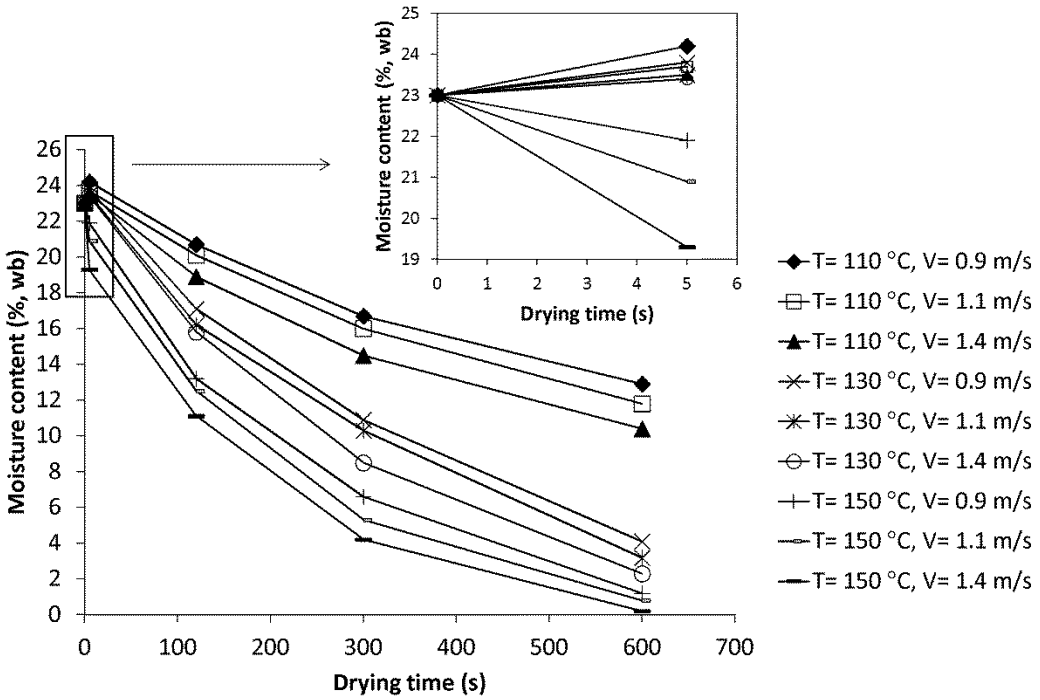

FIG. 5.10. Moisture content of wet distiller's spent grain compacts under different superheated steam processing conditions. The insert indicates moisture changes in the first 5 s of drying in superheated steam. Each data point is the average of three measurements (T denotes the temperature and V denotes the velocity of superheated steam).

5.3.2 Temperature measurements

Temperature changes of the compact with drying time are shown in Figs. 5.11 to 5.13. As mentioned earlier, initially a short warm-up period of few seconds was observed until the temperature of the product reached the saturation point of steam (100ºC at the atmospheric pressure). As observed from Figs. 5.11 to 5.13, the heat supplied by the SS during the warm-up period was used to bring the temperature of the compact from its ambient temperature to 100ºC.

This caused a decrease of temperature/energy of the SS followed by its condensation on the compact surface. The warm-up period was followed by the falling rate drying period. There was no constant rate drying period observed for any of the

drying conditions because of the low initial moisture content of the compact used for drying. The falling rate drying period occurs when the compact temperature increases above the saturation temperature of steam. Average temperature readings inside the compact showed that at SS temperature of 110ºC with velocities corresponding to 0.9 and 1.1 m/s, it took between 5 and 10 s to reach 100ºC; whereas, for all other drying conditions it took between 0 and 5 s for the compact to reach its 100°C temperature. After reaching the saturation temperature, the temperature of the compact increased gradually for all drying conditions. During the falling rate drying period, the heat supplied to the material was used only for removing the moisture stored in the material. This is in agreement with the study reported by Zielinska et al. (2009).

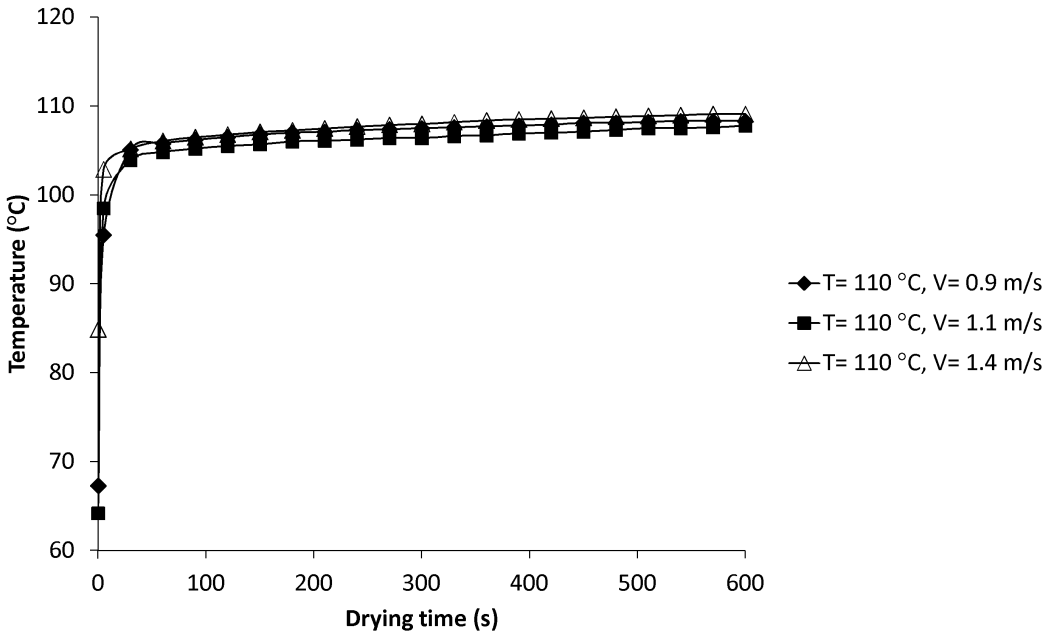

FIG. 5.11. Temperature changes of wet distiller's spent grain compacts as affected by drying time in superheated steam at temperature (T)=110°C and at 3 different superheated steam velocities, V. Each data point is the average of three measurements.

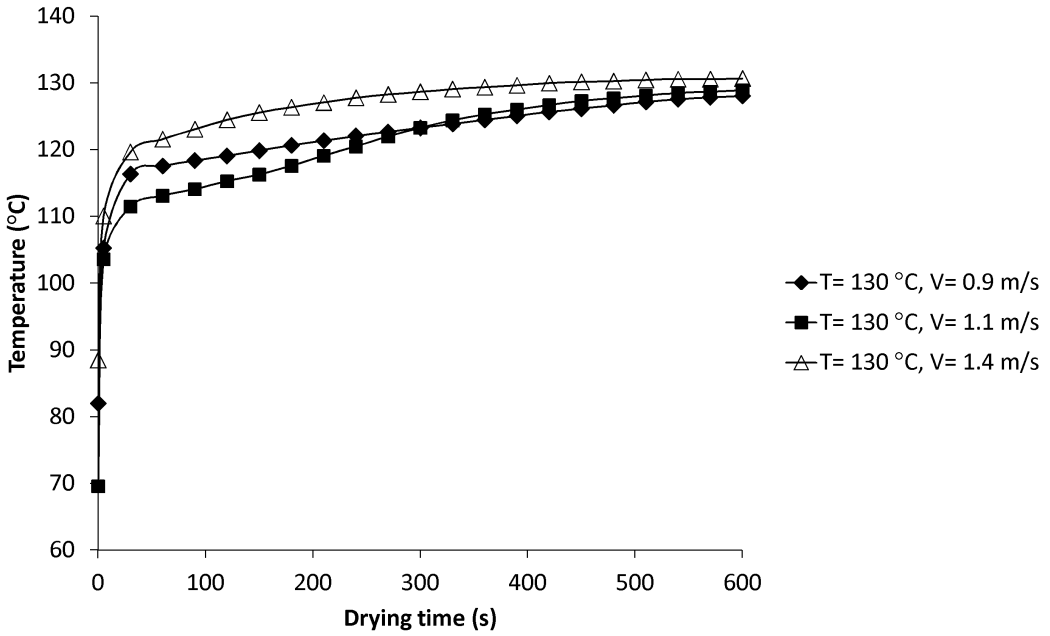

FIG. 5.12. Temperature changes of wet distiller's spent grain compacts as affected by drying time in superheated steam at temperature (T)=130°C and at 3 different superheated steam velocities, V. Each data point is the average of three measurements.

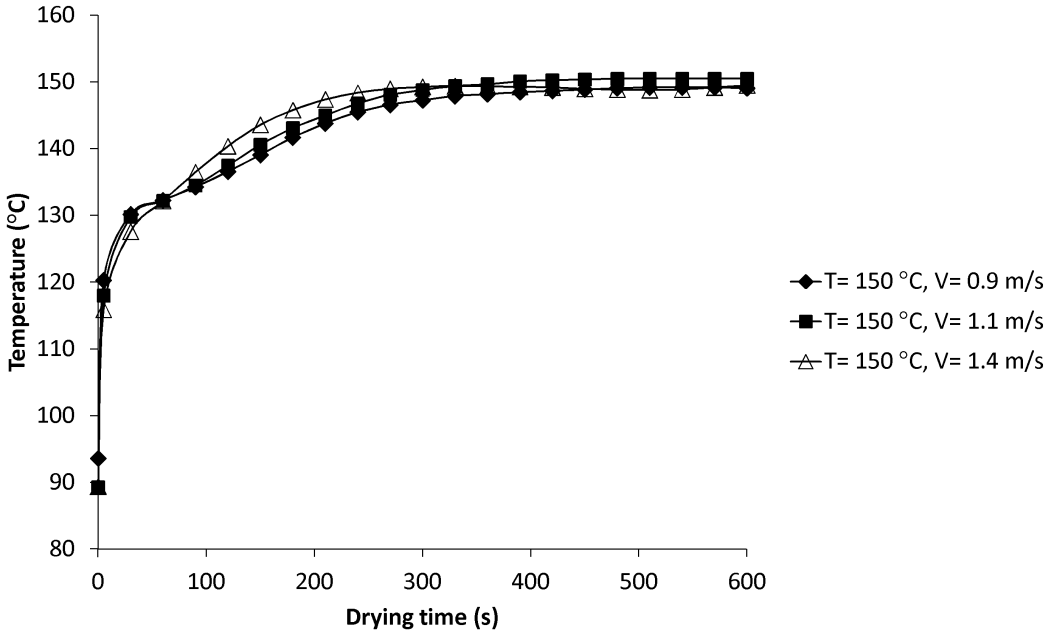

FIG. 5.13. Temperature changes of wet distiller's spent grain compacts as affected by drying time in superheated steam at temperature (T) =150°C and at 3 different superheated steam velocities, V. Each data point is the average of three measurements.

5.3.3 Percentage increase in volume

The results of the percentage increase in volume (Eq. 3.1) as a function of drying time for different drying conditions are shown in Figs. 5.14 to 5.16. The increase in volume was mainly due to the release of mechanical energy stored in the compact while drying. Dwianto et al. (1999a, 1999b) observed the release of stresses stored in the cell wall polymers of the Sugi wood under high temperature steam, which is in line with the results obtained from this study.

The release of mechanical energy was observed immediately after placing the compact in the drying medium, i.e., during the warm-up period. During this period, the initial condensation of steam along with the rapid raise in temperature of the compacts accelerated the release of mechanical energy in the compact. The release of mechanical energy in the compact can be due to the elastic extension of the polymer matrix causing building up of pressure within the compact. Iyota et al. (2001) reported that due to the sudden heating and rising of moisture content in the material during the warm-up period, the quality of the dried material as well as the drying processes is greatly influenced by the condensation phenomenon. Results showed that the percentage increase in volume was substantially higher for compacts dried at 110°C compared with 150°C. This may be due to the higher amount of initial steam condensation and low moisture removal rate at 110°C compared with 150°C. For a specific temperature and velocity, the percentage increase in volume was observed to decrease with drying time, i.e., the compact was observed to shrink with an increase in drying time. This shrinkage may be due to the reduction of moisture content of the compact with time while drying. Nathakaranakule et al. (2007) reported that chicken meat dried with SS at temperature

of 160°C had more shrinkage than that dried at 120°C; moreover, the percentage of shrinkage of dried chicken meat depended on the drying time. For reference, the post-hoc analysis for percentage increase in volume of WDG compacts while drying at different SS temperatures and velocities during the initial condensation period (5s) is shown in Appendices in A.3 to A.5.

Statistical analysis for this study was done to determine any significant difference in the results obtained for: (i) a specific temperature and specific velocity for four different drying times of 5, 120, 300, and 600 s, (ii) a specific temperature and specific time for three different SS velocities of 0.9, 1.1 and 1.4m/s, (iii) a specific velocity and specific time for three different SS temperatures of 110, 130 and 150°C. Statistical analysis of the percentage increase in volume showed that for different drying times, a significant difference ($P \leq 0.05$) was observed for each drying conditions expect for 110°C (0.9 and 1.1 m/s). While considering the effect of different SS velocities, a statistically significant difference ($P \leq 0.05$) was only observed for 110°C at 120, 300 and 600 s of drying. When drying with different SS temperatures, a statistically significant difference ($P \leq 0.05$) was observed for different treatment conditions except when the SS velocity was 0.9 m/s, with 120 s drying time, and when SS velocity was 1.4 m/s with 300 s of drying time.

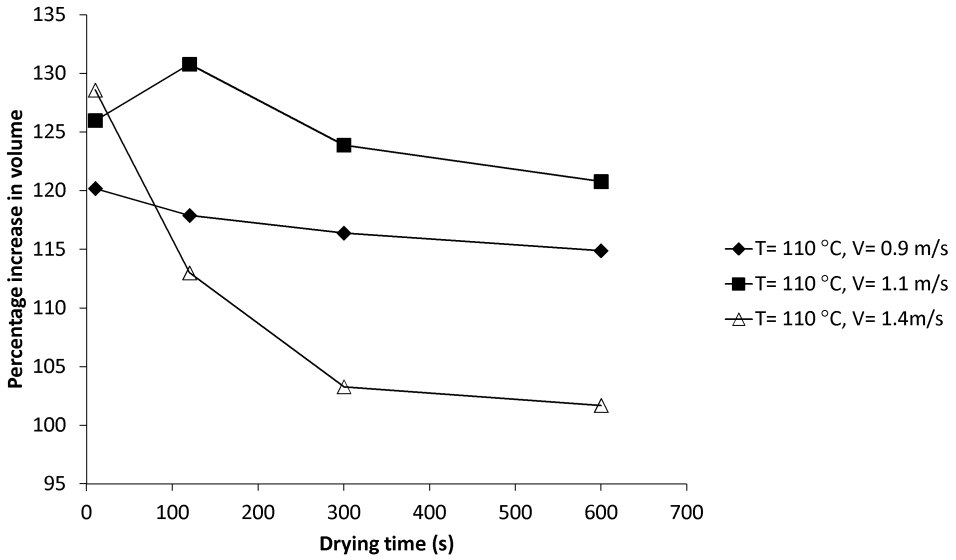

FIG. 5.14. Percentage increase in volume as affected by drying time in superheated steam at temperature (T) =110°C and at 3 different superheated steam velocities, V. Each data point is the average of three measurements. Values of standard deviation corresponding to each data point in this figure are provided in Appendix B.5.

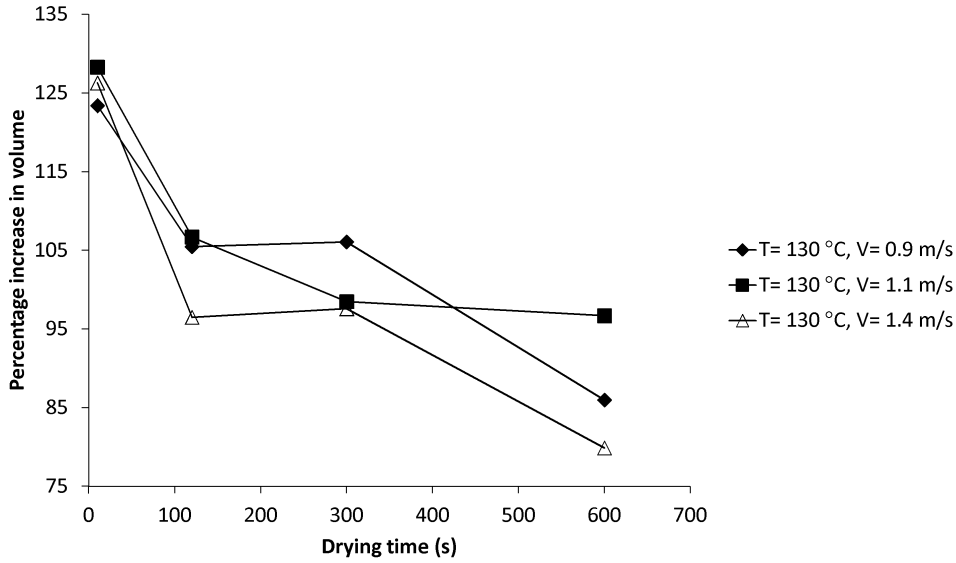

FIG. 5.15. Percentage increase in volume as affected by drying time in superheated steam at temperature (T) = 130°C and at 3 different superheated steam velocities, V. Each data point is the average of three measurements. Values of standard deviation corresponding to each data point in this figure are provided in Appendix B.5.

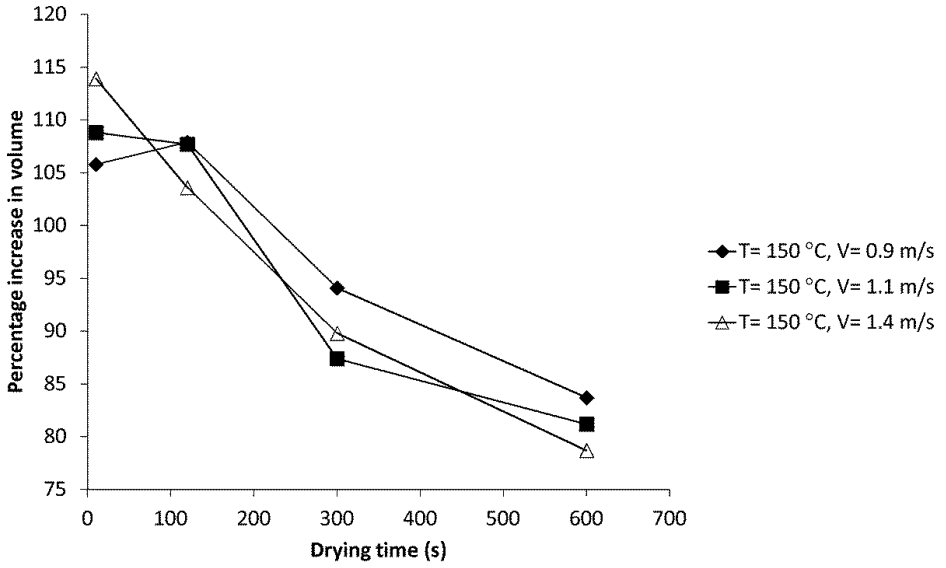

FIG. 5.16. Percentage increase in volume as affected by drying time in superheated steam at temperature (T) = 150°C and at 3 different superheated steam velocities, V. Each data point is the average of three measurements. Values of standard deviation corresponding to each data point in this figure are provided in Appendix B.5.

5.3.4 Compacts density variation

The density of compacts at different drying times was affected by their moisture content, drying temperature, and the percentage increase in volume. Density influences the strength of the compacts while drying. Zamorano et al. (2011) and Gunduz et al. (2009) reported that compacts with lower density and tensile strength brake easily during handling, transportation, and storage. The percentage decrease in compact density (Eq. 3.1) during SS drying is shown in Figs. 5.17 to 5.19. The sudden reduction of compact density during the warm-up period of SS drying indicates a reduction in strength of the compacts. A large reduction in the compact density along with excess moisture deposited due to initial condensation can make the compact more susceptible to breakage during the initial stage of SS drying.

Statistical analysis of the percentage change in density showed that for different drying times, a significant difference ($P \leq 0.05$) was obtained when drying at 110°C (0.9 and 1.4 m/s) and when drying at 130°C (1.4 m/s). When drying with different SS velocities, a statistically significant difference was only obtained when drying at 110°C under all drying times tested. When drying with different SS temperatures, no statistically significant difference ($P \leq 0.05$) was observed for any of the treatment conditions. For reference, the post-hoc analysis for percentage decrease in density of WDG compacts while drying at 110°C with different SS velocities of 0.9, 1.1 and 1.4 m/s during the initial condensation period (5s) is shown in Appendix A.6.

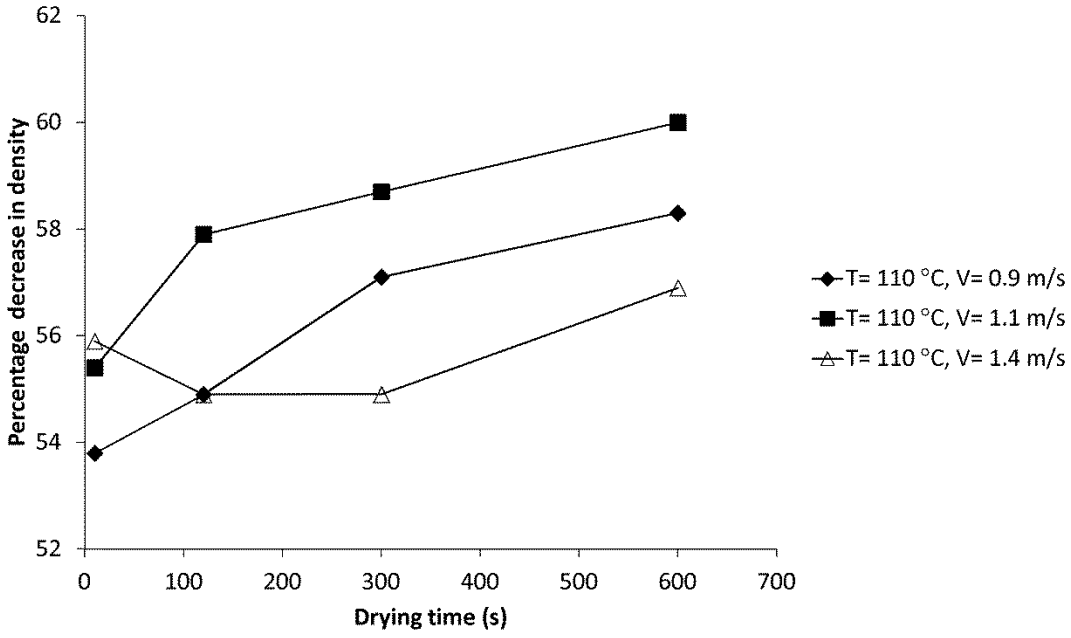

FIG. 5.17. Percentage decrease in density as affected by drying time in superheated steam at temperature (T) = 110°C and at 3 different superheated steam velocities, V. Each data point is the average of three measurements. Values of standard deviation corresponding to each data point in this figure are provided in Appendix B.6.

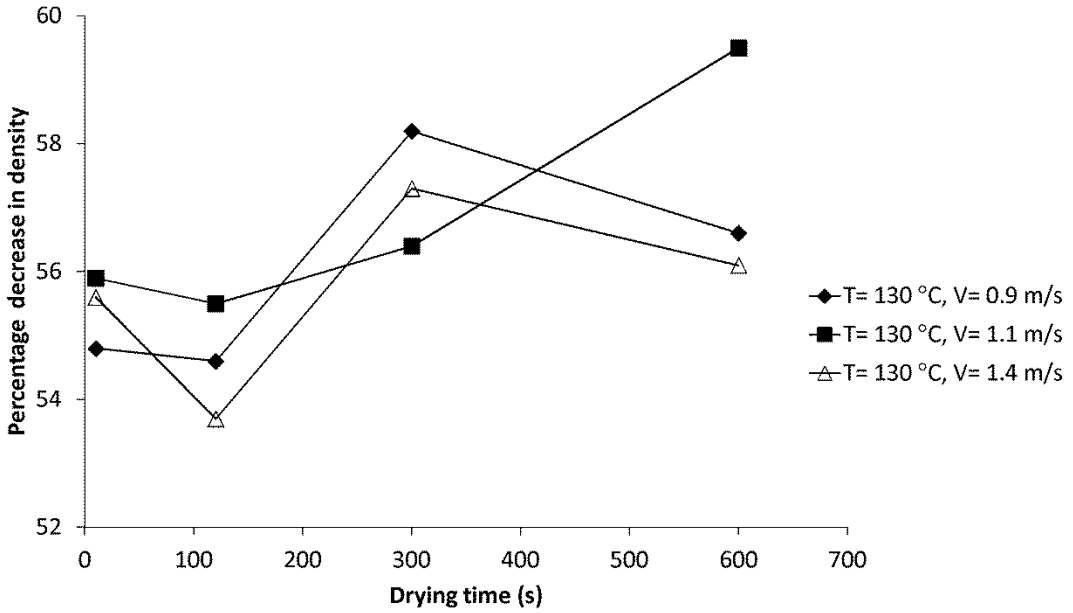

FIG. 5.18. Percentage decrease in density as affected by drying time in superheated steam at temperature (T) = 130°C and at 3 different superheated steam velocities, V. Each data point is the average of three measurements. Values of standard deviation corresponding to each data point in this figure are provided in Appendix B.6.

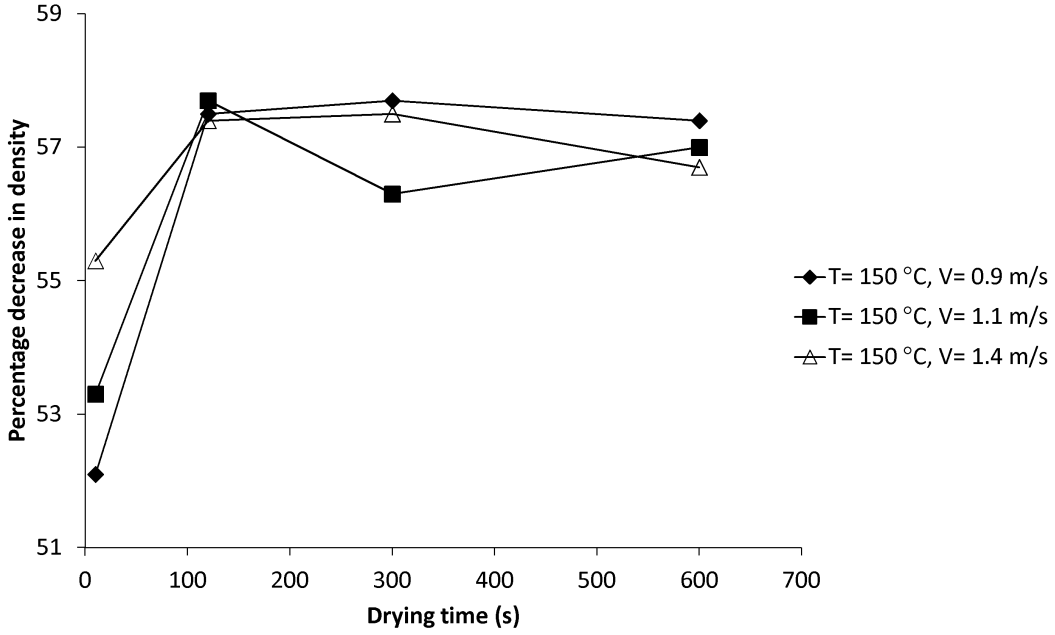

FIG. 5.19. Percentage decrease in density as affected by drying time in superheated steam at temperature (T) = 150°C and at 3 different superheated steam velocities, V. Each data point is the average of three measurements. Values of standard deviation corresponding to each data point in this figure are provided in Appendix B.6.

5.3.5 Diametral compression test

Methodology for this section is described in section 4.3. After exposing the compacts to different drying periods a 4.0 mm slice of the cylindrical compact was cut and used for diametral compression testing. Due to the high fibrous nature of WDG, the fracture line of the compacts was difficult to identify during diametral compression testing. Crushing resistance as well as tensile strength (Eq. 4.10) was determined for the compacts after they had been exposed to SS for various time periods.

The values of crushing resistance and tensile strength of the compacts are shown in Table 5.6. During the early period of drying, the compacts were not brittle and did not break between the compression plates. Due to the presence of high moisture, the compact behavior under compression resembled the behavior of a viscoelastic material. As seen from the results, the strength of the compact dried at 150°C increased quickly with time compared with those dried at 110°C. Results showed that, for a 600 s drying period, the compacts dried at 110°C had lower strength compared with those dried at 150°C. This higher strength may be attributed to the fact that at higher SS temperature (150°C), the amount of initial condensate deposited was low and the moisture removal rate was high due to higher heat transfer rates.

Statistical analysis of the crushing resistance of the compact showed that with the increase in drying time, crushing resistance values showed a significant difference ($P \leq 0.05$) for 110°C (1.4 m/s), 130°C (0.9 and 1.4 m/s) and for 150°C (0.9 and 1.4 m/s) (Table 5.6). While considering the effect of different SS velocities, a statistically significant difference ($P \leq 0.05$) was only observed for 150°C at 120 and 300 s of drying. When drying with different SS temperatures, a statistically significant difference

($P \leq 0.05$) was observed when the SS velocity was 0.9 and 1.4 m/s for 600 s of drying time.

Statistical analysis of the maximum tensile stress of the compact showed that with the increase in drying time a statistically significant difference ($P \leq 0.05$) for maximum tensile stress was observed for 110°C (1.4 m/s), 130°C (0.9, 1.4 m/s) and for 150°C (0.9, 1.1, 1.4 m/s). For different SS velocities, there was no statistically significant difference ($P \leq 0.05$) for any of the drying conditions studied. For different SS temperatures, a statistically significant difference ($P \leq 0.05$) was observed when the SS velocity was 0.9 and 1.4m/s for 600 s drying time.

Table 5.6. Variation of crushing resistance and maximum tensile stress of wet distiller's spent grain compacts dried under superheated steam at different conditions (values in parenthesis indicate standard deviations, n= 3).

Temperature (°C)	Velocity (m/s)	Time (s)	Crushing resistance (N)	Maximum tensile stress (kPa)
110	0.9	600	17.2 (1.7)	391.6 (42.1)
110	1.1	600	19.2 (4.2)	426.6 (87.8)
110	1.4	300	15.5 (1.0)	360.9 (19.3)
110	1.4	600	19.9 (2.2)	454.4 (46.9)
130	0.9	300	21.3 (4.1)	475.1 (102.5)
130	0.9	600	31.4 (1.1)	732.0 (46.0)
130	1.1	300	22.6 (6.2)	525.7 (153.1)
130	1.1	600	28.2 (6.5)	651.5 (157.9)
130	1.4	300	21.7 (4.0)	492.0 (87.2)
130	1.4	600	33.8 (3.4)	815.2 (78.5)
150	0.9	120	18.4 (1.7)	416.7 (44.0)
150	0.9	300	23.5 (2.2)	545.7 (48.7)
150	0.9	600	29.4 (3.9)	674.5 (99.1)
150	1.1	120	22.8 (1.7)	507.9 (35.8)
150	1.1	300	30.0 (1.5)	700.1 (40.3)
150	1.1	600	31.3 (5.8)	733.1 (126.9)
150	1.4	120	17.8 (2.6)	395.2 (60.9)
150	1.4	300	22.1 (4.8)	526.1 (125.2)
150	1.4	600	30.5 (3.0)	717.1 (71.4)

5.3.6 Physical characteristics of WDG compacts under oven-drying

The WDG compacts were oven dried to compare them with SS drying. Single compacts were dried in the convection hot-air oven for a 600 s period at temperatures of 110, 130 and 150°C. Percentage increase in volume, density change, crushing strength and tensile strength of the compact were determined after the oven-drying. Moisture content of the compacts for a 600 s drying period at 110, 130 and 150°C were 6.1, 4.6

and 3.5% wb, respectively. The volumetric and density changes for oven-dried compacts are shown in Fig. 5.20. The percentage increase in volume and percentage decrease in density was lower for oven-dried compacts compared with SS dried ones (Figs 5.14 to 5.19).

Crushing resistance and maximum tensile stress for oven-dried compacts are shown in Table 5.7. Since oven-dried compacts had smaller volume and higher density compared with SS dried compacts for 600 s drying period, oven-dried compacts had higher strength compared with SS dried ones (Table 5.6). It was found that for oven-dried compacts (velocity =1.4 m/s), crushing resistance was 147.8 (for 110°C), 39.7 (for 130°C) and 48.8% (for 150°C) higher compared with SS dried compacts. There were a 160.3 (for 110°C), 37.8 (for 130°C) and 52.7% (for 150°C) increases in maximum tensile stress for oven-dried compacts compared with SS dried ones. The comparison between the SS dried and oven-dried compacts clearly indicates the influence of SS in accelerating the release of mechanical energy stored in the compacts. As discussed earlier, the specific conditions prevailing inside the SS drying chamber during the initial stage of SS drying may have resulted in a higher reduction of compacts' strength as compared with those dried in the hot-air oven.

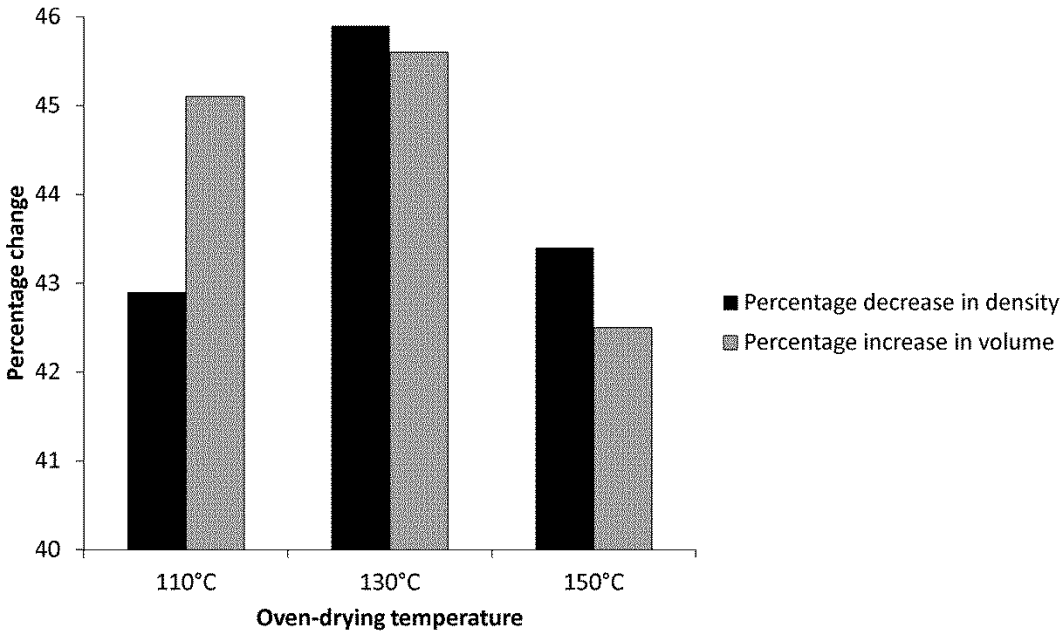

FIG. 5.20. Percentage decrease in density and percentage increase in volume of wet distiller's spent grain compacts dried in convection hot-air oven at 110, 130 and 150°C (n=3). Values of standard deviation corresponding to each data point in this figure are provided in Appendix B.7.

Table 5.7. Variation in crushing resistance and maximum tensile stress of wet distiller's spent grain compacts dried in convection hot-air oven for 600 seconds (values in parenthesis indicate standard deviations, n= 3).

Temperature (°C)	Time (s)	Crushing resistance (N)	Maximum tensile stress (kPa)
110	600	49.4 (2.3)	1182.6 (40.8)
130	600	47.2 (5.4)	1123.3 (135.7)
150	600	45.4 (8.1)	1095.2 (172.3)

5.4 Measurements of disintegration of DSG compacts during SS drying as affected by addition of solubles

The material presented in this chapter is the modified reproduction of work published by Johnson et al. (2014c) under the realm of this thesis**.** Compact used for this study had approximately 4-6 mm length, 12 mm diameter and 50% wb moisture content.

5.4.1 Particle size distribution

Methodology for particle size measurements and particle size distribution analysis is described in section 3.8.1 and section 4.6, respectively. Particle size distribution analysis is shown in Table 5.8. A graph of the PSD analysis of CDS is provided in Appendix A.1. The results show that the size of 90 percent of the sample in WDG lies below 1283.6 µm; whereas for CDS, the size of 90 percent of the sample lies below 563.9 µm. The d(0.5) represents the median for a volume distribution, it is the size at which 50% of the sample is below or above. DeBrouckere mean or D[4,3] is a moment mean and is analogous to the center of gravity of the particle size distribution. It shows the central value of the frequency the distribution would move around, and it is most sensitive to the proportion of large or coarse particulates in the sample.

Table 5.8. Analysis of particle size distribution of wet distiller's spent grain (WDG) and condensed distiller's solubles (CDS).

	WDG	CDS
d(0.9) (µm)	1283.6	563.9
d(0.5) (µm)	565.7	103.2
d(0.1) (µm)	52.4	8.2
D[4,3] (µm)	619.2	207.2

5.4.2 Chemical composition analysis

Table 5.9 shows the compositional analysis of WDG and CDS. The methods used to determine each composition are listed in Table 5.9. Values of cellulose were calculated as the difference between ADF and acid detergent lignin (labelled as

"Lignin" in Table 5.9) and the values of hemicellulose were calculated as the difference between NDF and ADF (Van Soest and Robertson, 1980; Jung, 1997; Moller, 2009).

Previous studies show that the presence of starch and protein in feed improves the binding of particles during the densification process (Alebiowu and Itiola, 2002; Thomas et al., 1998; Tabil et al, 1997). Starch gelatinization and protein denaturation normally take place in the presence of heat, moisture or mechanical shear forces (Kaliyan and Morey, 2009; Thomas et al., 1999). The presence of fat/oil in feed can produce pellets of lower strength and durability (Briggs et al., 1999; Angulo et al., 1996). Fat is hydrophobic and acts as a lubricant among feed particles, and between the feed and the die-hole wall. Fat even inhibits the binding characteristics of water soluble constituents such starch, protein and fiber (Thomas et al., 1999). Moreover, fat imparts a low friction in the die causing a reduction in the pelleting pressure (Tumuluru et al., 2011). Thus, the presence of higher amount of starch and protein, and lower amount of fat in CDS as compared with WDG may have provided favorable binding properties to the compacts with higher quantities of CDS.

Cellulose has a strong, non-hydrolysable crystalline structure while hemicellulose has an easily hydrolysable amorphous structure. Therefore, with the application of heat, lignin and cellulose impart binding properties to the feed (Kalyan and Morey, 2009). Grover and Mishra (1996) reported that under high temperature and pressure hemicellulose and lignin degraded into lower molecular weight compounds providing a favorable binding property. Though WDG has more lignin, cellulose and hemicellulose than CDS, the absence of heat during the densification process may have inhibited the binding properties of these components.

Table 5.9. Compositional analysis of wet distiller's spent grain (WDG) and condensed distiller's solubles (CDS). Each test was run in duplicate and the results are expressed on a dry matter basis. Values in parenthesis indicate standard deviation. NDF denotes the neutral detergent fiber and ADF denotes the acid detergent fiber.

	Methods used	CDS	WDG
Lignin (%)	(AOAC, 2005a)	1.77 (0.12)	2.21 (0.03)
ADF (%)	(AOAC, 2005a)	14.47 (0.20)	19.20 (0.26)
NDF (%)	(AOAC, 2005b)	21.73 (0.20)	46.56 (0.69)
Crude Fiber (%)	(AOCS, 2005)	4.51 (0.11)	7.95 (0.08)
Crude Protein (%)	(AOAC, 2005c)	48.82 (0.71)	29.49 (0.10)
Fat (%)	(AOAC, 2005d)	9.93 (0.18)	13.03 (0.06)
Starch (%)	Enzymatic UV-Method (Beutler, 1984)	5.76 (0.06)	3.77 (0.04)
Cellulose (%)		12.70 (0.16)	16.99 (0.18)
Hemicellulose (%)		7.26 (0.2)	27.37 (0.52)

5.4.3 Initial condensation and variation in dimensions of the compact

In the first 5 s of SS drying at 150°C a condensation of moisture on the surface of compacts was observed. This was reflected in a 1.8, 1.3, 0.9, 0.7 and 0.7% increase in moisture content of the compact which had various content of solubles of 0, 10, 30, 50 and 70%, respectively. Figs 5.21 and 5.22 show the WDG compacts with 0 and 70% solubles at various stages of drying in SS and the effect of SS on dimensions of the compacts. An immediate increase in the dimensions of WDG compact with 0% solubles after a 5 s exposure to SS is clearly visible in Fig. 5.21B*. For WDG compact with 70% solubles, the compacts turn comparatively darker in color with the reduction in moisture content (Figs 5.22C* and 5.22D*).

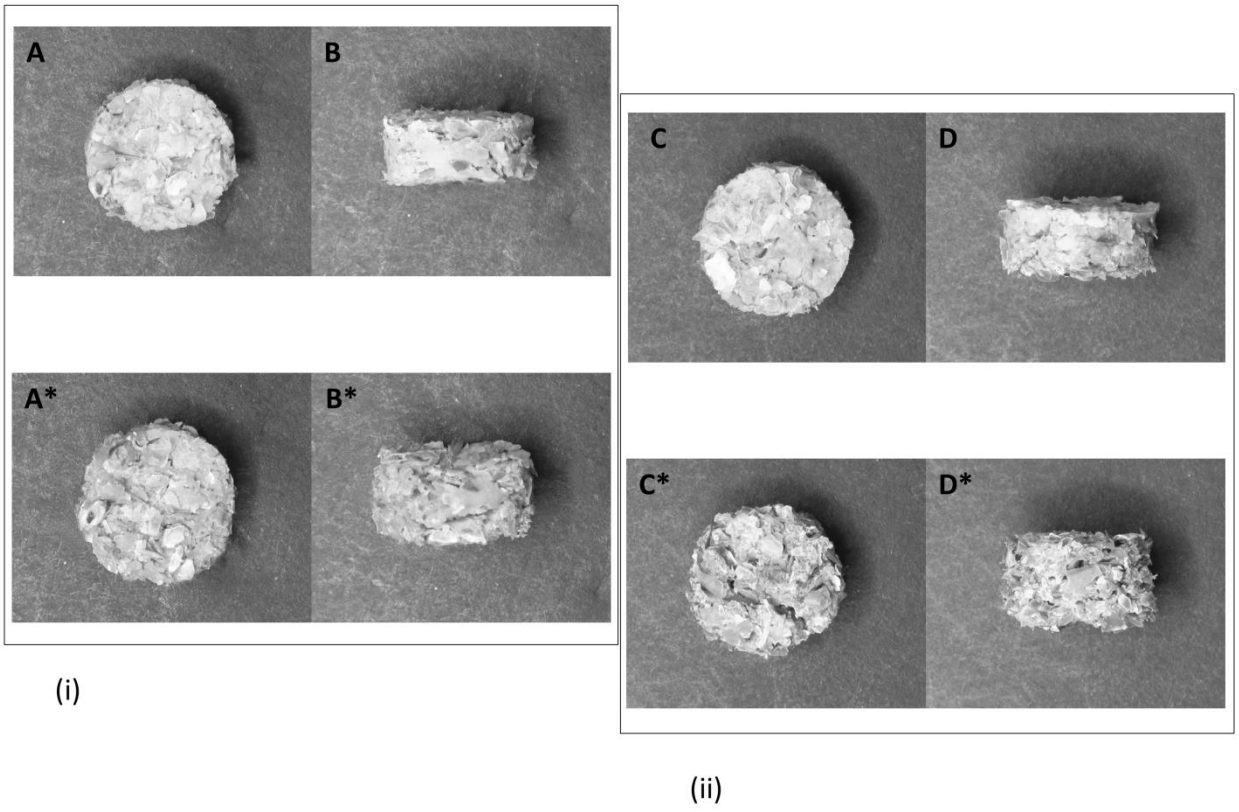

FIG. 5.21. (i) Wet distiller's spent grain compact with 0% solubles after 5 s of superheated steam drying. Pictures labelled as A and B refer to compacts before drying and pictures labelled as A* and B* show compacts after 5 s of drying. (ii) Wet distiller's spent grain compacts with 0% solubles after reaching 20% wb moisture while drying in superheated steam. Pictures labelled as C and D represent compacts before drying and pictures C* and D* show compacts after reaching 20% moisture content.

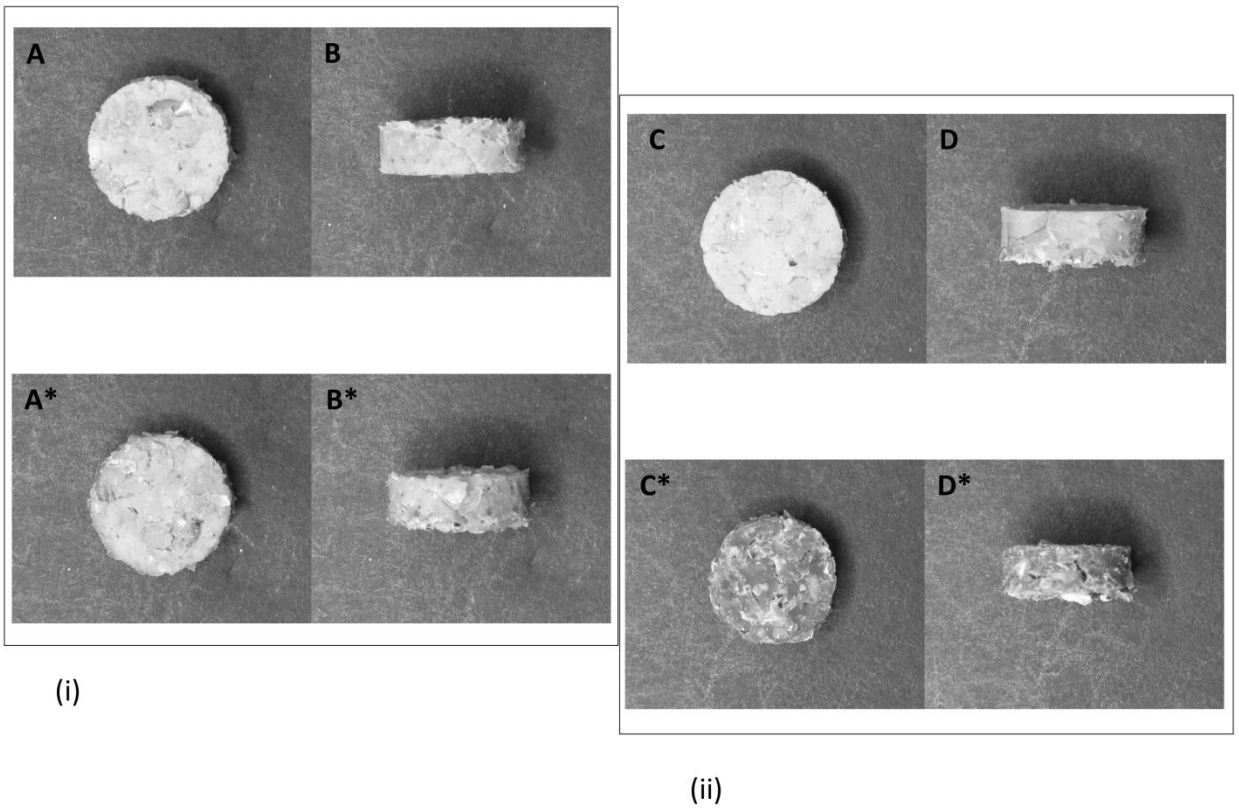

FIG. 5.22. (i) Wet distiller's spent grain compacts with 70% solubles after 5 s of superheated steam drying (A, B refers to compacts before drying, and A*, B* are compacts after 5 s drying). (ii) Wet distiller's spent grain compacts with 70% solubles after reaching a moisture content of 20% wb in superheated steam drying (C and D shows compacts before drying and C* and D* represents compacts after they reached 20% moisture content).

The percentage changes in length, diameter and volume of the compact are shown in Figs. 5.23, 5.24 and 5.25, respectively. In the figures 5.24 and 5.25, the negative values indicate a decrease in the diameter of the processed compact from the initial value of an unprocessed compact due to shrinkage of the compact during drying. Results showed that length of the compact increased at a higher percentage compared with diameter. The increases in dimensions were observed immediately after exposing the compact to SS. The addition of solubles diminished the increase in dimensions and at the end the volume. After the initial increase of dimensions, the compact shrank as

drying continued. Also, the highest change in geometry was observed for compacts without solubles added and during the condensation period.

The phenomenon of expansion of the compact in SS may be explained in terms of biomass compaction and relaxation processes. Relaxation of the compact is defined as the increase in dimensions or volume of the compact after compression (Doelker, 1993). During the compaction process, there is an increase in the density of the compact associated with the extent of material compression, which is fully reversible. In addition, during compaction, a compact is formed containing an amount of stress quantified as the stored energy. During the compact relaxation period, the stored energy is released leading to an increase in porosity of the compact. This stored energy can be regarded as the driving force during compact relaxation. Particle bonding is the counteracting force that prevents the expansion of the compact. Particle bonding is developed during the plastic deformation and fragmentation phase of the compaction process (Santos and Sousa, 2007). The increases in porosity and, at the same time, dimensions of the compacts are the net result of the stored energy that causes compact relaxation and the particle bonding that prevents compact relaxation (van der Voort Maarschalk et al., 1996; Papadimitropoulos and Duncan-Hewitt, 1992). When the compacts are exposed to vapor condensation in the initial stage of SS drying, the compacts tend to relax and increase their size immediately. Iyota et al. (2001) reported that during the warm-up period that includes initial condensation, the quality of the dried material is significantly affected due to the sudden heating and rising of moisture in the material. These initial conditions stimulate the release of mechanical energy stored in the compact.

The percentage increases in length and diameter of the compact were observed to decrease with the higher levels of solubles. Solubles have a sticky nature and a smaller particle size distribution as compared with WDG. The stickiness of the solubles act as a binding agent between the particles of the compact. van der Voort Maarschalk (1996) showed that interparticle bonding increases with decreasing particle size distribution. Thus, increasing the amount of solubles resulted in an increase in number of small particles and hence higher number of bonds. In addition, the presence of higher amount of starch and protein in CDS and lower amount of fat as compared with WDG (Table 5.9) may have triggered the binding mechanism during the densification process. The binding property of the solubles along with the higher number of bonds reduced the relaxation of the compact with SS drying. Statistical analysis of the results showed that, for the corresponding soluble contents, percentage increase in length, diameter and volume of compacts at different moisture contents (including the condensation period) were significantly different ($P \leq 0.05$). Also, for the corresponding moisture contents (including the condensation period), percentage increase in length, diameter and volume of compacts at different soluble contents were significantly different. For reference, the post-hoc analysis for percentage increase in length, diameter and volume of DSG compacts with different soluble levels during the initial condensation period (5s) is shown in Appendices in A.7 to A.9.

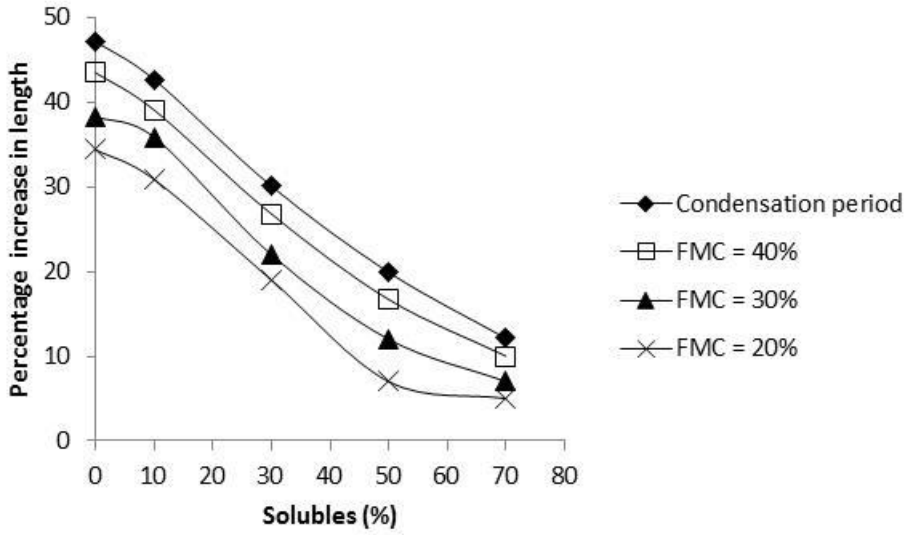

FIG. 5.23. Percentage increase in the length of the compact as affected by the addition of solubles during the condensation period and during drying from the condensation period to the final moisture content (FMC) of 40, 30 and 20% wb. Values of standard deviation corresponding to each data point in this figure are provided in Appendix B.8.

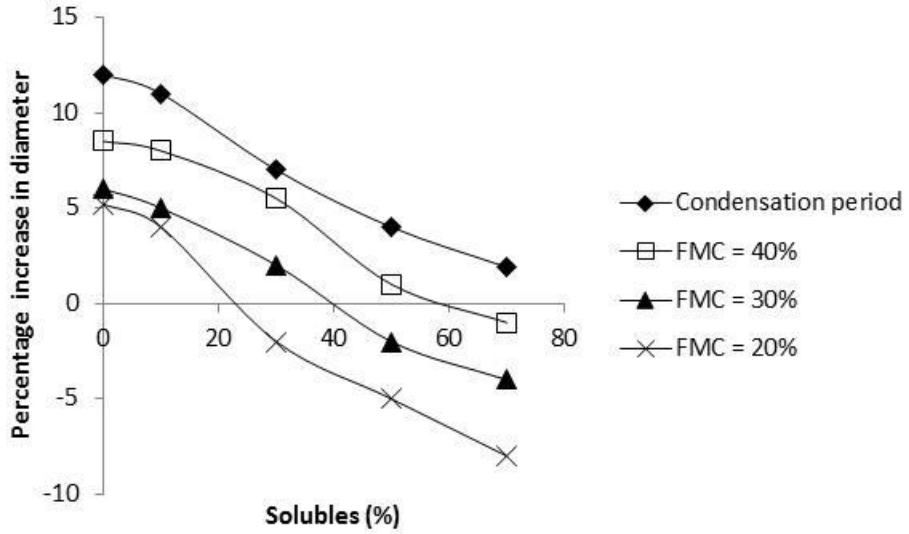

FIG. 5.24. Percentage increase in the diameter of the compact as affected by the addition of solubles during the condensation period and during drying from the condensation period to the final moisture content (FMC) of 40, 30 and 20% wb. Negative values indicate a decrease in the diameter from the initial value of an unprocessed compact. Values of standard deviation corresponding to each data point in this figure are provided in Appendix B.9.

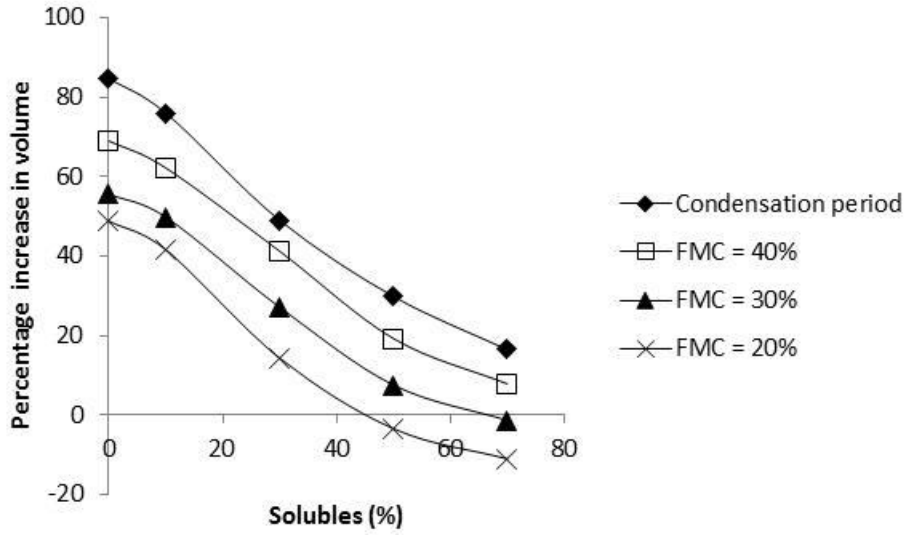

FIG. 5.25. Percentage increase in the volume of the compact as affected by the addition of solubles during the condensation period and during drying from the condensation period to the final moisture content (FMC) of 40, 30 and 20% wb. Negative values indicate a decrease in volume from the initial volume of an unprocessed compact. Values of standard deviation corresponding to each data point in this figure are provided in Appendix B.10.

5.4.4 Hardness of compacts

The methodology for finding hardness of the compact is described in section 3.7.4. The final mechanical characteristics of a compact are the consequence of the consolidation and expansion phenomena. A reduction in hardness was observed immediately after placing the compact in the SS dryer for 5s. For example, there was an 83 and 23% reduction in hardness as compared with unprocessed compacts, respectively for compacts with 0 and 70% solubles, after a 5s exposure of the compact to SS. This reduction in hardness can be related to the relaxation of the compact in the SS dryer.

As drying progressed, the compact was observed to regain its hardness with decreasing moisture content. Kaliyan (2008) reported that when a wet compact is

subjected to a drying process the water in the compact evaporates and the capillary bonding and viscous forces are replaced by solid bridges giving the dry strength to the compact. The dry strength can be lower or higher in comparison to the strength of a wet pellet depending on the type of binder present in the compact (Gupta, 2010). With the addition of solubles there was a considerable increase in the hardness of the compact. This may be due to the lower expansibility of the compact after the addition of solubles. As discussed earlier, the sticky nature of the solubles, the binding facilitating chemical composition, along with the fine fractions may have imparted more hardness to the compacts. The hardness of the compact with and without the addition of solubles at different moisture levels is shown in Fig. 5.26. Statistical analysis of the results showed that for the corresponding soluble contents, hardness of compacts at different moisture contents were significantly different ($P \leq 0.05$). Also, for the corresponding final moisture contents, hardness of compacts at different soluble contents were significantly different ($P \leq 0.05$).

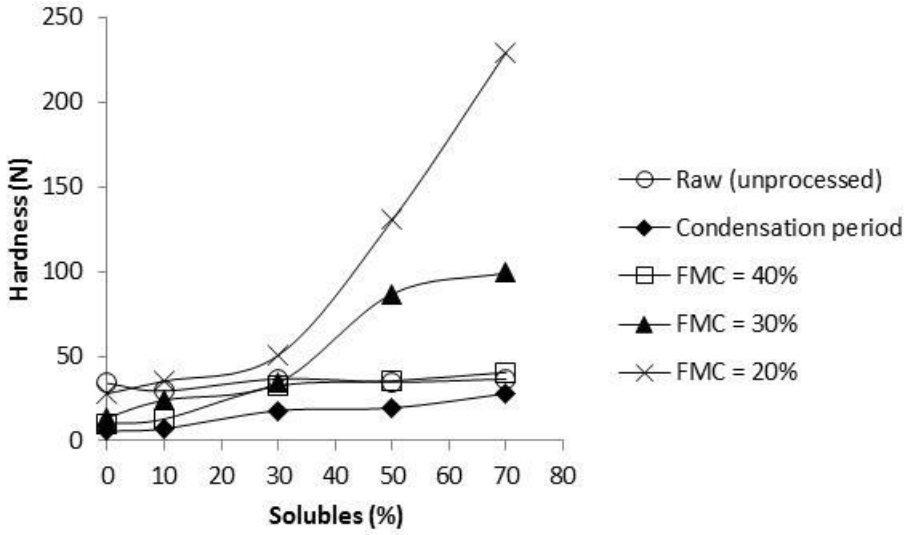

FIG. 5.26. Variation in the hardness of the compact as affected by the addition of solubles for unprocessed compacts and for compacts exposed to condensation in the first 5 s of superheated steam drying and during superheated steam drying from the condensation period to the final moisture content (FMC) of 40, 30 and 20% wb. Values of standard deviation corresponding to each data point in this figure are provided in Appendix B.11.

5.4.5 Asymptotic modulus

Asymptotic modulus (Eq. 4.5) is an indication of the compacts ability to sustain unrelaxed stresses. The compact is said to be a strong one when the compact can sustain stresses without dissipation. Thus, E_A is an indication of the solidity of the compact. A higher E_A value indicates that the compact is stronger.

Asymptotic moduli of the compact with and without the addition of solubles at different moisture levels are shown in Fig. 5.27. Results show that there is a reduction in E_A of the compact immediately after exposing it to condensation in the first 5 s of SS drying. This indicates that the compact is losing its solidity due to processing with SS. As drying continues, E_A tends to increase indicating an increase in compact solidity with a decrease in moisture content. Rey and Vandamme (2013) modeled the shrinking and stiffening properties of cellulose sponge upon drying. Their results showed that due

to drying the volume of the sponge decreased by more than half and its bulk modulus increased by almost two orders of magnitude. The stiffening of the sponge upon drying was due to geometrical nonlinearities induced by closing of the pores under the action of capillary pressure and due to the nonlinear elastic properties of the cellulose material itself. The increase in E_A of the spent grain compact during drying may be due to the stiffening of the compact as described by Rey and Vandamme (2013). With the addition of solubles the compact increased its E_A indicating a higher strength for the compact.

Statistical analysis showed that for the corresponding soluble contents, E_A of compacts at different moisture contents were significantly different ($P \leq 0.05$). Also, for the corresponding final moisture contents, E_A of compacts at different soluble contents were significantly different ($P \leq 0.05$). For reference, the post-hoc analysis for hardness and E_A of DSG compacts with different soluble levels during the initial condensation period (5s) is shown in Appendices in A.10 and A.11.

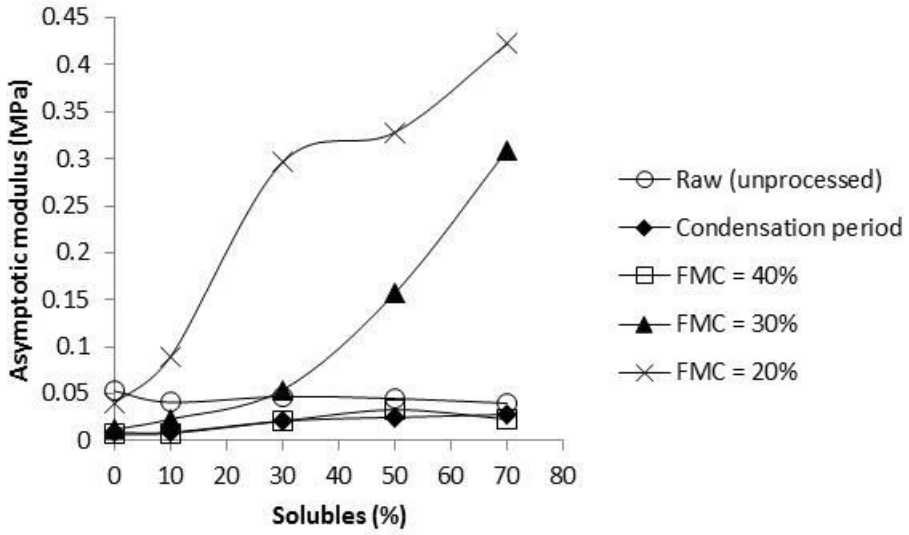

FIG. 5.27. Asymptotic modulus of the compact as affected by the addition of solubles for unprocessed compacts and for compacts exposed to condensation in the first 5 s of superheated steam drying and during superheated steam drying from the condensation period to the final moisture content (FMC) of 40, 30 and 20% wb. Values of standard deviation corresponding to each data point in this figure are provided in Appendix B.12.

5.4.6 Stepwise regression modeling and validation

Methodology for stepwise regression modeling and evaluation of the prediction model is described in section 4.4 and section 4.5, respectively. A forward stepwise regression method was used to find suitable independent variables in order to predict the E_A of the compacts. The variables chosen for the development of the model were soluble content, moisture content and hardness. A value of 4.000 was used as the F-to-enter value and 3.900 was chosen as the F-to-remove value. All variables with smaller F values (below 3.900) would be removed from the final equation by the program. Soluble content was intentionally included in the equation 5.1.

Stepwise regression analysis showed that the dependent variable E_A can be predicted from a linear combination of the independent variables soluble content and

moisture content. The regression model developed for the prediction of E_A is given by Eq. 5.1, where MC denotes the moisture content. Coefficient of determination obtained for the equation was 0.770 and $\underline{R^2}$ value was 0.752. Coefficient of determination values closer to 1 implies that the developed equation provides a good description of the relation between the independent and dependent variables. The $\underline{R^2}$ is also a measure of the strength of the regression model and it considers the number of independent variables which indicate the degrees of freedom. Larger values of $\underline{R^2}$ closer to 1 indicate that the independent variables are highly correlated.

$$E_A = 0.137 + (0.000738 \times \text{Solubles}) - (0.00367 \times \text{MC}) + (0.00145 \times \text{Hardness}) \quad (5.1)$$

Predicted E_A values determined using Eq. (5.1) was compared with the experimental E_A values (Fig. 5.28). For the model validation, mean absolute percentage error (MAPE) obtained was 163.6 and R^2 value obtained was 0.824. Generally, R^2 values above 0.5 are considered acceptable (Santhi et al., 2001, Van Liew et al., 2003, as cited in Moriasi et al., 2007). Chang et al. (2007) used multiple regression analysis to develop two predictive models of lower heating value for municipal solid waste; (1) original proposed model (OPM) and (2) simplified model (SM). The R^2 values of the developed equation for OPM and SM were 0.9831 and 0.9753, respectively, whereas the $\underline{R^2}$ were 0.9827 and 0.9738, respectively. Their mean absolute percentage error (Eq (4.14)) of the prediction equation during evaluation varied between 5.56 and 33.18. Their study concluded that the predictability of regression equations could be improved significantly through a selection of suitable physical components and multiple

regression analysis. Results obtained from the current study show that MAPE is in the unacceptable range, but the R^2 of 0.824 indicates that the model developed provides a good description of the relation between the dependent and independent variables.

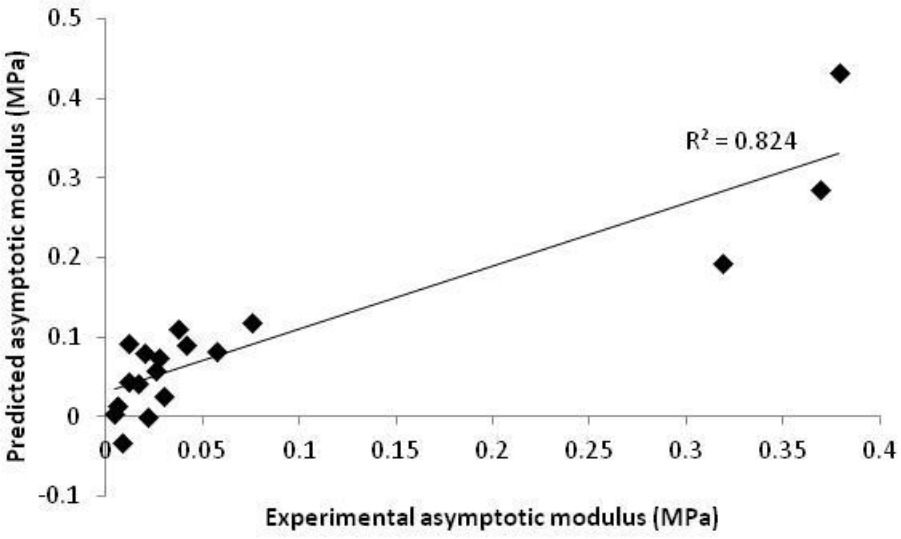

FIG. 5.28. A comparison between the experimental asymptotic modulus values and the values predicted by Eq. 5.1.

5.5 Effect of particle size on the disintegration of distiller's spent grain compacts while drying in superheated steam dryer

The material presented in this chapter is the modified reproduction of work published by Johnson et al. (2014a) and the work under review by Johnson et al. (2014d) under the realm of this thesis**.** Compact used for this study had approximately 4-7 mm length, 12 mm diameter and 50% wb moisture content.

5.5.1 Particle size distribution analysis

Methodology for particle size measurements and particle size distribution analysis is described in section 3.8.1 and section 4.6, respectively. Parameters used for representing the PSD are listed in Table 5.10. Results shows that d(0.9) is directly

proportional to d(0.1), d(0.5), Sauter mean diameter and DeBroukere mean diameter, whereas, d(0.9) is inversely proportional to specific surface area. This is in confirmation with the results obtained from the study by Afoakwa et al. (2008). In current experiments, span varied from 2.2 - 3.7. A higher span value indicates a lack of homogeneity in size and a greater variability in a particle size. The PSD curves obtained are shown in Figs. 5.29 to 5.31.

5.5.2 Superheated steam condensation

As long as the surface temperature of the compact was below the saturation point of steam, condensation on the sample surface was observed. This resulted in an increase in moisture of the compact by 1.8, 0.4 and 0.5% wb for samples of d(0.9)= 1283.6 µm, d(0.9)= 1069.3 µm and d(0.9)= 812.8 µm, respectively.

Table 5.10. Particle size distribution analysis for wet distiller's spent grain samples without grinding (d(0.9)= 1283.6 µm) and with grinding (d(0.9)= 1069.3 µm and d(0.9)= 812.8 µm). The d(0.9) denotes the specific size below which 90% of the particles lie.

	d(0.9)= 1283.6 µm	d(0.9)= 1069.3 µm	d(0.9)= 812.8 µm
Span	2.18	2.76	3.73
Uniformity	0.68	0.88	1.15
Specific surface area (m^2/g)	0.08	0.12	0.16
D[3,2] (µm)	66.6	46.3	33.2
D[4,3] (µm)	619.2	473.7	330.7
d(0.1) (µm)	52.4	28.2	16.4
d(0.5) (µm)	565.7	377.4	213.6

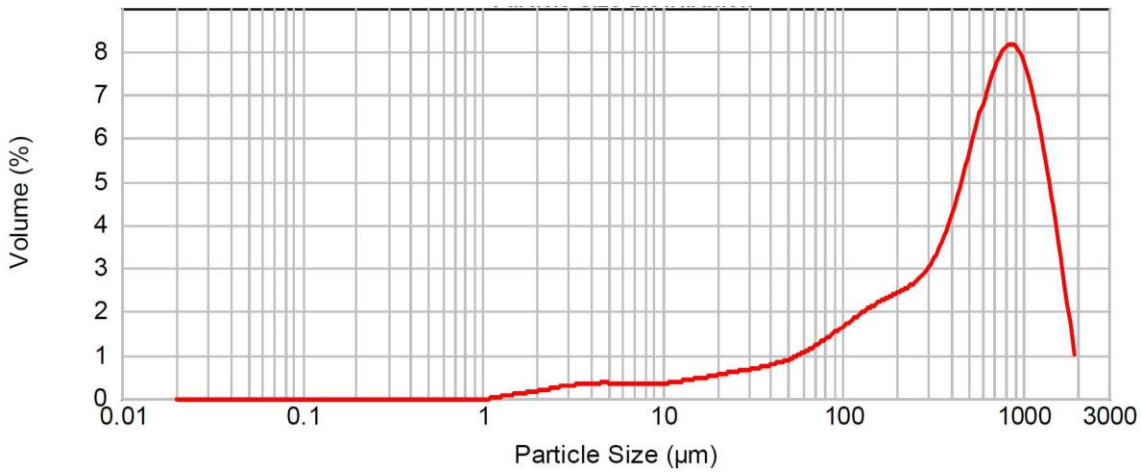

FIG. 5.29. Particle size distribution curve for d(0.9)= 1283.6 µm (graph obtained from the Malvern Mastersizer indicating average of three particle size distribution readings).

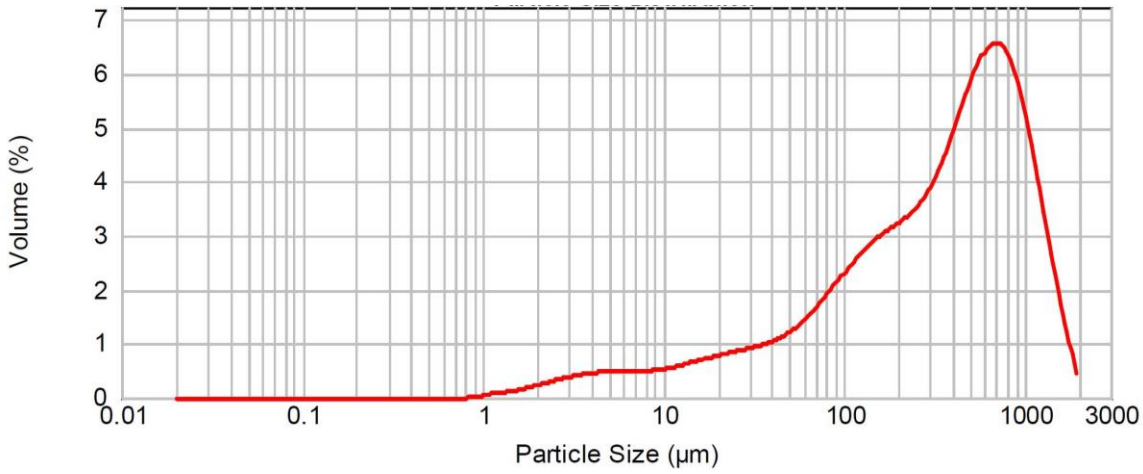

FIG. 5.30. Particle size distribution curve for d(0.9)= 1069.3 µm (graph obtained from the Malvern Mastersizer indicating average of three particle size distribution readings).

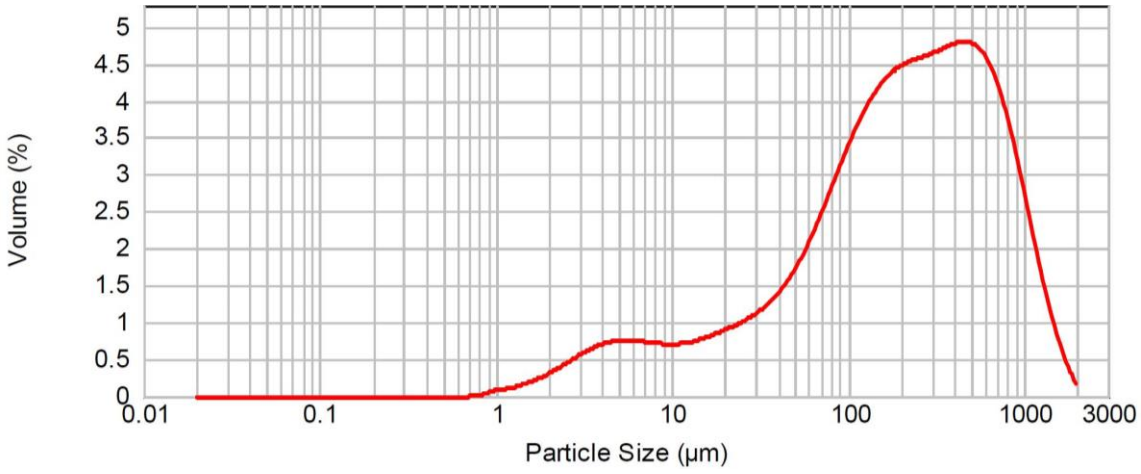

FIG. 5.31. Particle size distribution curve for d(0.9)= 812.8 µm (graph obtained from the Malvern Mastersizer indicating average of three particle size distribution readings).

5.5.3 Variation in volume of the compact in SS

Figs 5.32 and 5.33 show the WDG compacts, with PSD of d(0.9)= 1283.6 µm, d(0.9)= 1069.3 µm and d(0.9)= 812.8 µm, after 5 s of SS drying and after reaching moisture content of 20% wb, respectively. The increase in dimensions of the compact

with SS drying conditions and PSD can be observed from the figures. Percentage increase in volume of the compact (Eq. 3.1) is shown in Fig. 5.34. After exposing the compact to SS, volume of the compact increased immediately. Doelker (1993) defined the relaxation of the compact as the increase in dimensions or volume of the compact after compression. After compressing the biomass, the densified product contains a certain amount of stress quantified by the stored energy. This stored energy is considered the driving force for the relaxation of a compact; whereas, particle bonding is the resisting force that acts against the relaxation of the compact. Thus, an increase in the volume of the compact is the net result of the stored energy and the particle bonding force (van der Voort Maarschalk, 1996; Papadimitropoulos and Duncan-Hewitt, 1992).

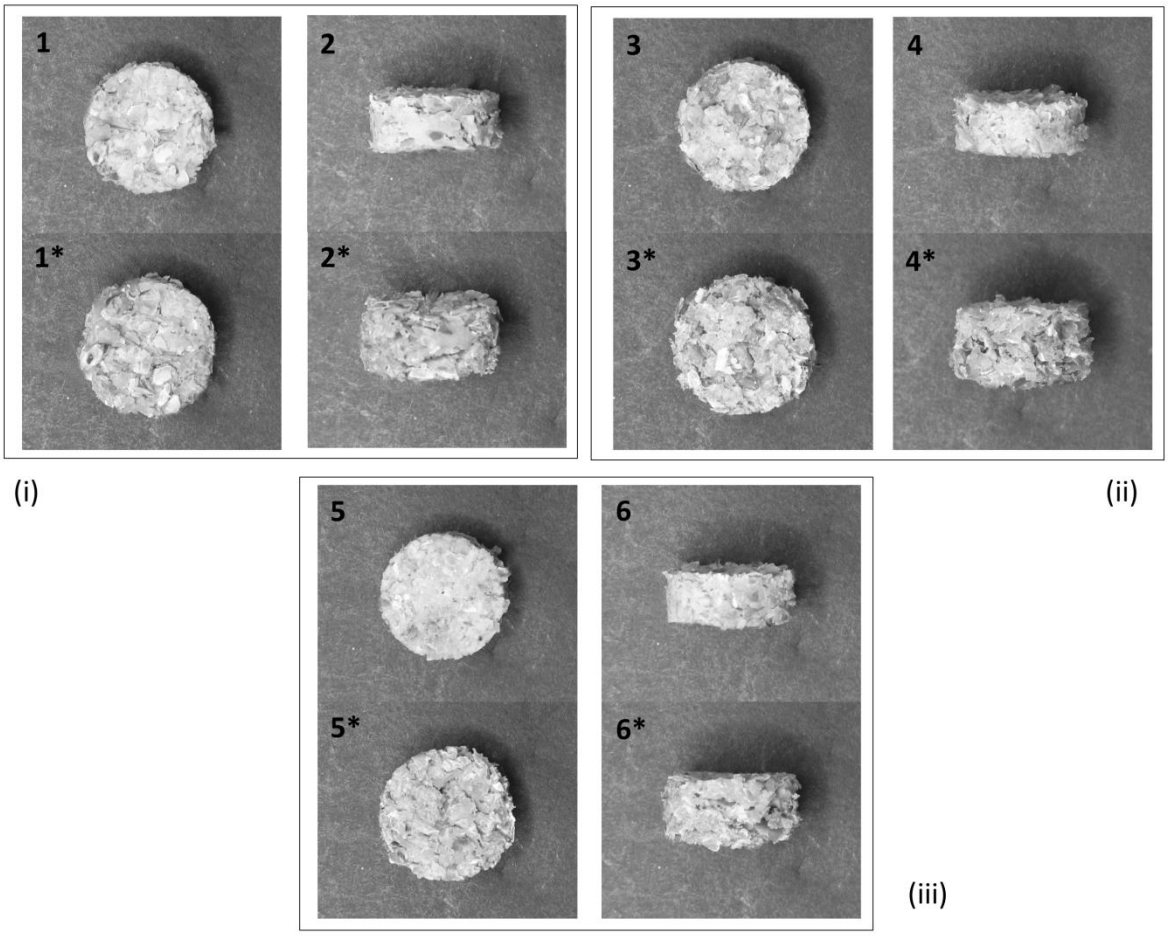

FIG. 5.32. (i) Wet distiller's spent grain compact with particle size distribution of d(0.9)= 1283.6 µm after 5 s of exposure to superheated steam (1*, 2*); pictures numbered as 1 and 2 indicates compacts before drying. (ii) Wet distiller's spent grain compacts with particle size distribution of d(0.9)= 1069.3 µm after 5 s of exposure to superheated steam (3*, 4*); pictures numbered as 3 and 4 indicates compacts before drying. (iii) Wet distiller's spent grain compacts with particle size distribution of d(0.9)= 812.8 µm after 5 s of exposure to superheated steam (5*, 6*); pictures numbered as 5 and 6 indicates compacts before drying.

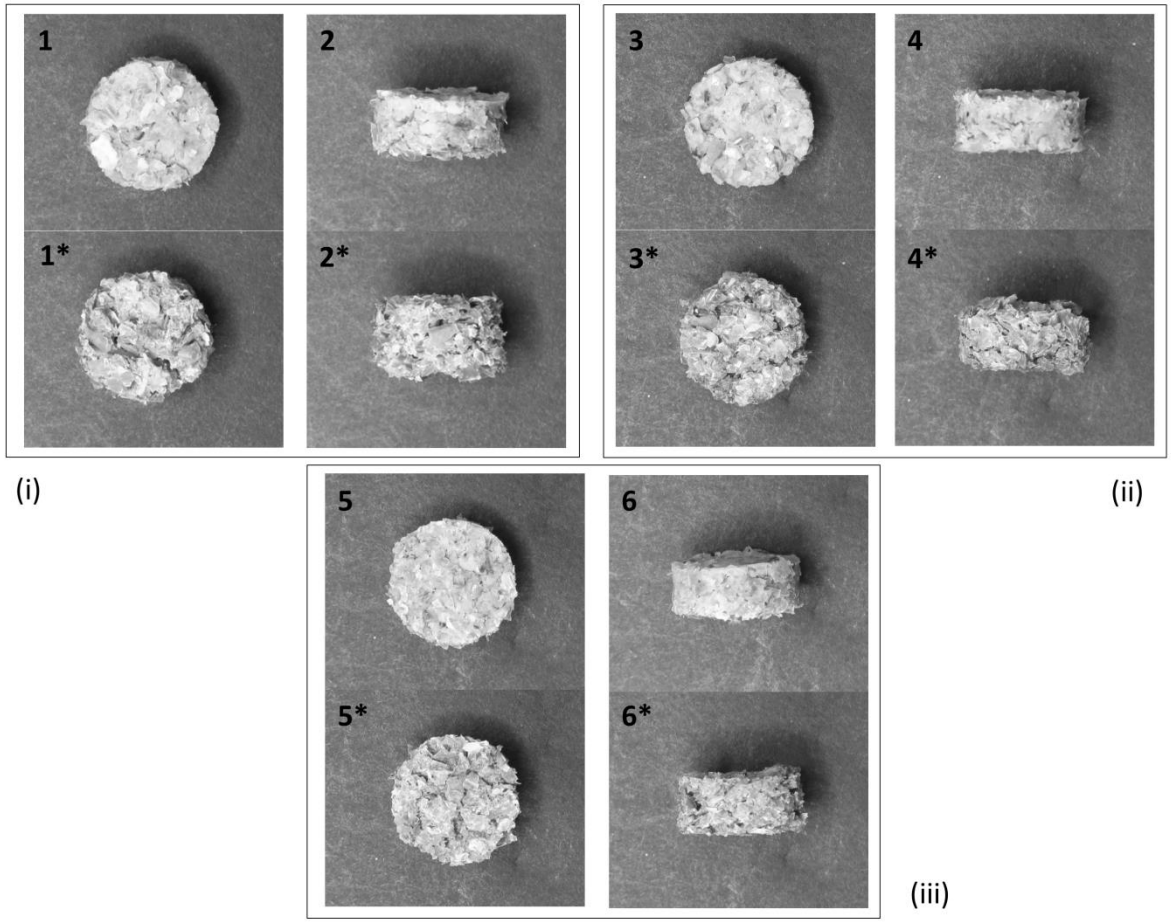

FIG. 5.33. (i) Wet distiller's spent grain compact with particle size distribution of d(0.9)= 1283.6 µm after reaching 20% wb moisture during drying in superheated steam (1*, 2*); pictures numbered as 1 and 2 indicates compacts before drying. (ii) Wet distiller's spent grain compacts with particle size distribution of d(0.9)= 1069.3 µm after reaching 20% wb moisture during drying in superheated steam (3*, 4*); pictures numbered as 3 and 4 indicates compacts before drying. (iii) Wet distiller's spent grain compacts with particle size distribution of d(0.9)= 812.8 µm after reaching 20% wb moisture during drying in superheated steam (5*, 6*); pictures numbered as 5 and 6 indicates compacts before drying.

A compacted sample relaxed (increased its volume) immediately after exposing it to SS. Iyota et al. (2001) reported that during the initial stage of SS drying process, i.e., during the warm-up period, the quality of the dried material is significantly affected by the sudden heating and rising moisture of the material. The initial condensation of

SS along with the rapid raise in temperature of the compact during the warm-up period may have stimulated the release of mechanical energy stored inside the compact. The increase in volume of the compact during the warm-up period was observed to decrease with the reduction in particle size of the compact. Studies done by Afoakwa et al. (2008) and van der Voort Maarschalk (1996) showed that with the decreasing particle size of a material the interparticle bonding increased. A decrease in PSD of the compacts may have increased the number of particles along with the number of bonds and hence, a reduction in relaxation (increase in volume) of the compact was observed. However, after the initial increase in the compacts volume, shrinkage of the compact occurred as it dried.

Post-hoc analysis for percentage increase in volume is provided in Appendix A.12. The comparatively lager values of percentage increase in volume for d(0.9) = 1283.6 µm may have influenced the overall significance levels ($P \leq 0.05$). There is no significant difference ($P \leq 0.05$) in the percentage increase in volume between particle sizes of d(0.9)= 1069.3 to 812.8 µm. However when the particle size distribution was at d(0.9) = 1283.6 µm a significant difference ($P \leq 0.05$) was observed. The statistical analysis discussed below are based on an overall significance level of $P \leq 0.05$. Statistical analysis showed that percentage increase in the volume of compacts at different moisture contents were significantly different ($P \leq 0.05$) among samples d(0.9)= 1283.6 µm, d(0.9)= 1069.3 µm and d(0.9)= 812.8 µm. Also, for the corresponding moisture contents, percentage increase in volume of compacts at different PSD was significantly different ($P \leq 0.05$).

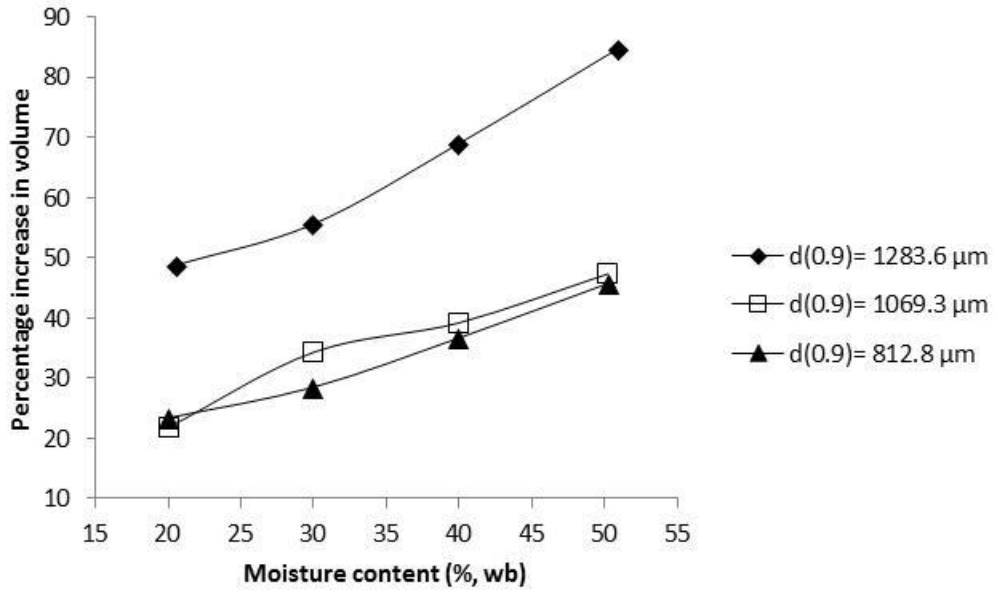

FIG. 5.34. Percentage increase in volume of the compact as affected by the variation of particle size distribution during the warm-up period of the first 5 s of superheated steam drying and at different moisture levels of 40, 30 and 20% wb. Values of standard deviation corresponding to each data point in this figure are provided in Appendix B.13.

5.5.4 Hardness of WDG compacts

The methodology for finding hardness of the compact is described in section 3.7.4. Hardness of the compacts was greatly influenced by the increase in volume of the compact due to drying in SS. During the initial condensation period, the hardness of the compact was reduced significantly. There was an 83, 56 and 55% reduction in hardness for d(0.9)= 1283.6 µm, d(0.9)= 1069.3 µm and d(0.9)= 812.8 µm, respectively after 5 s of SS drying compared with the raw compacts. However, as drying progressed and moisture decreased, the compact hardened.

With the decrease in particle size the hardness of the compact while drying in SS was observed to increase. This may be due to a reduction in relaxation of the compact with the decrease in particle size. Studies done by Afoakwa et al. (2008) showed a

significant ($P < 0.001$) reduction in firmness and consistency of dark chocolate with an increase in particle size from 18 to 50 µm. With a reduction in particle size the number of particles in the sample increases along with the specific surface area. This enhances particle surface–surface contacts providing lower compact relaxation rates and higher values for hardness. The hardness of the compact for different PSD is shown in Fig. 5.35. Statistical analysis showed that for the corresponding PSD, hardness of compacts at different moisture contents (including raw compacts) were significantly different ($P \leq 0.05$); whereas for the corresponding moisture contents, the hardness of compacts at different PSD was significantly different ($P \leq 0.05$) for 5s drying in SS and drying to 40, 30 and 20% mc, but there were no statistically significant difference ($P \leq 0.05$) found among the raw compacts.

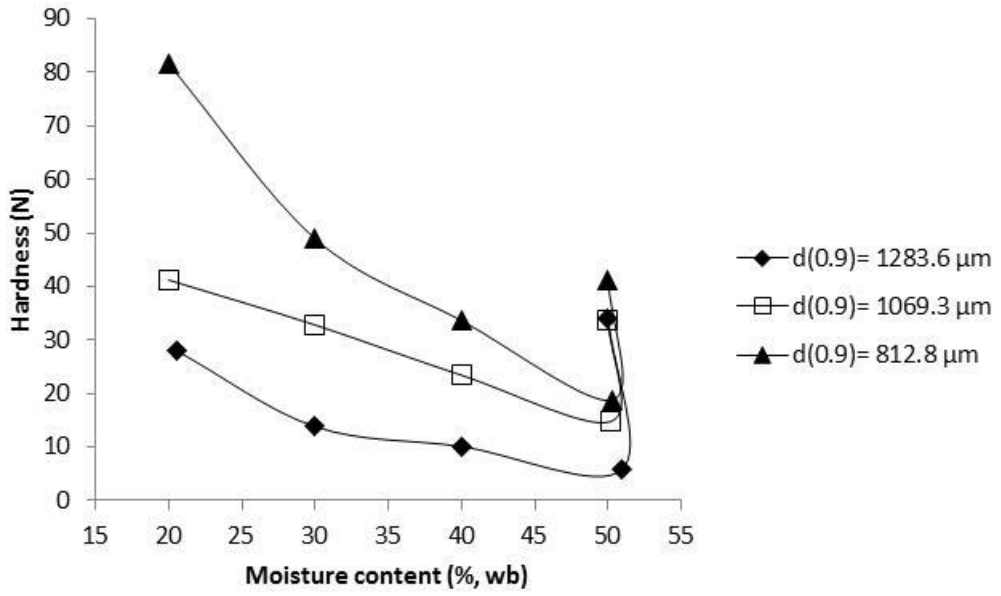

FIG. 5.35. Variation in the hardness of the compact as affected by different particle size distribution for raw compacts and for compacts exposed to superheated steam during the 5s warm-up period and after reaching moisture levels of 40, 30 and 20% wb in superheated steam. Values of standard deviation corresponding to each data point in this figure are provided in Appendix B.14.

5.5.5 Asymptotic modulus

Asymptotic modulus (Eq. 4.5) is considered as a short-term index for the measure of compact solidity. Higher values of E_A indicate that the compact has more ability to sustain stresses without dissipation. Results showed that during the warm-up period, due to the release of mechanical energy, the compact loses its solidity. A reduction in E_A during the initial stage is an indication that the compact is becoming more fragile and is more susceptible to breakage. There were 83, 58 and 64% reductions in E_A for d(0.9)= 1283.6 µm, d(0.9)= 1069.3 µm and d(0.9)= 812.8 µm, respectively for a 5 s of SS drying period compared with the raw compacts. However, as drying

progressed the compact was observed to shrink and the E_A increased with the drying time.

With the decrease in the particle size of the compact, an increase in E_A was observed which may be due to an increase in particle bonding with an increase in number of particles in the compact. Particles having a larger size may act as predetermined fissure points in a compact; whereas a mixture of different particle sizes having smaller particle diameters occupy the voids between the particles with few inter-particle spaces. A study done by Shaw and Tabil (2007) showed that decreasing the screen size of particles by milling significantly increased the asymptotic modulus of the three grinds of flax shive, oat hull, and wheat straw pellets. Asymptotic moduli of the compacts for different PSD are shown in Fig. 5.36.

Statistical analysis of the results showed that, for the corresponding PSD, E_A of compact at different moisture contents were significantly different ($P \leq 0.05$). Also, for the corresponding moisture contents, E_A of compact at different PSD were significantly different ($P \leq 0.05$) (expect for the raw compacts, which was not significantly different). For reference, the post-hoc analysis for hardness and E_A of WDG compacts with different PSD during the initial condensation period (5s) is shown in Appendices in A.13 and A.14.

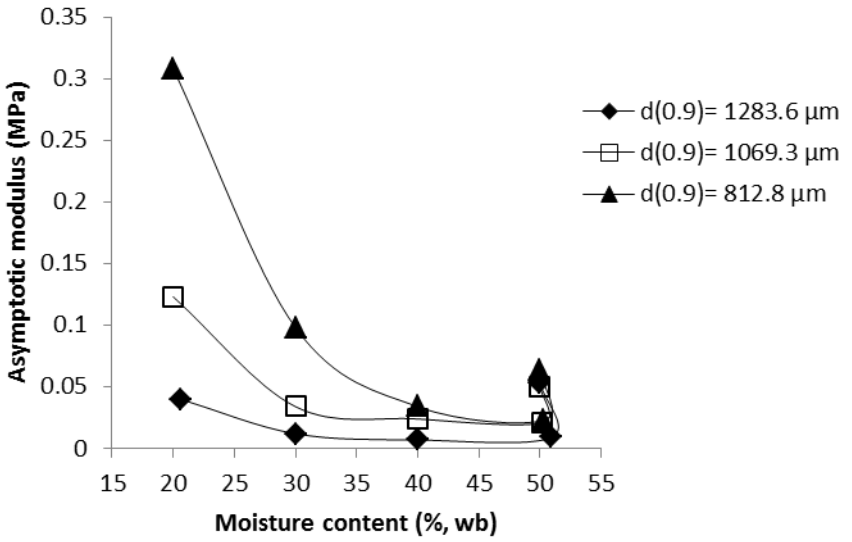

FIG. 5.36. Asymptotic modulus of the compact as affected by particle size distribution for raw compacts and for compacts exposed to particle size distribution during the 5 s of the warm-up period and after reaching moisture levels of 40, 30 and 20% wb in superheated steam. Values of standard deviation corresponding to each data point in this figure are provided in Appendix B.15.

5.5.6 Stepwise forward regression modeling

For selecting the appropriate independent variables for predicting the E_A of compacts, forward stepwise regression method was used. Volume mean diameter (D[4.3]) and moisture content and hardness were the independent variables selected for the stepwise forward regression analysis. For the current study, F-to-enter was chosen as 4.000 and F-to-remove was chosen as 3.900. During the model development, the stepwise regression method eliminates all variables with F values smaller than 3.900 and retains those variables with F values above 3.900.

Since particle size distribution has a major role in the disintegration of the compacts during drying in SS, D[4.3] was intentionally included in the equation. Stepwise regression analysis showed that the dependent variable E_A can be predicted from a linear combination of the independent variables volume mean diameters and

hardness. The variable moisture content was eliminated from the model by the variable picking algorithm. The model developed for the prediction of E_A using the multiple linear regression method is given by Eq. 5.2, the R^2 value obtained for the equation was 0.762 and the $\underline{R^2}$ obtained was 0.741.

$$E_A = -0.0823 + (0.0000668 \times D[4.3]) + (0.00377 \times \text{Hardness}) \quad (5.2)$$

The model was validated using the remaining 30% of the data that were not used for model development. The predicted (Eq. 5.2) and experimental E_A values (Fig. 5.37) were compared giving R^2 equal to 0.941.

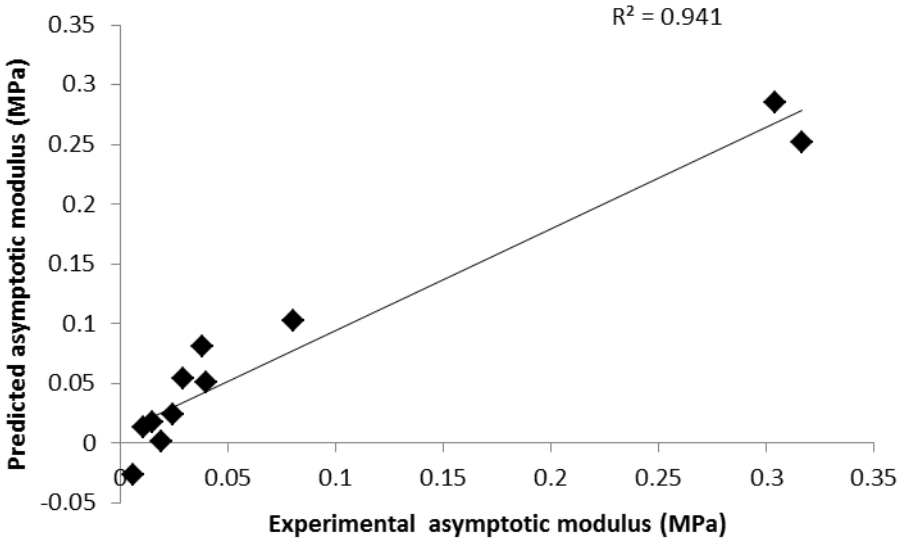

FIG. 5.37. A comparison between the experimental asymptotic modulus values and the values predicted by Eq. 5.2.

Grossman et al. (1996) used stepwise multiple linear regression to quantify leaf carbon, nitrogen, lignin, cellulose, dry weight, and water compositions from leaf level reflectance (L). Stepwise multiple regression produced R^2 values between 0.41 and 0.82

for the first and the second derivative log (1/L) spectra while using artificially constructed datasets that randomized the association between nitrogen concentration and reflectance spectra. For the current study, a R^2 value of above 0.5 obtained while comparing the predicted and experimental E_A values indicates that the model developed provides a good description of the relation between E_A and the independent variables (Santhi et al., 2001, Van Liew et al., 2003, as cited in Moriasi et al., 2007).

6. THESIS CONCLUSIONS

The results from the analysis of flow characteristics of DSG prepared using the same drying method indicates that both bulk density and AOR were affected by particle size. For DSG fractions dried using different drying methods (drying in SS at 150°C, air-drying at 45 and 150°C), bulk densities were in the range of 0.379-0.435 g/cm^3 and AOR ranged from 46.0 to 50.4°. When condensed distiller's solubles were added (10-30%) to DSG and then dried in SS, the bulk density varied from 0.391 to 0.444 g/cm^3 and AOR ranged from 46.5 to 49.8°. The AOR values indicated that dried DSG fell under poor flowing category for all treatments.

Analysis of the Jones model showed that, there was a non-significant increase ($P \leq 0.05$) in the compressibility of DSG when its moisture content was between 15 to 25% wb; whereas, a significant decrease ($P \leq 0.05$) in compressibility was observed when 15 and 30% solubles were added. Results showed that asymptotic modulus (E_A) can be used to characterize the DSG compacts affected by different compressive pressures and moisture contents for all treatments.

The release of mechanical energy stored in a compact was accelerated by processing in SS. The increase in volume of the compact (78 to 130%) was observed immediately after exposing the compacts to SS. This increase in volume was accompanied by a reduction in the compact strength and ultimately leading to the disintegration and agglomeration of the compact inside the dryer. After the initial increase in volume, as SS drying continued, the compacts shrank and regained strength depending on the SS processing conditions. Drying compacts at a higher SS temperature (150°C for the current study) has a few advantages due to the lower SS

condensation and higher moisture removal rate; in addition, higher temperature helps in regaining the strength of the compact at a faster rate after the sudden initial reduction of the strength of the compact during the initial condensation period. Volume of WDG compacts dried in the hot-air oven increased 42 to 46%. The crushing resistance of oven-dried compacts was 49 to 148% higher than SS dried compacts for a 600 s drying time.

The initial increase in volume of DSG compacts during the course of SS drying could be reduced by the addition of solubles or by reducing particle size of the samples before compacting. When the soluble content in the compact increased from 0 to 70% (w/w), the increase in the volume of compacts was reduced from 85 to 16%; the hardness rose from 6 to 28 N; and the asymptotic modulus (E_A) increased from 0.009 to 0.028 MPa during the initial SS condensation period. With a decrease in PSD (d(0.9)) of WDG from 1284 to 813 µm, the increase in the volume of compact was reduced from 85 to 46%; the hardness increased from 6 to 19 N; and the E_A increased from 0.009 to 0.023 MPa during the same initial condensation period of SS drying.

The study also evaluated the possibility of predicting the E_A of the compact with different soluble contents and PSD in separate studies. For studies involving the solubles and PSD, R^2 values of 0.824 and 0.941 were obtained, respectively. The R^2 values indicate that the model developed provides a good description of the relation between E_A and the independent variables. It is anticipated that the knowledge obtained from this project will help to develop new process or technology to effectively utilize distiller's spent grain.

Major Contributions to Knowledge

1. The AOR values indicated that dried DSG fell under poor flowing category.
2. Asymptotic modulus can be used to characterize the DSG compacts that are affected by different compressive pressures and moisture contents.
3. Drying of DSG compacts in SS showed that the release of mechanical energy stored in a compact or the expansion of the compact was accelerated by SS.
4. The increase in volume of a compact was observed immediately after exposing it to SS. The increase in volume was accompanied by a reduction in the compact's strength and ultimately leading to its disintegration and agglomeration during drying.
5. After the initial increase in volume, as SS drying continued, the compacts shrank and regained their strength depending on the SS processing conditions.
6. Drying compacts at a higher SS temperature (e.g., 150 versus 110°C for the current study) has advantages such as a higher moisture removal rate and reduced disintegration of compacts due to shorter duration of SS condensation. Higher SS temperature also helps in regaining the strength of the compact at a faster rate during drying.
7. The initial increase in volume of DSG compacts during the course of SS drying could be reduced by the addition of solubles or by reducing the particle size of the samples before compacting them.

7. RECOMMENDATIONS FOR FUTURE RESEARCH

Though the current research covered many aspects of the disintegration behavior of compacted DSG in SS, as far as future studies are concerned the following questions need to be answered:

1. How do the pellets produced from a commercial pelleting mill behave in an industrial SS drying unit?

The current study used lab scale compaction equipment and SS drying unit. The study could be expanded to analyze the properties of pellets produced from a commercial pelleting unit while drying in an industrial SS drying unit. The processing conditions are different in a commercial pelleting unit. Studies need to be conducted to find how such changes in processing conditions affect the extent of relaxation and strength of the pellets.

2. What is the effect of adding binders, increasing temperature or steam conditioning on the quality of the pellets and on their disintegration characteristics in SS?

A study could be conducted to find the effect of binders or additives, increasing feed temperature and steam conditioning on the disintegration behavior of compacted DSG. This study is important as many researches have reported substantial differences in the pellet durability as affected by changes in the above factors.

3. How does the integrity of compacts in SS vary with different biomass types?

The current study was focused on DSG compacts but the properties of the compacts change depending on the biomass grind. Hence a study could be conducted to find the effect of different biomass grinds, such as wheat straw, barley straw etc., on the properties of the compacts while drying in SS.

4. How does the grinding of DSG affect the overall economics of the pelleting operation?

Grinding of particles before compaction is an energy consuming unit operation. But, if the particle grinding can lead to a reduction in the disintegration of the pellets and the clogging of the pelleting unit, the overall profitability of the operation may be higher. However, an economic analysis of the particle grinding and the pelleting operation is needed for verifying the feasibility of the grinding operation.

5. How does the compacted DSG dissipate its stored energy during drying in SS?

A molecular level study may be required for revealing the interaction between SS and the interparticle bonds of the compact. Exploration of the chemical properties of compacts and SS could be beneficial in finding more specific answers.

8. REFERENCES

AACC. 2000. Method 44–19: Air-oven method, drying at 135°C. *In Approved Methods of the American Association of Cereal Chemists, Vol. II, 10th ed*. St. Paul, MN: AACC.

Abbott, J., J. O'Palka and C.F. McGuire. 1991. Dried distillers' grains with solubles: particle size effects on volume and acceptability of baked products. *Journal of Food Science* 56(5): 1323- 1326.

Adapa, P. K. 2011. Densification of selected agricultural crop residues as feedstock for the biofuel industry. Unpublished Ph.D thesis. Saskatchewan, SK: Department of Chemical and Biological Engineering, University of Saskatchewan.

Adapa, P., L.G. Tabil and G.J. Schoenau. 2009. Compaction characteristics of barley, canola, oat and wheat straw. *Biosystems Engineering* 104(3): 1-10.

Adapa, P.K., L.G. Tabil, G.J. Schoenau and S. Sokhansanj. 2004. Pelleting characteristics of fractionated sun-cured and dehydrated alfalfa grinds. *Applied Engineering in Agriculture* 20(6): 813-820.

Afoakwa, E. O., A. Paterson, M. Fowler and J. Vieira. 2008. Particle size distribution and compositional effects on textural properties and appearance of dark chocolates. *Journal of Food Engineering* 87(2): 181–190.

Ahmad, M.Z., S. Akhter, M. Anwar, M. Rahman, M.A. Siddiqui and F.J. Ahmad. 2012. Compactibility and compressibility studies of Assam Bora rice starch. *Powder Technology* 224: 281–286.

Ahmed E. M. and R. C. Fluck. 1972. Textural properties of stored and irradiated peaches: II. Rheological properties. *Journal of Texture Studies* 3(3): 319–328.

Aishima, T. and A. Nobuhara. 1977. Objective specification of food flavour. Analysis of gas chromatographic profiles of soy sauce flavour by stepwise regression analysis. *Food Chemistry* 2: 81-93.

Alebiowu, G. and O.A. Itiola. 2002. Compression characteristics of native and pregelatinized forms of sorghum, plantain, and corn starches and the mechanical properties of their tablets. *Drug Development and Industrial Pharmacy* 28(6): 663–672.

Al-Mashat, S.H.I. and C.A. Zuritz. 1993. Stress relaxation behavior of apple pomace and effect of temperature, pressing aid and compaction rate on juice yield. *Journal of Food Engineering* 20(3): 247–66.

Al-Widyan, M.I. and H.F. Al-Jalil. 2001. Stress–density relationship and energy requirement of compressed olive cake. *American Society of Agricultural and Biological Engineers* 17(6): 749–53.

Al-Widyan, M.I., H.F. Al-Jalil, M.M. Abu-Zreig and N.H. Abu-Hamdeh. 2002. Physical durability and stability of olive cake briquettes. *Canadian Biosystems Engineering* 44(3): 41–45.

Angulo, E., J. Brufau and E. Esteve-Garcia. 1996. Effect of a sepiolite product on pellet durability in pig diets differing particle size and in broiler starter and finisher diets. *Animal Feed Science and Technology* 63(1-4): 25–34.

AOAC. 2005a. AOAC Official Method 973.18: Fiber (acid detergent) and lignin (H2SO4) in animal feed. In *Official Methods of Analysis of AOAC International*, AOAC International. Gaithersburg, MD: AOAC.

AOAC. 2005b. AOAC Official Method 2002.04: Amylase-treated neutral detergent fiber in feeds. In *Official Methods of Analysis of AOAC International*, AOAC International. Gaithersburg, MD: AOAC.

AOAC. 2005c. AOAC Official Method 968.06: Protein (crude) in animal feed. In *Official Methods of Analysis of AOAC International*, AOAC International. Gaithersburg, MD: AOAC.

AOAC. 2005d. AOAC Official Method 920.39: Fat (crude) or ether extract in animal feed. In *Official Methods of Analysis of AOAC International*, AOAC International. Gaithersburg, MD: AOAC.

AOCS. 2005. AOCS Official Method Ba 6a-05: Crude fibre analysis in feeds by filter bag technique. In *Official Methods and Recommended practices of the AOCS*, Association of Oil Chemists Society. Champaign, IL: AOCS.

Applegate, T. and L. Adeola. 2008. Use of dry distillers' grains with solubles by poultry. BioEnergy newsletter. Purdue University Extension Department of Animal Sciences.

ASAE. 2008. ASAE Standard S319.4: Method of determining and expressing fineness of feed materials by sieving. In *American Society of Agricultural and Biological Engineers Standards.* St. Joseph, MI: ASABE.

ASAE. 2003a. ASAE Method S-269.4: Cubes, pellets, and crumbles – definitions and methods for determining density, durability, and moisture content. In *American Society of Agricultural and Biological Engineers Standards.* St. Joseph, MI: ASABE.

ASAE. 2003b. ASAE Method S-358.2: Moisture measurement – forages. In *American Society of Agricultural and Biological Engineers Standards*, *50th ed*. St. Joseph, MI: ASABE.

ASTM. 1998. ASTM Method D-440-86: Standard test method of drop shatter test for coal. In *Annual book of ASTM Standards*. West Conshohocken, PA: ASTM.

ASTM. 2006. ASTM Standard B 417: Standard test method for apparent density of non-free-flowing metal powders using the Carney funnel, Vol 02.05. In *American Society for Testing and Materials*. West Conshohocken, PA: ASTM.

ASTM. 2011. ASTM Method D7369. Standard test method for determining the resilient modulus of bituminous mixtures by indirect tension test. In *American Society for Testing and Materials.* West Conshohocken, PA: ASTM.

Aqa, S. and S. C. Bhattacharya. 1992. Densification of preheated sawdust for energy conservation. *Energy* 17(6): 575–578.

Bargale, P.C. and J. Irudayaraj. 1995. Mechanical strength and rheological behaviour of barley kernels. *International Journal of Food Science and Technology* 30(5): 609-23.

Beeby, C. and O.E. Potter. 1985. Steam drying. In *Drying '85,* ed. R. Toei, A.S. Mujumdar, 41–58. New York, NY: Hemisphere Publishing Corporation.

Belyea, R.L., K.D. Rausch and M.E. Tumbleson. 2004. Composition of corn and distillers dried grains with soluble from dry grind ethanol processing. *Bioresource Technology* 94(3): 293-298.

Beutler, H.O. 1984. Methods of Enzymatic Analysis (3rd edition), Volume VI, ed. H.U. Bergmeyer, 2-10. New York: Academic Press.

Bhadra, R., K, Muthukumarappan and K.A. Rosentrater. 2009. Flowability properties of commercial distillers dried grains with solubles (DDGS). *Cereal Chemistry* 86(2): 170– 180.

Bhattacharya, S. 2010. Stress relaxation behaviour of moth bean flour dough: Product characteristics and suitability of model. *Journal of Food Engineering* 97(4): 539–546.

Blahovec, J. 2001. Improved rate controlled model for stress relaxation in vegetable tissue. *International Agrophysics* 15(2), 73-78.

Bookwalter, G.N., K. Warner, J.S. Wall and Y.V. Wu. 1984. Corn distillers' grains and other by-products if alcohol production in blended foods. II. Sensory, stability, and processing studies. *Cereal Chemistry* 61(6): 509-513.

Boye, J. and Y. Arcand. 2013. Current trends in green technologies in food production and processing. *Food Engineering Reviews* 5: 1–17.

Briggs, J.L., D.E. Maier, B.A. Watkins and K.C. Behnke. 1999. Effects of ingredients and processing parameters on pellet quality. *Poultry Science* 78(10): 1464–1471.

Brochetti, D. and M.P. Penfield. 1989. Sensory characteristics of bakery products containing distillers dried grains from corn, barley, and rye. *Journal of Food Quality* 12(6): 413–426.

Brochetti, D., M.P. Penfield and M.F. Heim-Edelman. 1991. Yeast bread containing distillers' dried grain: dough development and bread quality. *Journal of Food Quality* 14(4): 331-334.

Bunell, R.H. and J.C. Bauernfeind. 1962. Chemistry, uses and properties of carotenoids in foods. *Food Technology* 16: 42–43.

Burkholder, T. and R. Lieber. 1996. Stepwise regression is an alternative to splines for fitting noisy data. *Journal of Biomechanics* 29(2): 235-238.

Calzada, J.F. and M. Peleg. 1978. Mechanical interpretation of compressive stress-strain relationships of solid foods. *Journal of Food Science* 43(4): 1087-1092.

Canadian Biomass, 2014. Canadian Biomass Magazine. http://www.canadianbiomassmagazine.ca/content/view/4228/57/ (2014/04/15).

Carr Jr, R. L. 1965. Evaluating flow properties of solids. *Chemical Engineering* 72(3): 163–168.

Carone, M.T., A. Pantaleo and A. Pellerano. 2011. Influence of process parameters and biomass characteristics on the durability of pellets from the pruning residues of Olea europaea L. *Biomass and Bioenergy* 35(1): 402-410.

Cenkowski S., C. Pronyk, D. Zmidzinska and W.E. Muir. 2007. Decontamination of food products with superheated steam. *Journal of Food Engineering* 83(1): 68–75.

Cenkowski, S., M.E. Sosa-Morales and M.C. Flores-Alvarez. 2012. Protein content and antioxidant activity of distillers' spent grain dried at 150°C with superheated steam and hot air. *Drying Technology: An International Journal* 30(11-12): 1292-1296.

Chang, Y.F., C.J. Lin, J.M. Chyan, I.M. Chen and J.E. Chang. 2007. Multiple regression models for the lower heating value of municipal solid waste in Taiwan. *Journal of Environmental Management* 85(4): 891–899.

Chen, Z., W. Wu and P.K. Agarwal. 2000. Steam-drying of coal. Part 1. Modeling the behavior of a single particle. *Fuel* 79: 961–973.

Cheryan, M. 2002. Corn oil and protein extraction method. United States Patent 6,433,146.

Ciolkosz, D. 2009. Renewable and Alternative Energy Fact Sheet. Biomass Energy Center and Department of Agricultural and Biological Engineering. Publications Distribution Center, The Pennsylvania State University, PA.

Clementson, C.L. and K.E. Ileleji. 2010. Variability of bulk density of distillers dried grains with solubles (DDGS) during gravity-driven discharge. *Bioresource Technology* 101(14): 5459–5468.

Cliff, M.A., M.C. Dever, J.W. Hall and B. Girard. 1996. Development and evaluation of multiple regression models for prediction of sweet cherry liking. *Food Research International* 28(6): 583-589.

Crenshaw, T.D. 2001. Calcium, Phosphorus, Vitamin D, and Vitamin K in swine nutrition. In: *Swine Nutrition*, 2nd Edition, eds A.J. Lewis and L.L. Southern. CRC Press.

Dawson, K.R., J. O'Palka, N. W. Hether, L. Jackson and P. W. Gras. 1984. Taste panel preference correlated with lipid composition of barley dried distillers' grains. *Journal of Food Science* 49(3): 787-790.

Dev, S.R.S. and V.G.S. Raghavan. 2012. Advancements in drying techniques for food, fiber, and fuel. *Drying Technology: An International Journal* 30(11-12): 1147-1159.

Doelker, E. 1993. Comparative compaction properties of various microcrystalline cellulose types and generic products. *Drug Development and Industrial Pharmacy* 19 (17-18): 2399- 2471.

Douglas, W.J.M. 1994. Drying paper in superheated steam. *Drying Technology: An International Journal* 12(6): 1341–1355.

Dresse, P.C. and R.C. Hoseney. 1982. Baking properties of the bran fraction from brewer's spent grains. *Cereal Chemistry* 59(2): 89-91.

Dwianto, W., T. Morooka, M. Norimoto and T. Kitajima. 1999a. Stress relaxation of sugi wood (Cryptomeria japonica D. Don) in radial compression under high temperature steam. *Holiforschung* 53(5): 541-546.

Dwianto, W., T. Morooka, M. Norimoto and T. Kitajima. 1999b. Method for measuring viscoelastic properties of wood under high temperature and high pressure steam conditions. *Journal of Wood Science* 45(5): 373-377.

Ezhil, C. 2010. Superheated Steam Drying of Foods-A Review. *World Journal of Dairy and Food Sciences* 5(2): 214-217.

FAO. 2011. Bioenergy, Food Security. http://www.fao.org/bioenergy/foodsecurity/befsci/en/ (2011/04/28).

Fahad, M. K. 1996. Stresses and failure in the diametral compression test. *Journal of Materials Science* 31(14): 3723-3729.

Farely, R. and F.H.H. Valentin. 1967/68. Effect of particle size upon strength of powders. *Powder Technology* 45(1): 344–354.

Fausett, H., C. Gayser and A.K. Dash. 2000. Evaluation of quick disintegrating calcium carbonate tablets. *AAPS PharmSciTech* 1(3): 37–43.

Fell J. T. and J. M. Newton. 1970. Determination of tablet strength by the diametral-compression test. *Journal of Pharmaceutical Sciences* 59(5): 688–691.

Fiasco, B.A., G. Rubenthaler, M. Borhan and F.M. Dong. 1990. Baking properties of bread and cookies incorporating distillers' or brewer's grain from wheat or barley. *Journal of Food Science* 55(2): 424-429.

Fitzpatrick, J. 1998. Sludge processing by anaerobic digestion and superheated steam drying. *Water Research* 32(10): 2897-2902.

Franke, M. and A. Rey. 2006. Pelleting quality, 78–79. World Grain.

Frette, V., K. Christensen, A. Malthesorenssen, J. Feder, T. Jossang and P. Meakin. 1996. Avalanche dynamics in a pile of rice. *Nature* 379(4): 49-52.

Frocht, M.M. 1947. *Photoelasticity*. New York: John Wiley & Sons.

Ganesan ,V., K.A. Rosentrater and K. Muthukumarappan. 2008a. Flowability and handling characteristics of bulk solids and powders – a review with implications for DDGS. *Biosystems Engineering* 101(4): 425–435.

Ganesan, V., K. Muthukumarappan and K.A. Rosentrater. 2008b. Flow properties of DDGS with varying soluble and moisture contents using jenike shear testing. *Powder Technology* 187(2): 130–137.

Ganesan, V., K. Muthukumarappan and K.A. Rosentrater. 2008c. Effect of moisture content and soluble level on the physical, chemical, and flow properties of distillers dried grains with solubles (DDGS). *Cereal Chemistry* 85(4): 464–470.

Gamero, M., S.M. Fiszman and L. Durán. 1993. Stress relaxation of fruit gels. Evaluation of models and effects of composition. *Journal Food Science* 58(5):1125–1128.

Garcia-Maraver, A., A. F. Ramos-Ridao, D.P. Ruiz and M. Zamorano. 2010. Quality of pellets from olive grove residual biomass. In *Proceedings of International*

Conference on Renewable Energies and Power Quality (ICREPQ'10). Granada, Spain. March 23-25.

Ghani, I.M.M. and S. Ahmad. 2010. Stepwise multiple regression method to forecast fish landing. *Procedia Social and Behavioural Sciences* 8: 549–554.

Gilpin, A.S., T.J. Herrman, K.C. Behnke and F.J. Fairchild. 2002. Feed moisture, retention time, and steam as quality and energy utilization determinants in the pelleting process. *Applied Engineering in Agriculture* 18(3): 331–338.

Grover, P.D. and S.K. Mishra. 1996. Biomass briquetting: technology and practices. Field document no. 46. Bangkok, Thailand: Regional wood energy development program in Asia, Food and Agriculture Organization of the United Nations.

Guillen-Casla, V., N. Rosales-Conrado, M.E. Leon-Gonzalez, L.V. Perez-Arribas and L. M. Polo-Diez. 2011. Principal component analysis (PCA) and multiple linear regression (MLR) statistical tools to evaluate the effect of E-beam irradiation on ready-to-eat food. *Journal of Food Composition and Analysis* 24(3): 456–464.

Gunduz, G., S. Korkut, D. Aydemir and I. Bekar. 2009. The density, compression strength and surface hardness of heat treated hornbeam ("Carpinus betulus") wood. Maderas. *Ciencia y tecnología* 11(1): 61-70.

Gupta, R. C. 2010. *Theory and Laboratory Experiments in Ferrous Metallurgy*. New Delhi, India: PHI Learning Pvt. Ltd.

Grossman, Y.L., S.L. Ustin, S. Jacquemoud, E.W. Sanderson, G. Schmuck and J. Verdeboutt. 1996. Critique of stepwise multiple linear regression for the extraction of leaf biochemistry information from leaf reflectance data. *Remote Sensing of Environment* 56(3): 182-193.

Head, D.S., S. Cenkowski, S. Arntfield and K. Henderson. 2010. Superheated steam processing of oat groats. *LWT-Food Science and Technology* 43(4): 690-694.

Herrero, A.M., K. Heia and M. Careche. 2004. Stress relaxation test for monitoring post mortem textural changes of ice-stored cod (Gadus morhua L.). *Journal of Food Science* 69(4): 178-182.

Hertz, H. 1895. Gesammelte Werke (CollectedWorks), Vol.1. Leipzig, Germany.

Holley, C.A. 1983. The densification of biomass by roll briquetting. *Proceedings of the Institute for Briquetting and Agglomeration* (IBA) 18: 95-102.

Hondros, G. 1959. The evaluation of Poisson's ratio and the modulus of materials of a low tensile resistance by the Brazilian (indirect tensile) test with particular reference to concrete. *Australian Journal of Applied Science* 10(3): 243–268.

Hwang, K.T., S.L. Cuppett, C.L. Weller and M.A. Hanna. 2002a. Properties, composition, and analysis of grain sorghum wax. *Journal of the American Oil Chemists' Society* 79(6): 521–527.

Hwang, K.T., S.L. Cuppett, C.L. Weller and M.A. Hanna. 2002b. HPLC of grain sorghum wax classes highlighting separation of aldehydes from wax esters and steryl esters. *Journal of Separation Science* 25(9): 619–623.

Ileleji, K.E., K.S. Prakash, R.L. Stroshine and C.L. Clementson. 2007. An investigation of particle segregation in corn processed dried distillers grains with soluble (DDGS) induced by three handling scenarios. *Bulk Solids and Powder Science and Technology* 2: 84–94.

Ileleji, K.E. and K.A. Rosentrater. 2008. On the physical properties of dried distillers grains with solubles (DDGS). ASAE Paper No. 084576. St. Joseph, MI:

ASABE.

Ileleji, K.E. and B. Zhou. 2008. The angle of repose of bulk corn stover particles. *Powder Technology* 187(2): 110–118.

Iyota, H., T. Inoue, J. Yamagata and N. Nishimura. 2008. Effect of time-dependent humidity profiles from air to superheated steam on drying of a wetted starch sphere. *Drying Technology* 26(2): 211-221.

Iyota, H., N. Nishimura, M. Yoshida and T. Nomura. 2001. Simulation of superheated drying considering initial steam condensation. *Drying Technology: An International Journal* 19(7): 1425–1440.

Irvine, Jr. T.F. and Liley, P.E. 1984. Steam and gas tables with computer equations. Orlando: Academic Press Inc.

Johansson, A., C. Fyhr and A. Rasmuson. 1997. High temperature convective drying of wood chips with air and superheated steam. *International Journal of Heat and Mass Transfer* 40(12): 2843-2858.

Johnson, P., S. Cenkowski and J. Paliwal. 2010. Issues with utilisation of brewers' spent grain. *Stewart Postharvest Review* 6(4): 1-8.

Johnson, P., S. Cenkowski and J. Paliwal. 2011a. Bulk Density and Angle of Repose of Distiller's Spent Grain under Different Drying Methods and Soluble Concentrations. *Canadian Society for Bioengineering Conference*. Paper No. CSBE11-18. Winnipeg, MB. July 10-13.

Johnson, P., S. Cenkowski and J. Paliwal. 2011b. Current and Potential Applications of Distiller's Spent Grain. *Canadian Society for Bioengineering Conference*. Paper No. CSBE11-316. Winnipeg, MB. July 10-13.

Johnson, P., Cenkowski, S., Paliwal, J., 2013a. Superheated steam drying characteristics of single cylindrical compacts produced from wet distiller's spent grain. *Canadian Society for Bioengineering Conference*. Paper No. CSBE13-11. Saskatoon, SK. July 7-10.

Johnson, P., Cenkowski, S., Paliwal, J., 2013b. Compaction and relaxation characteristics of single compacts produced from distiller's spent grain. *Journal of Food Engineering* 116(2): 260–266.

Johnson, P., S. Cenkowski, J. Paliwal and S. Arntfield. 2014a. Significance of Particle Size Distribution on the Disintegration of Compacted Spent Grain during Drying in Superheated Steam. *CSBE/SCGAB Annual International Meeting*. Paper No. 1908835. Montreal, QC. July 13-16.

Johnson, P., S. Cenkowski and J. Paliwal. 2014b. Analysis of the disintegration of distiller's spent grain compacts as affected by drying in superheated steam. *Drying Technology: An International Journal* 32(9): 1060-1070.

Johnson, P., S. Cenkowski and J. Paliwal. 2014c. Effect of solubles on Disintegration of distiller's spent grain compacts during superheated steam drying. *Drying Technology: An International Journal*. DOI: 10.1080/07373937.2014.967403 (Accepted, in press).

Johnson, P., S. Cenkowski and J. Paliwal. 2014d. Analyzing the Effect of Particle Size on the Disintegration of Distiller's Spent Grain Compacts while Drying in Superheated Steam Dryer (under review).

Jones, W.D. (1960). *Fundamental Principles of Powder Metallurgy*, 242-370. London, UK: Edward Arnold Publishers Ltd.

Julson J.L., G. Subbarao, D.D. Stokke, H.H. Gieselman and K. Muthukumarappan. 2004. Mechanical Properties of Biorenewable Fiber/Plastic Composites. *Journal of Applied Polymer Science* 93(5): 2484–2493.

Jung, H.J. 1997. Analysis of forage fiber and cell walls in ruminant nutrition. *Journal of Nutrition* 127(5): 810S–813S.

Kaliyan, N. and R.V. Morey. 2009. Factors affecting strength and durability of densified biomass products. *Biomass and Bioenergy* 33(3): 337–359.

Kaliyan, N. 2008. *Densification of Biomass*. Michigan: ProQuest LLC.

Kamath, S., V.M. Puri and H.B. Manbeck. 1994. Flow property measurement using the Jenike cell for wheat flour at various moisture contents and consolidation times. *Powder Technology* 81(3): 293–297.

Kashaninejad, M., B. Kashaninejad and L. G. Tabil. 2010. Enhancing compaction characteristics of barley straw by microwave/chemical pretreatment. In *Proceedings of the XVIIth World Congress of the International Commission of Agricultural and Biosystems Engineering (CIGR)*, Québec City, QC. June 13-17.

Kemp, I. C., B.C. Fyhr, S. Laurent, M.A. Roques, C.E. Groenewold, E. Tsotsas, A.A. Sereno, C.B. Bonazzi, J. Bimbenet and M. Kind. 2001. Methods for processing experimental drying kinetics data. *Drying Technology: An International Journal* 19(1): 15-34.

Kingsly A.R.P., K.E. Ileleji and R.L. Stroshine. 2013. Stress relaxation behavior of corn distillers dried grains with solubles (DDGS) in relation to caking. *Powder Technology* 235: 866–872.

Kleinschmit, D.H., D.J. Schingoethe, K.F. Kalscheur and A.R. Hippen. 2006. Evaluation of various sources of corn distillers dried grains plus solubles for lactating dairy cattle. *Journal of Dairy Science* 89(12): 4784–4794.

Konstance, R.P. and V.H. Holsinger. 1992. Development of rheological test methods for cheese. *Food Technology* 46(1): 105-109.

Kozanoglu, B., A.C. Vazquez, J.W. Chanes and J.L. Patino. 2006. Drying of seeds in a superheated steam vacuum fluidized bed. *Journal of Food Engineering* 75(3): 383–387.

Lam, P.S., S. Sokhansanj, X. Bi, C.J. Lim, L.J. Naimi, M. Hoque, S. Mani, A.R. Womac, X.P. Ye and S. Narayan. 2008. Bulk density of wet and dry wheat straw and switchgrass particles. *Applied Engineering in Agriculture* 24(3): 351-358.

Larson, E.M., R.A. Stock, T.J. Klopfenstein, M.H. Sindt and R.P. Huffman. 1993. Feeding value of wet distillers by-products for finishing ruminants. *Journal of Animal Science* 71(8): 2228–2236.

Lawton, J.W. 2002. Zein: a history of processing and use. *Cereal Chemistry* 79(1): 1–18.

Li, Y. and H. Liu. 2000. High-pressure densification of wood residues to form an upgraded fuel. *Biomass and Bioenergy* 19(3): 177–186.

Lindley, J.A. and M. Vossoughi. 1989. Physical properties of biomass briquettes. *Transactions of the ASAE* 32(2): 361–366.

Liu, C. and C. E. Wyman. 2005. Partial flow of compressed-hot water through corn stover to enhance hemicellulose sugar recovery and enzymatic digestibility of cellulose. *Bioresource Technology* 96(18): 1978–1985.

Liu S.X., M. Singh and G. Inglett. 2011. Effect of incorporation of distillers' dried grain with solubles (DDGS) on quality of cornbread. *LWT - Food Science and Technology* 44(3): 713-718.

Maga, J. A. and K.E. van Everen. 1989. Chemical and sensory properties of whole wheat pasta products supplemented with wheat-derived dried distillers grain (DDG). *Journal of Food Processing & Preservation* 13(1): 71-78.

Maier, D.E. and J. Gardecki. 1992. Feed mash conditioning field case studies. ASAE Paper No. 92-1541. St. Joseph, MI, ASABE.

Malvern Instruments. 1997. Getting started, MAN 0101, Issue1.3. Malvern Instruments Ltd. Spring Lane South, Malvern. Worcestershire, UK.

Mammarella E.J., D.A. De Piante Vicín and A.C. Rubiolo. 2002. Evaluation of stress-strain for characterization of the rheological behavior of alginate and carrageenan gels. *Brazilian Journal of Chemical Engineering* 19(4): 403- 410.

Mani, S., L.G. Tabil and S. Sokhansanj. 2003. An overview of compaction of biomass grinds. *Powder Handling and Processing* 15(3): 160–168.

Mani, S., L.G. Tabil and S. Sokhansan. 2004. Evaluation of compaction equations applied to four biomass species. *Canadian Biosystems Engineering* 46(3): 3.55-3.61.

Mani, S., L.G. Tabil and S. Sokhansanj. 2006. Effects of compressive force, particle size and moisture content on mechanical properties of biomass pellets from grasses. *Biomass and Bioenergy* 30(7): 648–654.

Mani, S., L.G. Tabil and S. Sokhansanj. 2006b. Specific energy requirement for compacting corn stover. *Bioresoure Technology* 97(12): 1420–1426.

Markowski, M., S. Cenkowski, D. W. Hatcher, J. E. Dexter and N. N. Edwards. 2003. The effect of superheated-steam dehydration kinetics on textural properties of Asian noodles. *Transactions of the ASAE* 46(2): 389–395.

Marquina, P.L., J. Burgos and R. Oria. 2001. Application of a compression—relaxation test for the characterization of burlat sweet cherry. *Journal of Texture Studies* 32(1): 15–30.

McCabe, W.L., J.C. Smith and P. Harriott. 1993. *Unit Operations of Chemical Engineering,* 5th edition. Jurong, Singapore: McGraw-Hill International Publication.

McMullen, J., O.O. Fasina, C.W. Wood and Y. Feng. 2005. Storage and handling characteristics of pellets from poultry litter. *Applied Engineering in Agriculture* 21(4): 645–651.

Mickley, H.S., T.K. Sherwood and C.E. Reed. 1957. *Applied Mathematics in Chemical Engineering*, 2nd edition, 8-14. New York: McGraw-Hill Book Co.

Mingard, K., R. Morrell, P. Jackson, S. Lawson, S. Patel and R. Buxton. 2009. Good practice guide for improving the consistency of particle size measurement. Measurement Good Practice Guide No. 111. Industry and Innovation of Division, National Physical Laboratory. CERAM Research. Particles CIC, University of Leeds. Particle Technology Ltd., Teddington, Middlesex: UK.

Moller, J. 2009. Gravimetric determination of acid detergent fiber and lignin in feed: interlaboratory study. *The Journal of AOAC INTERNATIONAL* 92(1): 74-90.

Morad, M.M., C. A. Doherty and L.W. Rooney. 1984. Utilization of dried distillers' grain from sorghum in baked food systems. *Cereal Chemistry* 61(5): 409-414.

Moreyra, R. and M. Peleg. 1980. Compressive deformation patterns of selected food powders. *Journal of Food Science* 45(4): 866-868.

Moriasi, D.N., J.G. Arnold, M.W. Van Liew, R.L. Bingner, R.D. Harmel and T. L. Veith. 2007. Model evaluation guidelines for systematic quantification of accuracy in watershed simulations. *Transactions of the ASABE* 50(3): 885−900.

Mosqueda, M.R., L.G. Tabil and C. Christensen. 2013. Effect of drying conditions and level of condensed distillers solubles on protein quality of wheat distillers dried grain with solubles. *Drying Technology: An International Journal* 31(7): 811-824.

Mujumdar, A.S. 1991. Drying technologies of the future. *Drying Technology: An International Journal* 9(2): 325-347.

Mujumdar, A.S. and C.L. Law. 2010. Drying technology: Trends and applications in postharvest processing in postharvest processing. *Food and Bioprocess Technology* 3(6): 843-852.

Muntoz, A.M., R.M. Pangbom and A.C. Noble. 1986. Sensory and mechanical attributes of gel texture. I. Effect of gelatin concentration. *Journal of Texture Studies* 17(1): 1-16.

Murphy, P.A., S. Hendrich, C. Landgren and C. Bryant. 2006. Food mycotoxins: an update. *Journal of Food Science* 71(5): 51-65.

Nakamura, T., T.J. Klopfenstein, D.J. Gibb and R.A. Britton. 1994. Growth efficiency and digestibility of heated proteins fed to growing ruminants. *Journal of Animal Science* 72(3): 774–782.

Nathakaranakule, A., W. Kraiwanichkul and S. Soponronnarit. 2007. Comparative study of different combined superheated-steam drying techniques for chicken meat. *Journal of Food Engineering* 80(4): 1023-1030.

Nichols, J.R., D.J. Schingoethe, H.A. Maiga, M.J. Brouk and M.S. Piepenbrink. 1998. Evaluation of corn distiller's grains and ruminally protected lysine and methionine for lactating dairy cows. *Journal of Dairy Science* 81(2):482–491.

Nielsen, B.R., H. Stapelfeldt and L.H. Skibsted. 1997. Early Prediction of the Shelf-life of Medium-heat Whole Milk Powders Using Stepwise Multiple Regression and Principal Component Analysis. *International Diary Journal* 7(5): 341-348.

NRCAN, 2013. Natural Resources Canada (NRCAN). http://www.nrcan.gc.ca/energy/alternative-fuels/fuel-facts/ethanol/3493 (2014/04/15).

Oba, M., G.B. Penner, T.D. Whyte and K. Wierenga. 2010. Effects of feeding triticale dried distiller's grains plus soluble as a nitrogen source on productivity of lactating dairy cows. *Journal of Dairy Science* 93(5): 2044-2052.

Obernberger, I. and G. Thek. 2004. Physical characterisation and chemical composition of densified biomass fuels with regard to their combustion behaviour. *Biomass and Bioenergy* 27(6): 653–669.

Oksman, K. and C. Clemons. 1998. Mechanical properties and morphology of impact modified polypropylene–wood flour composites. *Journal of Applied Polymer Science* 67(9): 1503–1513.

Pakowski, Z., B. Krupinska and R. Adamski. 2007. Prediction of sorption equilibrium both in air and superheated steam drying of energetic variety of willow Salix viminalis in a wide temperature range. *Fuel* 86(12-13): 1749-1757.

Pang, S. and M. Dakin. 1999. Drying rate and temperature profile for superheated steam vacuum drying and moist air drying of softwood lumber. *Drying Technology: An International Journal* 17(6): 1135–1147.

Papadimitropoulos, E. A. and W.C. Duncan-Hewitt. 1992. Predicting the post consolidation relaxation behavior of sodium chloride tablets. *Journal of Pharmaceutical Sciences* 81(7): 701-704.

Parsons, C.M., C. Martinez, V. Singh, S. Radhakrishman and S. Noll. 2006. Nutritional value of conventional and modified DDGS for poultry. Multi-State Poultry Nutrition and Feeding Conference. Indianapolis, IN. May 24-25.

Payne, J.D. 1978. Improving quality of pellet feeds. *Milling Feed and Fertilizer* 162: 34–41.

Payne, J.D. 2006. Troubleshooting the pelleting process. In *Feed technology technical report series*, 17-23. Singapore: American Soybean Association, International Marketing Southeast Asia.

Peleg, M. 1979. Characterization of the stress relaxation curves of solid foods. *Journal of Food Science* 44(1): 277–281.

Peleg, M. 1980. Linearization of relaxation and creep curves of solid biological materials. *Journal of Rheology* 24(4): 451–463.

Peleg, M. 1987. The basics of food rheology. In *Food Texture, Instrumental and Sensory Measurement*, ed. H.R. Moskowitz, 3-33. New York: Marcel Dekker.

Peleg, M. and M.D. Normand. 1983. Comparison of two methods for stress relaxation data presentation of solid foods. *Rheologica Acta* 22(1): 108-113.

Peleg, M. and N. Pollak. 1982. The problem of equilibrium conditions in stress relaxation analysis of solid foods. *Journal of Texture Studies* 13(1): 1-11.

Peleg, M. and R. Moreyra. 1979. Effect of moisture on the stress relaxation pattern of compacted powders. *Powder Technology* 23(2): 277–279.

Pettersson, D., H. Klas and P. Aman. 1987. Nutritional value for chickens of dried distillers- spent-grain from barley and dehulled barley. *Animal Feed Science and Technology* 17(2): 145-156.

Pfost, H.B. 1964. The effect of lignin binders, die thickness and temperature on the pelleting process. *Feed Stuffs* 36(20): 54.

Pietsch, W. 2002. Agglomeration processes – phenomena, technologies, equipment. Weinheim, Germany: Wiley-VCH.

Pons M. and S.M. Fiszman. 1996. Instrumental texture profile analysis with particular reference to gelled systems. *Journal of Texture Studies* 27(6): 597- 624.

Powers, W.J., H.H. Van Horn, B. Harris, Jr. and C.J. Wilcox. 1995. Effects of variable sources of distillers dried grains plus solubles on milk yield and composition. *Journal of Dairy Science* 78(2): 388-396.

Prachayawarakorn, S. and S. Soponronnarit. 2010. Chapter 10, Superheated-steam drying applied in food engineering. In *Innovation in Food Engineering: New Techniques and Products*, eds M. L. Passos and C. P. Ribeiro, 331-359. USA: CRC Press (Taylor and Francis).

Prentice, N. and B.C.D Appolonia. 1977. High-fiber bread containing brewer's spent grain. *Cereal Chemistry* 54: 1084-1095.

Prentice, N., L.T.L. Kissell, R.C. Lindsay and W. T. Yamazaki. 1978. High-fiber cookies containing brewers' spent grain. *Cereal Chemistry* 55(5): 712-721.

Procopio, A. T., A. Zavaliangos and J. C. Cunningham. 2003. Analysis of the diametrical compression test and the applicability to plastically deforming materials. *Journal of Materials Science* 38(17): 3629–3639.

Pronyk, C., S. Cenkowski and W.E. Muir. 2010. Drying kinetics of instant Asian noodles processed in superheated steam. *Drying Technology: An International Journal* 28(2): 304-314.

Pronyk, C., S. Cenkowski, W.E. Muir and O.M. Lukow. 2008. Effects of superheated steam processing on the textural and physical properties of Asian noodles. *Drying Technology: An International Journal* 26(2): 192-203.

Rasco, B.A., A.E. Hashisaka, F.M. Dong and M.A. Einstein. 1989. Sensory evaluation of baked foods incorporated different levels of distillers' dried grains with solubles from soft white winter wheat. *Journal of Food Science* 54(2): 337-342.

Rasco, B.A., S.E. Downy and F.M. Dong. 1987a. Consumer acceptability of baked goods containing distillers' dried grains with solubles from soft white winter wheat. *Cereal Chemistry* 64(3): 139-143.

Rasco, B.A., S.E. Downey, F.M. Dong and J. Ostrander. 1987b. Consumer acceptability and color of deep-fried fish coated with wheat or corn distillers' dried Grains with solubles (DDGS). *Journal of Food Science* 52(6): 1506-1508.

Ratti, C. 2001. Hot air and freeze-drying of high-value foods: a review. *Journal of Food Engineering* 49(4): 311-319.

Ratti, C (ed.). 2008. Advances in Food Dehydration: Technology & Engineering. CRC Press. Reddy, N.R., M.D. Pierson and F.W. Cooler. 1986. Supplementation of wheat muffins with dried distillers grain flour. *Journal of Food Quality* 9(4): 243-249.

Reddy, J.A. and R. Stoker. 1991. Bakery product from distiller's grain. United States Patent 5225228.

Reese, D.E. and A.J. Lewis. 1989. Nutrient content of Nebraska corn. Nebraska Cooperative Extension Service. Nebraska Swine Report. Pub No. EC89-219, 5-7.

Rey, J. and M. Vandamme. 2013. On the shrinkage and stiffening of a cellulose sponge upon drying. *Journal of Applied Mechanics* 80(2): 020908-1– 6.

Rosendahl, L (ed.). 2013. Biomass Combustion Science, Technology and Engineering: Woodhead Publishing Series in Energy No. 40. Cambridge: Woodhead Publishing Ltd.

Rosenau, J., J. Calzada and M. Peleg. 1978. Some rheological properties of a cheese-like product prepared by direct acidification. *Journal of Food Science* 43(3): 948- 950.

Rosentrater, K. A. 2006a. Understanding distillers dried grain storage, handling, and flowability challenges. *Distillers Grains Quarterly* 1(1): 18–21.

Rosentrater, K.A. 2006b. Some physical properties of distillers dried grains with solubles (DDGS). *Applied Engineering in Agriculture* 22(4): 589–595.

Rosentrater, K. A. and K. Muthukumarappan. 2006. Corn ethanol co-products: generation, properties, and future prospects. *International Sugar Journal* 108(1295): 648–657.

Rosentrater, K. 2008a. US researchers investigate use of ethanol co-products as fillers for plastics. *Additives for Polymers* 2008(8): 4.

Rosentrater, K.A. 2008b. Adding value to distillers grains by pelleting. In *Proceedings from Corn Utilization and Technology Conference*, 1-6. Kansas City, MO. June 2-4.

Runge, C. and B. Senauer. 2007. How biofuels could starve the poor. Foreign Affairs 86: 41-53. http://www.foreignaffairs.com/articles/62609/c-ford-runge-and-benjamin-senauer/how-biofuels-could-starve-the-poor (2011/04/23).

Sa-adchom, P., T. Swasdisevi, A. Nathakaranakule and S. Soponronnarit. 2011. Mathematical model of pork slice drying using superheated steam. *Journal of Food Engineering* 104(4): 499-507.

Saikia, M. and Baruah, D. 2013. Analysis of physical properties of biomass briquettes prepared by wet briquetting method. *International Journal of Engineering Research and Development* 6(5): 12-14.

Salas-Bringas, C., L. Plassen, O.I. Lekang and R. B. Schüller. 2007. Measuring physical quality of pelleted feed by texture profile analysis, a new pellet tester and comparisons to other common measurement devices. *Annual Transactions of the Nordic Rheology Society* 15: 149-157.

Santhi, C., J.G. Arnold, J.R. Williams, W.A. Dugas, R. Srinivasan and L.M. Hauck. 2001. Validation of the SWAT model on a large river basin with point and

nonpoint sources. *Journal American Water Resources Association* 37(5): 1169-1188.

Santos, H.M.M and J.J.M.S Sousa. 2007. Pharmaceutical Manufacturing Handbook: Production and Processes. USA: Wiley.

Sastry, K.V.S. and D.W. Fuerstenau. 1973. Mechanisms of agglomerate growth in green pelletization. *Powder Technology* 7(2): 97-105.

Schwab, C.G. 1995. Protected proteins and amino acids for ruminants. In *Biotechnology in Animal Feeds and Animal Feeding*, eds R. J. Wallace and A. Chesson. Weinheim, Germany: V.C.H. Press.

Schlicher, M. 2005. The flowability factor. Ethanol Producer Magazine. http://www.ethanolproducer.com/article.jsp?article_id=115 (2011/05/25).

Semple R.L., A.S. Frio, P.A. Hicks and J.V. Lozare. 1989. Mycotoxin Prevention and Control in Food Grains. UNDP/FAO/REGNET and the ASEAN Grain Postharvest Program. Bangkok, Thailand.

Shankar, T. J., S. Sokhansanj, S. Bandyopadhyay and A. S. Bawa. 2008. A case study on optimization of biomass flow during single-screw extrusion cooking using genetic algorithm (GA) and response surface method (RSM). *Food and Bioprocess Technology* 3(4): 498-510.

Shaw, M. D. and L.G. Tabil. 2007. Compression and relaxation characteristics of selected biomass grinds. ASAE Paper No. 076183. St. Joseph, MI, ASABE.

Shi, Y., Z. Xiao, Z. Wang, X. Liu and D. Yang. 2011. Numerical simulation on superheated steam fluidized bed drying: II. Experiments and numerical simulation. *Drying Technology: An International Journal* 29(11): 1332–1342.

Shibata, H. and A.S. Mujumdar. 1994. Steam drying technologies: Japanese R&D. *Drying Technology: An International Journal* 12(6): 1485–1524.

Shinohara, K., Y. Idemitsu, K. Gotoh and T. Tanaka. 1968. Mechanism of gravity flow of particles from a hopper. *Industrial and Engineering Chemistry Process Design and Development* 7(3): 378–383.

Shrivastava, M., P. Shrivastava and K.K. Khankari. 1989. Densification characteristics of rice husk under cold and hot compression. In *Agricultural Engineering: Proceedings of the 11th International Congress on Agricultural Engineering*, eds. V.A. Dodd and P. M. Grace, 2441-2443. Rotterdam, The Netherlands: A.A. Balkema Pub.

SHRP Protocol. 1993. P07, for SHRP Test Designation. AC07, Resilient Modulus for Asphalt Concrete.

Shurson, J. and S. Noll. 2005. Feed and alternative uses for DDGS. Energy From Agriculture: New Technologies, Innovative Programs and Success Stories: Department of Animal Science, University of Minnesota.

SigmaStat 3.5. 2006. Chapter 10, Prediction and Correlation. In *SigmaStat 3.5 User's Manual*, 575-608. Point Richmond, CA, USA: Systat Software Inc.

Singh, V., R.A. Moreau and K.B. Hicks. 2003. Yield and phytosterol composition of oil extracted from grain sorghum and its wet-milled fractions. *Cereal Chemistry* 80(2): 126–129.

Singh, V. and S.R. Eckhoff. 1996. Effect of soak time, soak temperature, and lactic acid on germ recovery parameters. *Cereal Chemistry* 73(6): 716–720.

Singh, V. and S.R. Eckhoff. 1997. Economics of germ preparation for dry-grind ethanol

facilities. *Cereal Chemistry* 74: 462–466.

Singh, R., S. Mangaraj and S.D. Kulkarni. 2006. Particle size analysis of tomato powder. *Journal of Food Processing and Preservation* 30(1): 87–98.

Singh V.J., K.D. Rausch, P. Yang, H. Shapouri, R.L. Belyea and M.E. Tumbleson. 2001. Modified Dry Grind Ethanol Process. Technical Bulletin UILU *2001*-7021. Urbana, IL: Agricultural Engineering Department, University of Illinois.

Skoch, E.R., K.C. Behnke, C.W. Deyoe and S.F. Binder. 1981. The effect of steam-conditioning rate on the pelleting process. *Animal Feed Science and Technology* 6(1): 83–90.

Sokhansanj S., S. Mani, X. Bi, P. Zaini and L.G. Tabil. 2005. Binderless pelletization of biomass. *ASAE Annual International Meeting*. ASAE Paper No. 056061. St Joseph, Tampa, FL, USA. July 17–20.

Sokhansanj, S., R.T. Patil, O.O. Fasina, J. Irudayaraj and G. Ahmadnia. 1991. Procedures for evaluating durability and density of forage cubes and pellets. *Canadian Society for Agricultural Engineering.* Paper No. 91-402. Saskatoon, SK, Canada. July 29-31.

Somjai, T., S. Achariyaviriya, A. Achariyaviriya and K. Namsanguan. 2009. Strategy for longan drying in two-stage superheated steam and hot air. *Journal of Food Engineering* 95(2): 313-321.

Speckhahn, A., G. Srzednicki and D.K. Desai. 2010. Drying of beef in superheated steam. *Drying Technology: An International Journal* 28(9): 1072-1082.

Spiehs, M.J., M.H. Whitney and G.C. Shurson. 2002. Nutrient database for distiller's dried grains with solubles produced from new ethanol plants in Minnesota and South Dakota. *Journal of Animal Science* 80(10): 2639-2645.

Srinivasan, R., R.A. Moreau, C. Parsons, J.D. Lane and V. Singh. 2008. Separation of fiber from distillers dried grains using sieving and elutriation. *Biomass and Bioenergy* 32(5): 468–472.

Stroem, L.K., D.K. Desai and A.F.A. Hoadley. 2009. Superheated steam drying of Brewer's spent grain in a rotary drum. *Advanced Powder Technology* 20(3): 240–244.

Szczesniak, A. S. 1963. Classification of textural characteristics. *Journal of Food Science* 28(4): 385-389.

Szczesniak, A. S. and B. J. Hall. 1975. Application of the General Foods Texturometer to specific food products. *Journal of Texture Studies* 6(1): 117-138.

Tabil, L., P. Adapa and M. Kashaninejad. 2011. Biomass feedstock pre-processing – Part 2: Densification. In *Biofuel's Engineering Process Technology,* ed. M. A. S. Bernardes, 439-464. Brazil: InTech.

Tabil, L.G., S. Sokhansanj and R.T. Tyler. 1997. Performance of different binders during alfalfa pelleting. *Canadian Agricultural Engineering* 39(1): 17–23.

Tabil, L.G. and S. Sokhansanj. 1996. Process conditions affecting the physical quality of alfalfa pellets. *Applied Engineering in Agriculture* 12(3): 345–350.

Taechapairoj, C., I. Dhuchakallaya, S. Soponronnarit, S. Wetchacama and S. Prachayawarakorn. 2003. Superheated steam fluidized bed paddy drying. *Journal of Food Engineering* 58(1): 67-73.

Tang, Z. and S. Cenkowski. 2000. Dehydration dynamics of potatoes in superheated steam and hot air. *Canadian Agricultural Engineering* 42(1): 43-49.

Tang, Z., S. Cenkowski and M. Izydorczyk. 2005. Thin-layer drying of spent grains in superheated steam. *Journal of Food Engineering*. 67(4): 457–465.

Tavasoli, A., M.G. Ahangari, C. Soni and A.K. Dalai. 2009. Production of hydrogen and syngas via gasification of the corn and wheat dry distiller grains (DDGS) in a fixed-bed micro reactor. *Fuel Processing Technology* 90(4): 472–482.

Temmerman M., F. Rabier, P.D. Jensen, H. Hartmann and T. Bohm. 2006. Comparative study of durability test methods for pellets and briquettes. *Biomass and Bioenergy* 30(11): 964-972.

Thomas, M. and A.F.B. van der Poel. 1996. Physical quality of pelleted animal feed. 1. Criteria for pellet quality. *Animal Feed Science and Technology* 61(1-4): 89–112.

Thomas, M., D.J. van Zuilichem and A.F.B. van der Poel. 1997. Physical quality of pelleted animal feed. 2. Contribution of processes and its conditions. *Animal Feed Science and Technology* 64(2):173–92.

Thomas, M., P.T.H.J. Huijnen, T. van Vliet, D.J. van Zuilichem and A.F.B. van der Poel. 1999. Effects of process conditions during expander processing and pelleting on starch modification and pellet quality of tapioca. *Journal of the Science of Food and Agriculture* 79(11): 1481–1494.

Thomas, M., T. van Vliet and A.F.B. van der Poel. 1998. Physical quality of pelleted animal feed. 3. Contribution of feedstuff components. *Animal Feed Science and Technology* 70(1-2): 59–78.

Timoshenko, S.P. and J. N. Goodier. 1970. Theory of elasticity. New York: McGraw-Hill.

Tjardes, K. and C. Wright. 2002. Feeding corn distiller's co-products to beef cattle. Extension Extra 2036: College of Agriculture and Biological Sciences, South Dakota State University.

Torres, J.D., A. Tárrega and E. Costell. 2010. Storage stability of starch-based dairy desserts containing long-chain inulin: Rheology and particle size distribution. *International Dairy Journal* 20(1): 46‑52.

Tsen, C.C., W. Eyestone and J.L. Weber. 1982. Evaluation of the quality of cookies supplemented with distillers' dried grain flours. *Journal of Food Science* 47(2): 684-685.

Tsen C.C., J.L. Weber and W. Eyestone. 1983. Evaluation of distillers' dried grain flour as a bread ingredient. *Cereal Chemistry* 60(4): 295-297.

Tumuluru, J.S., L. Tabil, A. Opoku, M.R. Mosqueda and O. Fadeyi. 2010. Effect of process variables on the quality characteristics of pelleted wheat distiller's dried grains with soluble. *Biosystems Engineering* 105(4): 466–475.

Tumuluru, J.S., C.T. Wright, J.R. Hess and K.L. Kenney. 2011. A review of biomass densification systems to develop uniform feedstock commodities for bioenergy application. *Biofuels, Bioproducts and Biorefining* 5(6): 683–707.

Turner, R. 1995. Bottom line in feed processing: achieving optimum pellet quality. *Feed Management* 46: 30–33.

UNEP, 2009. *United Nations Environment Programme.* http://www.unep.org/dtie/ (2011/04/23).

US Grains Council. 2008. Physical and chemical characteristics of DDGS. In *DDGS User Handbook*. www.grains.org (2011/05/25).

van Deventer, H.C. 2004. Industrial superheated steam drying. TNO-report. R 2004/239. Apeldoorn, The Netherlands: TNO Environment, Energy and Process Innovation.

van Deventer, H.C. and R.M.H. Heijmans. 2001. Drying with superheated steam. *Drying Technology: An International Journal* 19(8): 2033–2045.

van der Voort Maarschalk, K., K. Zuurman, H. Vromans, G. K. Bolhuis and C. F. Lerk. 1996. Porosity expansion of tablets as a result of bonding and deformation of particulate solids. *International Journal of Pharmaceutics* 140(2): 185-193.

Van Liew, M.W., T. L. Veith, D.D. Bosch and J.G. Arnold. 2007. Suitability of SWAT for the conservation effects assessment project: A comparison on USDA-ARS experimental watersheds. *Journal of Hydrologic Engineering* 12(2): 173-189.

Van Soest, P.J. and J.B. Robertson. 1980. Systems of analysis for evaluating fibrous feeds. In *Standardization of Analytical Methodology in Feeds*, eds W.J. Pigden, C. C. Balch, M. Graham, 49–60. Canada: International Research Development Center.

Wall, J.S., Y.V. Wu, W.F. Kwolek, G.N. Bookwalter, K. Warner and M.R. Gumbmann. 1984. Corn distillers grains and other by-products of alcohol production in blended foods. I. Compositional and nutritional studies. *Cereal Chemistry* 61(6): 504-509.

Wang, L., C.L. Weller, V.L. Schlegel, T.P. Carr and S.L. Cuppett. 2008. Supercritical CO_2 extraction of lipids from grain sorghum dried distillers grains with solubles.

Bioresource Technology 99(5): 1373-82.

Weir, C. E. 1952. Effect of moisture on compressibility of natural high polymers. *Journal of Research of the National Bureau of Standards* 49(3): 135-139.

Whitney, M.H., M.J. Spiehs and G.C. Shurson. 2001. Availability of phosphorus in distiller's dried grains with solubles for growing swine. *Journal of Animal Science* 79: 108 (Suppl.1).

Whitney, M.H., M.J. Spiehs, G.C. Shurson and S.K. Baidoo. 2000. Apparent ileal digestibilities of corn distiller's dried grains with solubles produced by new ethanol plants in Minnesota and South Dakota. *Journal of Animal Science* 78: 185 (Suppl. 1).

Winowiski, T. 1985. Optimizing pelleting temperature. *Feed Management* 36(7): 28–33.

Winowiski, T.S. 1995. Factors that affect pellet quality and trouble-shooting the pelleting process. Technical bulletin on feed technology, vol. FT23-. Singapore: American Soybean Association.

Wood, J.F. 1987. The functional properties of feed raw materials and the effect on the production and quality of feed pellets. *Animal Feed Science and Technology* 18(1): 1–17.

Woods, B., H. Husain and A.S. Mujumdar. 1994. Techno -economic assessment of potential superheated steam drying applications in Canada. Report 9138 U 888. Montreal, QC: Canada Electrical Association.

Wright, P.J.F. 1955. Comments on an indirect tensile test on *concrete* cylinders. *Magazine of Concrete Research* 7(20): 87-96.

Wu, Y.V. and A.C. Stringfellow. 1982. Corn distillers' dried grains with solubles and corn distillers' dried grains: Dry fractionation and composition. *Journal of Food Science* 47(4): 1155-1157.

Xu, W., N. Reddy and Y. Yang. 2007. An acidic method of zein extraction from DDGS. *Journal of Agricultural and Food Chemistry* 55(15): 6279–6284.

Xu, W., N. Reddy and Y. Yang. 2009. Extraction, characterization and potential applications of cellulose in corn kernels and Distillers' dried grains with solubles (DDGS). *Carbohydrate Polymers* 76(4): 521–527.

Yamashiki, T., T. Matsui, K. Kowsaka, M. Saitoh, K. Okajima and K. Kamide. 1992. New class of cellulose fiber spun from the novel solution of cellulose by wet spinning method. *Journal of Applied Polymer Science* 44(4): 691–698.

Yan, H. and G.V. Barbosa-Canovas. 1997. Compression characteristics of agglomerated food powders: effect of agglomerate size and water activity. *Food Science and Technology International* 3(5): 351–359.

Yang, W.Z. and K.A. Beauchemin. 2006. Physically effective fiber: method of determination and effects on chewing, ruminal acidosis, and digestion by dairy cows. *Journal of Dairy Science* 89(7): 2618-2633.

York, P. and N. Pilpel. 1973. The tensile strength and compression behaviour of lactose, four fatty acids and their mixture in relation to tableting. *Journal of Pharmacy and Pharmacology* 25: 1-11.

Young, L.R., H.B. Pfost and A.M. Feyerherm. 1963. Mechanical durability of feed pellets. *Transactions of the ASAE* 6(2): 145–150.

Zamorano, M., V. Popov, M.L. Rodríguez and A. García-Maraver. 2011. A comparative study of quality properties of pelletized agricultural and forestry lopping residues. *Renewable Energy* 36(11): 3133-3140.

Zhang, L., D. Ruan and J. Zhou. 2001. Structure and properties of regenerated cellulose films prepared from cotton linters in NaOH/urea aqueous solution. *Industrial & Engineering Chemistry Research* 25(40): 5923–5928.

Zhou, Y.C., B.H. Xu, A.B. Yu and P. Zulli. 2002. Experimental and numerical study of the angle of repose of coarse spheres. *Powder Technology* 125(1): 45–54.

Zielinska, M. and S. Cenkowski. 2012. Superheated steam drying characteristic and moisture diffusivity of distillers' wet grains and condensed distillers' soluble. *Journal of Food Engineering* 109(3): 627-634.

Zielinska, M., S. Cenkowski and M. Markowski. 2009. Superheated steam drying of distillers' spent grains on a single inert particle. *Drying Technology: An International Journal* 27(12): 1279–1285.

APPENDICES

Appendix A

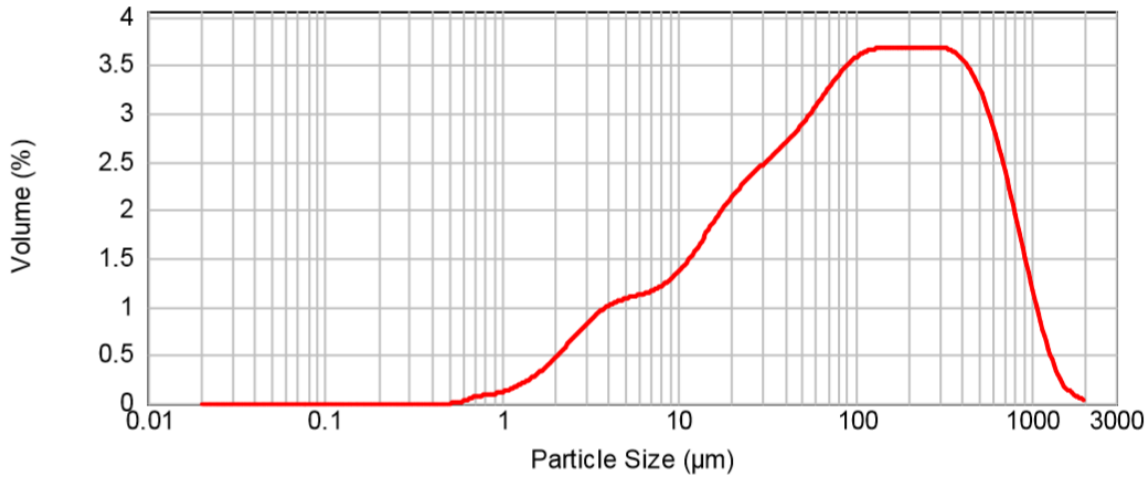

A.1. Particle size distribution of condensed distiller's solubles.
Note: Graph obtained from the Malvern Mastersizer indicating average of three particle size distribution readings.

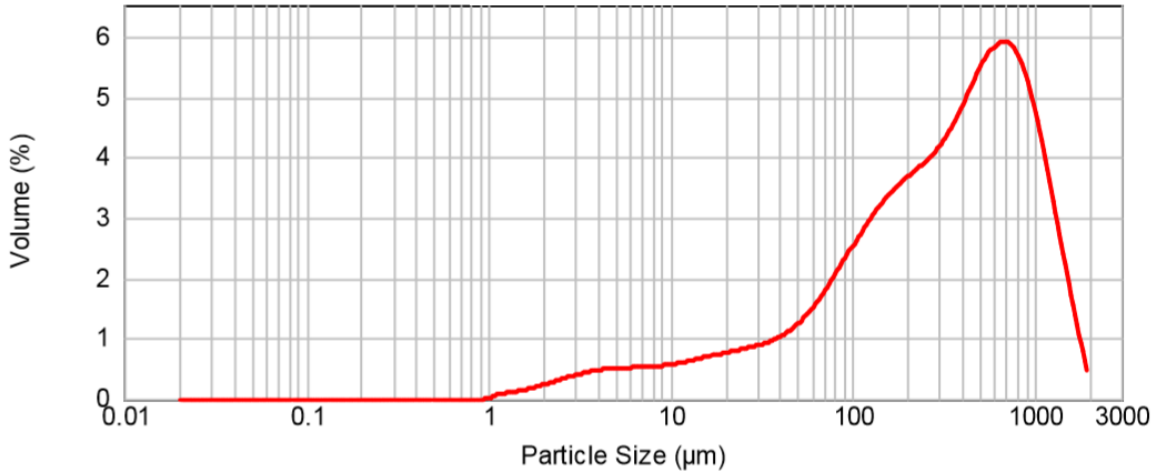

A.2. Particle size distribution of wet distiller's spent grain after grinding.
Note: Graph obtained from the Malvern Mastersizer indicating average of three particle size distribution readings.

Group Name	N	Missing	Mean	Std Dev	SEM
Col 1	3	0	120.192	5.175	2.988
Col 2	3	0	123.437	5.692	3.286
Col 3	3	0	105.823	3.826	2.209

All Pairwise Multiple Comparison Procedures (Holm-Sidak method):
Overall significance level = 0.05

Comparisons for factor:

Comparison	Diff of Means	t	Unadjusted P	Critical Level	Significant?
Col 2 vs. Col 3	17.614	4.349	0.00483	0.017	Yes
Col 1 vs. Col 3	14.369	3.548	0.0121	0.025	Yes
Col 2 vs. Col 1	3.245	0.801	0.454	0.050	No

A.3. Post-hoc analysis for percentage increase in volume of wet distiller's spent grain compacts while drying at different superheated steam temperatures during the initial condensation period (5s). Col 1, 2 and 3 represents percentage increase in volume for wet distiller's spent grain compacts dried with superheated steam temperatures of 110, 130 and 150°C, respectively at a superheated steam velocity of 0.9 m/s.

Group	N	Missing	Median	25%	75%
Col 1	3	0	125.663	123.495	128.596
Col 2	3	0	127.229	127.141	129.627
Col 3	3	0	107.931	102.316	115.391

All Pairwise Multiple Comparison Procedures (Tukey Test):

Comparison	Diff of Ranks	q	P<0.05
Col 2 vs Col 3	16.000	3.373	Yes
Col 2 vs Col 1	5.000	1.054	No
Col 1 vs Col 3	11.000	2.319	No

Note: The multiple comparisons on ranks do not include an adjustment for ties.

A.4. Post-hoc analysis for percentage increase in volume of wet distiller's spent grain compacts while drying at different superheated steam temperatures during the initial condensation period (5s). Col 1, 2 and 3 represents percentage increase in volume for wet distiller's spent grain compacts dried with superheated steam temperatures of 110, 130 and 150°C, respectively at a superheated steam velocity of 1.1 m/s.

Group Name	N	Missing	Mean	Std Dev	SEM
Col 1	3	0	128.635	2.538	1.465
Col 2	3	0	126.300	5.779	3.337
Col 3	3	0	113.903	1.784	1.030

All Pairwise Multiple Comparison Procedures (Holm-Sidak method):
Overall significance level = 0.05

Comparisons for factor:

Comparison	Diff of Means	t	Unadjusted P	Critical Level	Significant?
Col 1 vs. Col 3	14.732	4.764	0.00311	0.017	Yes
Col 2 vs. Col 3	12.397	4.009	0.00704	0.025	Yes
Col 1 vs. Col 2	2.335	0.755	0.479	0.050	No

A.5. Post-hoc analysis for percentage increase in volume of wet distiller's spent grain compacts while drying at different superheated steam temperatures during the initial condensation period (5s). Col 1, 2 and 3 represents percentage increase in volume for wet distiller's spent grain compacts dried with superheated steam temperatures of 110, 130 and 150°C, respectively at a superheated steam velocity of 1.4 m/s.

Group Name	N	Missing	Mean	Std Dev	SEM
Col 1	3	0	53.808	1.139	0.658
Col 2	3	0	55.359	0.607	0.351
Col 3	3	0	55.915	0.492	0.284

All Pairwise Multiple Comparison Procedures (Holm-Sidak method):
Overall significance level = 0.05

Comparisons for factor:

Comparison	Diff of Means	t	Unadjusted P	Critical Level	Significant?
Col 3 vs. Col 1	2.107	3.235	0.0178	0.017	No
Col 2 vs. Col 1	1.551	2.381	0.0547	0.025	No
Col 3 vs. Col 2	0.556	0.853	0.426	0.050	No

A.6. Post-hoc analysis for percentage decrease in density of wet distiller's spent grain compacts while drying at 110°C with different superheated steam velocities of 0.9, 1.1 and 1.4 m/s during the initial condensation period (5s). Col 1, 2 and 3 represents percentage decrease in density for wet distiller's spent grain compacts dried with superheated steam velocities of 0.9, 1.1 and 1.4 m/s, respectively at a superheated steam temperature of 110°C.

Group Name	N	Missing	Mean	Std Dev	SEM
Col 1	3	0	47.169	1.334	0.770
Col 2	3	0	42.733	2.689	1.552
Col 3	3	0	30.071	1.293	0.747
Col 4	3	0	19.908	1.944	1.123
Col 5	3	0	12.063	1.069	0.617

All Pairwise Multiple Comparison Procedures (Holm-Sidak method):
Overall significance level = 0.05

Comparisons for factor:

Comparison	Diff of Means	t	Unadjusted P	Critical Level	Significant?
Col 1 vs. Col 5	35.106	24.338	0.000000000313	0.005	Yes
Col 2 vs. Col 5	30.670	21.263	0.00000000118	0.006	Yes
Col 1 vs. Col 4	27.261	18.899	0.00000000373	0.006	Yes
Col 2 vs. Col 4	22.825	15.824	0.0000000209	0.007	Yes
Col 3 vs. Col 5	18.008	12.485	0.000000201	0.009	Yes
Col 1 vs. Col 3	17.098	11.853	0.000000328	0.010	Yes
Col 2 vs. Col 3	12.662	8.778	0.00000518	0.013	Yes
Col 3 vs. Col 4	10.163	7.046	0.0000352	0.017	Yes
Col 4 vs. Col 5	7.845	5.439	0.000285	0.025	Yes
Col 1 vs. Col 2	4.436	3.075	0.0117	0.050	Yes

A.7. Post-hoc analysis for percentage increase in length of distiller's spent grain compacts with different soluble levels during the initial condensation period (5s). Col 1, 2, 3, 4 and 5 represents percentage increase in length for wet distiller's spent grain compacts with soluble content of 0, 10, 30, 50 and 70% (w/w), respectively.

Group Name	N	Missing	Mean	Std Dev	SEM
Col 1	3	0	12.030	1.055	0.609
Col 2	3	0	11.019	1.917	1.107
Col 3	3	0	7.038	1.109	0.640
Col 4	3	0	4.033	1.955	1.129
Col 5	3	0	1.917	0.929	0.537

All Pairwise Multiple Comparison Procedures (Holm-Sidak method):
Overall significance level = 0.05

Comparisons for factor:

Comparison	Diff of Means	t	Unadjusted P	Critical Level	Significant?
Col 1 vs. Col 5	10.113	8.466	0.00000714	0.005	Yes
Col 2 vs. Col 5	9.102	7.620	0.0000180	0.006	Yes
Col 1 vs. Col 4	7.997	6.695	0.0000540	0.006	Yes
Col 2 vs. Col 4	6.986	5.848	0.000162	0.007	Yes
Col 3 vs. Col 5	5.122	4.288	0.00159	0.009	Yes
Col 1 vs. Col 3	4.992	4.179	0.00189	0.010	Yes
Col 2 vs. Col 3	3.981	3.332	0.00759	0.013	Yes
Col 3 vs. Col 4	3.005	2.516	0.0306	0.017	No
Col 4 vs. Col 5	2.116	1.772	0.107	0.025	No
Col 1 vs. Col 2	1.011	0.846	0.417	0.050	No

A.8. Post-hoc analysis for percentage increase in diameter of distiller's spent grain compacts with different soluble levels during the initial condensation period (5s). Col 1, 2, 3, 4 and 5 represents percentage increase in diameter for wet distiller's spent grain compacts with soluble content of 0, 10, 30, 50 and 70% (w/w), respectively.

Group Name	N	Missing	Mean	Std Dev	SEM
Col 1	3	0	84.701	2.289	1.322
Col 2	3	0	75.976	7.681	4.435
Col 3	3	0	49.015	1.609	0.929
Col 4	3	0	29.753	2.775	1.602
Col 5	3	0	16.393	1.047	0.605

All Pairwise Multiple Comparison Procedures (Holm-Sidak method):
Overall significance level = 0.05

Comparisons for factor:

Comparison	Diff of Means	t	Unadjusted P	Critical Level	Significant?
Col 1 vs. Col 5	68.308	21.511	0.00000000105	0.005	Yes
Col 2 vs. Col 5	59.583	18.763	0.00000000400	0.006	Yes
Col 1 vs. Col 4	54.948	17.304	0.00000000880	0.006	Yes
Col 2 vs. Col 4	46.223	14.556	0.0000000467	0.007	Yes
Col 1 vs. Col 3	35.686	11.238	0.000000540	0.009	Yes
Col 3 vs. Col 5	32.622	10.273	0.00000124	0.010	Yes
Col 2 vs. Col 3	26.961	8.490	0.00000697	0.013	Yes
Col 3 vs. Col 4	19.263	6.066	0.000121	0.017	Yes
Col 4 vs. Col 5	13.360	4.207	0.00181	0.025	Yes
Col 1 vs. Col 2	8.725	2.748	0.0206	0.050	Yes

A.9. Post-hoc analysis for percentage increase in volume of distiller's spent grain compacts with different soluble levels during the initial condensation period (5s). Col 1, 2, 3, 4 and 5 represents percentage increase in volume for wet distiller's spent grain compacts with soluble content of 0, 10, 30, 50 and 70% (w/w), respectively.

Group Name	N	Missing	Mean	Std Dev	SEM
Col 1	3	0	5.689	1.748	1.009
Col 2	3	0	7.241	0.718	0.415
Col 3	3	0	17.842	1.158	0.669
Col 4	3	0	19.416	5.005	2.890
Col 5	3	0	27.928	8.162	4.712

All Pairwise Multiple Comparison Procedures (Holm-Sidak method):
Overall significance level = 0.05

Comparisons for factor:

Comparison	Diff of Means	t	Unadjusted P	Critical Level	Significant?
Col 5 vs. Col 1	22.239	6.197	0.000102	0.005	Yes
Col 5 vs. Col 2	20.688	5.765	0.000181	0.006	Yes
Col 4 vs. Col 1	13.726	3.825	0.00335	0.006	Yes
Col 4 vs. Col 2	12.175	3.393	0.00685	0.007	Yes
Col 3 vs. Col 1	12.153	3.386	0.00693	0.009	Yes
Col 3 vs. Col 2	10.601	2.954	0.0144	0.010	No
Col 5 vs. Col 3	10.087	2.811	0.0185	0.013	No
Col 5 vs. Col 4	8.513	2.372	0.0391	0.017	No
Col 4 vs. Col 3	1.574	0.439	0.670	0.025	No
Col 2 vs. Col 1	1.551	0.432	0.675	0.050	No

A.10. Post-hoc analysis for hardness of distiller's spent grain compacts with different soluble levels during the initial condensation period (5s). Col 1, 2, 3, 4 and 5 represents hardness for wet distiller's spent grain compacts with soluble content of 0, 10, 30, 50 and 70% (w/w), respectively.

Group	N	Missing	Median	25%	75%
Col 1	3	0	0.00870	0.00687	0.0103
Col 2	3	0	0.00829	0.00820	0.00953
Col 3	3	0	0.0214	0.0203	0.0215
Col 4	3	0	0.0249	0.0212	0.0288
Col 5	3	0	0.0224	0.0183	0.0390

All Pairwise Multiple Comparison Procedures (Tukey Test):

Comparison	Diff of Ranks	q	P<0.05
Col 4 vs Col 2	26.000	3.357	No
Col 4 vs Col 1	25.000	3.227	Do Not Test
Col 4 vs Col 3	7.000	0.904	Do Not Test
Col 4 vs Col 5	2.000	0.258	Do Not Test
Col 5 vs Col 2	24.000	3.098	Do Not Test
Col 5 vs Col 1	23.000	2.969	Do Not Test
Col 5 vs Col 3	5.000	0.645	Do Not Test
Col 3 vs Col 2	19.000	2.453	Do Not Test
Col 3 vs Col 1	18.000	2.324	Do Not Test
Col 1 vs Col 2	1.000	0.129	Do Not Test

Note: The multiple comparisons on ranks do not include an adjustment for ties.

A result of "Do Not Test" occurs for a comparison when no significant difference is found between the two rank sums that enclose that comparison. For example, if you had four rank sums sorted in order, and found no significant difference between rank sums 4 vs. 2, then you would not test 4 vs. 3 and 3 vs. 2, but still test 4 vs. 1 and 3 vs. 1 (4 vs. 3 and 3 vs. 2 are enclosed by 4 vs. 2: 4 3 2 1). Note that not testing the enclosed rank sums is a procedural rule, and a result of Do Not Test should be treated as if there is no significant difference between the rank sums, even though one may appear to exist.

A.11. Post-hoc analysis for asymptotic modulus of distiller's spent grain compacts with different soluble levels during the initial condensation period (5s). Col 1, 2, 3, 4 and 5 represents asymptotic modulus for wet distiller's spent grain compacts with soluble content of 0, 10, 30, 50 and 70% (w/w), respectively.

Group Name	N	Missing	Mean	Std Dev	SEM
Col 1	3	0	84.701	2.289	1.322
Col 2	3	0	47.268	3.722	2.149
Col 3	3	0	45.828	11.548	6.667

All Pairwise Multiple Comparison Procedures (Holm-Sidak method):
Overall significance level = 0.05

Comparisons for factor:

Comparison	Diff of Means	t	Unadjusted P	Critical Level	Significant?
Col 1 vs. Col 3	38.873	6.679	0.000546	0.017	Yes
Col 1 vs. Col 2	37.433	6.432	0.000668	0.025	Yes
Col 2 vs. Col 3	1.440	0.247	0.813	0.050	No

A.12. Post-hoc analysis for percentage increase in volume of wet distiller's spent grain compacts with different particle size distribution during the initial condensation period (5s). Col 1, 2 and 3 represents asymptotic modulus for wet distiller's spent grain compacts with particle size distribution of d(0.9)=1283.6 µm, d(0.9)= 1069.3 and d(0.9)= 812.8 µm, respectively.

Group Name	N	Missing	Mean	Std Dev	SEM
Col 1	3	0	5.689	1.748	1.009
Col 2	3	0	14.769	1.537	0.887
Col 3	3	0	18.762	3.346	1.932

All Pairwise Multiple Comparison Procedures (Holm-Sidak method):
Overall significance level = 0.05

Comparisons for factor:

Comparison	Diff of Means	t	Unadjusted P	Critical Level	Significant?
Col 3 vs. Col 1	13.073	6.804	0.000494	0.017	Yes
Col 2 vs. Col 1	9.080	4.726	0.00324	0.025	Yes
Col 3 vs. Col 2	3.993	2.078	0.0829	0.050	No

A.13. Post-hoc analysis for hardness of wet distiller's spent grain compacts with different particle size distribution during the initial condensation period (5s). Col 1, 2 and 3 represents hardness for wet distiller's spent grain compacts with particle size distribution of d(0.9)=1283.6 µm, d(0.9)= 1069.3 and d(0.9)= 812.8 µm, respectively.

Group Name	N	Missing	Mean	Std Dev	SEM
Col 1	3	0	0.00859	0.00228	0.00132
Col 2	3	0	0.0208	0.00218	0.00126
Col 3	3	0	0.0230	0.00143	0.000824

All Pairwise Multiple Comparison Procedures (Holm-Sidak method):
Overall significance level = 0.05

Comparisons for factor:

Comparison	Diff of Means	t	Unadjusted P	Critical Level	Significant?
Col 3 vs. Col 1	0.0144	8.837	0.000117	0.017	Yes
Col 2 vs. Col 1	0.0122	7.481	0.000295	0.025	Yes
Col 3 vs. Col 2	0.00221	1.356	0.224	0.050	No

A.14. Post-hoc analysis for asymptotic modulus of wet distiller's spent grain compacts with different particle size distribution during the initial condensation period (5s). Col 1, 2 and 3 represents asymptotic modulus for wet distiller's spent grain compacts with particle size distribution of d(0.9)=1283.6 µm, d(0.9)= 1069.3 and d(0.9)= 812.8 µm, respectively.

Appendix B

B.1. Particle size distribution analysis of grinded wet distiller's spent grain (WDG).

Parameters	Grinded WDG
d(0.9) (µm)	1053.0
d(0.5) (µm)	335.0
d(0.1) (µm)	27.2
D[4,3] (µm)	452.4

B.2. Compact density of wet distiller's spent grain samples as affected by compressive pressure, initial moisture content and soluble content. Table corresponding to Figures 5.1 and 5.2.

Compressive pressure (MPa)	Moisture content (%,wb)	Soluble content (%, w/w)	Pellet density (kg/m^3)	
			Average	Std. dev.
60.3	15	0	983.5	3.07
90.5	15	0	1054.1	13.42
120.6	15	0	1080.5	14.29
135.7	15	0	1099.8	7.58
60.3	20	0	975.5	1.69
90.5	20	0	1050.8	10.13
120.6	20	0	1074.8	17.24
135.7	20	0	1094.9	11.31
60.3	25	0	945.5	2.13
90.5	25	0	1052.9	8.11
120.6	25	0	1058.1	6.07
135.7	25	0	1078.9	9.52
60.3	25	15	985.1	2.05
90.5	25	15	1042.3	6.99
120.6	25	15	1064.9	15.85
135.7	25	15	1076	14.57
60.3	25	30	1012.8	14.48
90.5	25	30	1044.4	1.6
120.6	25	30	1056.3	8.96
135.7	25	30	1086.4	12.4

B.3. Moisture content of wet distiller's spent grain compacts with different levels of compaction, initial moisture content and soluble content. Table corresponding to Figures 5.3 and 5.4.

Compressive Pressure (MPa)	Moisture content (%,wb)	Soluble content (%, w/w)	Moisture content (%, wb)	
			Average	Std. dev.
60.3	15	0	14.2	0.28
90.5	15	0	13.9	1.4
120.6	15	0	13.5	1.35
135.7	15	0	11.9	1.16
60.3	20	0	18	0.32
90.5	20	0	16.9	2.49
120.6	20	0	16.3	0.41
135.7	20	0	16	1.85
60.3	25	0	23.4	0.25
90.5	25	0	22.3	2.49
120.6	25	0	21.8	1.95
135.7	25	0	21.3	0.94
60.3	25	15	23.9	0.1
90.5	25	15	23.7	0.47
120.6	25	15	21.3	2.08
135.7	25	15	21	2.2
60.3	25	30	24.2	0.22
90.5	25	30	23.8	0.38
120.6	25	30	21.3	0.8
135.7	25	30	20.7	1.18

B.4. The effect of compressive pressure on asymptotic modulus of wet distiller's spent grain samples for different levels of initial moisture content and soluble content. Table corresponding to Figures 5.8 and 5.9.

Compressive Pressure (MPa)	Moisture content (%,wb)	Soluble content (%, w/w)	Asymptotic modulus (MPa)	
			Average	Std. dev.
60.3	15	0	24.1	2.8
90.5	15	0	46.2	3.82
120.6	15	0	67.7	6.85
135.7	15	0	133.2	3.21
60.3	20	0	33.3	1.71
90.5	20	0	68.4	10.47
120.6	20	0	81.6	13.2
135.7	20	0	150.8	13.1
60.3	25	0	50	6.41
90.5	25	0	95.1	8.29
120.6	25	0	152.6	8.3
135.7	25	0	174	3.14
60.3	25	15	41.1	3.01
90.5	25	15	111.3	3.42
120.6	25	15	141.7	5.12
135.7	25	15	131	8.96
60.3	25	30	29.8	3.52
90.5	25	30	69.7	4.6
120.6	25	30	134.8	8.73
135.7	25	30	156.3	10.52

B.5. Percentage increase in volume as affected by drying time in superheated steam at 3 different superheated steam temperatures and velocities. Table corresponding to Figures 5.14 to 5.16.

Temperature (°C)	Velocity (m/s)	Drying time (s)	Percentage increase in volume	
			Average	Std. dev.
110	0.9	5	120.2	5.17
110	0.9	120	117.9	1.68
110	0.9	300	116.4	1.81
110	0.9	600	114.9	3.48
110	1.1	5	126	3.41
110	1.1	120	130.8	7.71
110	1.1	300	123.9	3.77
110	1.1	600	120.8	3.78
110	1.4	5	128.6	2.54
110	1.4	120	113	2.7
110	1.4	300	103.3	5.94
110	1.4	600	101.7	6.04
130	0.9	5	123.4	5.69
130	0.9	120	105.5	5.07
130	0.9	300	106.1	7.99
130	0.9	600	86	8.26
130	1.1	5	128.3	1.88
130	1.1	120	106.7	7.07
130	1.1	300	98.5	9.12
130	1.1	600	96.7	9.41
130	1.4	5	126.3	5.78
130	1.4	120	96.5	3.95
130	1.4	300	97.6	4.39
130	1.4	600	79.9	5.6
150	0.9	5	105.8	3.83
150	0.9	120	107.9	7.91
150	0.9	300	94.1	5.53
150	0.9	600	83.7	11.63
150	1.1	5	108.8	8.75
150	1.1	120	107.7	2.31
150	1.1	300	87.4	13.4
150	1.1	600	81.2	14.72
150	1.4	5	113.9	1.78
150	1.4	120	103.6	9.46
150	1.4	300	89.8	9.43
150	1.4	600	78.7	8.08

B.6. Percentage decrease in density as affected by drying time in superheated steam at 3 different superheated steam temperatures and velocities. Table corresponding to Figures 5.17 to 5.19.

Temperature (°C)	Velocity (m/s)	Drying time (s)	Percentage decrease in density	
			Average	Std. dev.
110	0.9	5	53.8	1.14
110	0.9	120	54.9	0.59
110	0.9	300	57.1	0.37
110	0.9	600	58.3	0.63
110	1.1	5	55.4	0.61
110	1.1	120	57.9	1.6
110	1.1	300	58.7	0.79
110	1.1	600	60	0.79
110	1.4	5	55.9	0.49
110	1.4	120	54.9	0.77
110	1.4	300	54.9	1.41
110	1.4	600	56.9	1.2
130	0.9	5	54.8	1.22
130	0.9	120	54.6	1.08
130	0.9	300	58.2	1.68
130	0.9	600	56.6	2.06
130	1.1	5	55.9	0.4
130	1.1	120	55.5	1.65
130	1.1	300	56.4	1.89
130	1.1	600	59.5	2.09
130	1.4	5	55.6	1.13
130	1.4	120	53.7	0.87
130	1.4	300	57.3	0.95
130	1.4	600	56.1	1.41
150	0.9	5	52.1	0.84
150	0.9	120	57.5	1.61
150	0.9	300	57.7	1.09
150	0.9	600	57.4	2.56
150	1.1	5	53.3	2.13
150	1.1	120	57.7	0.62
150	1.1	300	56.3	3.29
150	1.1	600	57	3.34
150	1.4	5	55.3	0.32
150	1.4	120	57.4	2.32
150	1.4	300	57.5	2.05
150	1.4	600	56.7	1.95

B.7. Percentage decrease in density and percentage increase in volume of wet distiller's spent grain compacts dried in convection hot-air oven at 110, 130 and 150°C. Table corresponding to Figure 5.20.

Oven-dried					
Temperature (°C)	Time (s)	Percentage increase in volume		Percentage decrease in density	
		Average	Std. Dev	Average	Std. dev.
110	600	45.1	4	42.9	1.66
130	600	45.6	4.05	45.9	1.14
150	600	42.5	3.53	43.4	0.82

B.8. Percentage increase in the length of the compact as affected by the addition of solubles during the condensation period and during drying from the condensation period to the final moisture content of 40, 30 and 20% wb. Table corresponding to Figure 5.23.

Soluble (%, w/w)	Moisture content (%, wb)	Percentage increase in length	
		Average	Std. dev.
0	Initial condensation	47.2	1.33
0	40	43.5	1.62
0	30	38.3	1.13
0	20	34.4	1.7
10	Initial condensation	42.7	2.69
10	40	39.1	2.16
10	30	35.9	1.81
10	20	30.9	2.99
30	Initial condensation	30.1	1.29
30	40	26.8	1.68
30	30	22	3
30	20	19	2.7
50	Initial condensation	19.9	1.94
50	40	16.7	2.04
50	30	12	1.05
50	20	7	1.94
70	Initial condensation	12.1	1.07
70	40	10	1.99
70	30	7	1.02
70	20	5	1.1

B.9. Percentage increase in the diameter of the compact as affected by the addition of solubles during the condensation period and during drying from the condensation period to the final moisture content of 40, 30 and 20% wb. Table corresponding to Figure 5.24.

Soluble (%, w/w)	Moisture content (%, wb)	Percentage increase in diameter	
		Average	Std. dev.
0	Initial condensation	12	1.05
0	40	8.5	2.26
0	30	6	2.72
0	20	5.2	1.35
10	Initial condensation	11	1.92
10	40	8	0.98
10	30	5	1.01
10	20	4	1.02
30	Initial condensation	7	1.11
30	40	5.5	1.4
30	30	2	2.63
30	20	-2	2.64
50	Initial condensation	4	1.96
50	40	1	1.98
50	30	-2	1.03
50	20	-5	1.74
70	Initial condensation	1.9	0.93
70	40	-1	1.73
70	30	-4	0.99
70	20	-8	1.73

B.10. Percentage increase in the volume of the compact as affected by the addition of solubles during the condensation period and during drying from the condensation period to the final moisture content of 40, 30 and 20% wb. Table corresponding to Figure 5.25.

Soluble (%, w/w)	Moisture content (%, wb)	Percentage increase in volume	
		Average	Std. dev.
0	Initial condensation	84.7	2.29
0	40	69	9.01
0	30	55.6	9.16
0	20	48.8	5.45
10	Initial condensation	76	7.68
10	40	62.2	5.47
10	30	49.8	2.65
10	20	41.6	0.47
30	Initial condensation	49	1.61
30	40	41.2	3.56
30	30	27.1	9.45
30	20	14.3	5.38
50	Initial condensation	29.8	2.78
50	40	19.2	6.75
50	30	7.5	1.92
50	20	-3.5	3.96
70	Initial condensation	16.4	1.05
70	40	7.8	2.37
70	30	-1.4	2.98
70	20	-11.1	3.49

B.11. Variation in the hardness of the compact as affected by the addition of solubles for unprocessed compacts and for compacts exposed to condensation in the first 5 s of superheated steam drying and during superheated steam drying from the condensation period to the final moisture content of 40, 30 and 20% wb. Table corresponding to Figure 5.26.

Soluble (%, w/w)	Moisture content (%, wb)	Hardness (N)	
		Average	Std. dev.
0	50 (Raw)	34	3.33
0	Initial condensation	5.7	1.75
0	40	10.1	3.73
0	30	13.8	1.96
0	20	27.9	3.79
10	50 (Raw)	29.5	0.51
10	Initial condensation	7.2	0.72
10	40	12.9	0.96
10	30	24	4.51
10	20	35.3	2.08
30	50 (Raw)	36.6	1.63
30	Initial condensation	17.8	1.16
30	40	32.4	9.27
30	30	34.3	2.33
30	20	50.5	9.19
50	50 (Raw)	35.2	4.29
50	Initial condensation	19.4	5.01
50	40	35.4	3.88
50	30	86.8	18.8
50	20	130.4	14.56
70	50 (Raw)	36.6	1.64
70	Initial condensation	27.9	8.16
70	40	40.4	6.71
70	30	99.3	7.53
70	20	229.5	25.74

B.12. Asymptotic modulus of the compact as affected by the addition of solubles for unprocessed compacts and for compacts exposed to condensation in the first 5 s of superheated steam drying and during superheated steam drying from the condensation period to the final moisture content of 40, 30 and 20% wb. Table corresponding to Figure 5.27.

Soluble (%, w/w)	Moisture content (%, wb)	Asymptotic modulus (MPa)	
		Average	Std. dev.
0	50 (Raw)	0.053	0.012
0	Initial condensation	0.009	0.002
0	40	0.007	0.003
0	30	0.012	0.004
0	20	0.04	0.002
10	50 (Raw)	0.041	0.003
10	Initial condensation	0.009	0.001
10	40	0.008	0.003
10	30	0.023	0.005
10	20	0.089	0.011
30	50 (Raw)	0.047	0.006
30	Initial condensation	0.021	0.001
30	40	0.021	0.005
30	30	0.054	0.012
30	20	0.296	0.046
50	50 (Raw)	0.045	0.009
50	Initial condensation	0.025	0.005
50	40	0.033	0.022
50	30	0.157	0.14
50	20	0.328	0.057
70	50 (Raw)	0.04	0.011
70	Initial condensation	0.028	0.015
70	40	0.023	0.016
70	30	0.309	0.013
70	20	0.422	0.039

B.13. Percentage increase in volume of the compact as affected by the variation of particle size distribution during the warm-up period of the first 5 s of superheated steam drying and at different moisture levels of 40, 30 and 20% wb. Table corresponding to Figure 5.34.

Particle size distribution (μm)	Moisture content (%, wb)	Percentage increase in volume	
		Average	Std. dev.
d(0.9)=1283.6	Initial condensation	84.7	2.29
d(0.9)=1283.6	40	69	9.01
d(0.9)=1283.6	30	55.6	9.16
d(0.9)=1283.6	20	48.8	5.45
d(0.9)= 1069.3	Initial condensation	47.3	3.72
d(0.9)= 1069.3	40	39.2	1.86
d(0.9)= 1069.3	30	34.3	0.38
d(0.9)= 1069.3	20	21.8	2.88
d(0.9)= 812.8	Initial condensation	45.8	11.55
d(0.9)= 812.8	40	36.7	4.72
d(0.9)= 812.8	30	28.5	7.36
d(0.9)= 812.8	20	23.4	6.56

B.14. Variation in the hardness of the compact as affected by different particle size distribution for raw compacts and for compacts exposed to superheated steam during the 5s warm-up period and after reaching moisture levels of 40, 30 and 20% wb in superheated steam. Table corresponding to Figure 5.35.

Particle size distribution (μm)	Moisture content (%, wb)	Hardness (N)	
		Average	Std. dev.
d(0.9)=1283.6	50 (Raw)	34	3.33
d(0.9)=1283.6	Initial condensation	5.7	1.75
d(0.9)=1283.6	40	10.1	3.73
d(0.9)=1283.6	30	13.8	1.96
d(0.9)=1283.6	20	27.9	3.79
d(0.9)= 1069.3	50 (Raw)	33.6	4.66
d(0.9)= 1069.3	Initial condensation	14.8	1.54
d(0.9)= 1069.3	40	23.4	4.13
d(0.9)= 1069.3	30	32.8	2.47
d(0.9)= 1069.3	20	41.2	7.33
d(0.9)= 812.8	50 (Raw)	41.3	6.04
d(0.9)= 812.8	Initial condensation	18.8	3.35
d(0.9)= 812.8	40	33.6	4.06
d(0.9)= 812.8	30	48.9	12.48
d(0.9)= 812.8	20	81.6	10.55

B.15. Asymptotic modulus of the compact as affected by particle size distribution for raw compacts and for compacts exposed to superheated steam during the 5 s of the warm-up period and after reaching moisture levels of 40, 30 and 20% wb in superheated steam. Table corresponding to Figure 5.36.

Particle size distribution (μm)	Moisture content (%, wb)	Asymptotic modulus (MPa)	
		Average	Std. dev.
d(0.9)=1283.6	50 (Raw)	0.053	0.012
d(0.9)=1283.6	Initial condensation	0.009	0.002
d(0.9)=1283.6	40	0.007	0.003
d(0.9)=1283.6	30	0.012	0.004
d(0.9)=1283.6	20	0.04	0.002
d(0.9)= 1069.3	50 (Raw)	0.05	0.009
d(0.9)= 1069.3	Initial condensation	0.021	0.002
d(0.9)= 1069.3	40	0.024	0.005
d(0.9)= 1069.3	30	0.034	0.008
d(0.9)= 1069.3	20	0.123	0.058
d(0.9)= 812.8	50 (Raw)	0.064	0.012
d(0.9)= 812.8	Initial condensation	0.023	0.001
d(0.9)= 812.8	40	0.034	0.005
d(0.9)= 812.8	30	0.098	0.026
d(0.9)= 812.8	20	0.308	0.007

B.16. Variation of bulk density with particle size for thin-layer drying at low-air temperature of 45°C, high-air temperature at 150°C and superheated steam drying at150°C. The statistical analysis was performed in SAS using the Bartlett's Test.

Particle size (μm)	Bulk Density (g/cm^3)		
	Thin-layer low-temperature drying at 45°C	Thin-layer high-temperature drying at 150°C	Superheated steam drying
300	0.379 (0.003)^{F}	0.392 (0.003)^{D}	0.379 (0.007)^{F}
425	0.386 (0.004)^{E}	0.417 (0.004)^{B}	0.397 (0.002)^{C}
600	0.387 (0.004)^{E}	0.433 (0.002)^{A}	0.384 (0.004)^{E}
850	0.397 (0.002)^{C}	0.435 (0.003)^{A}	0.384 (0.004)^{E}

Values in parenthesis indicate standard deviations (n= 10). Means with the same letter are not significantly different.

B.17. Variation of bulk density as affected by the addition of the condensed distiller's solubles (CDS). The statistical analysis was performed in SAS using the Bartlett's Test.

Particle Size (μm)	Bulk Density (g/cm^3)		
	10% CDS	20%CDS	30%CDS
300	0.391 (0.004)^{G}	0.393 (0.004)^{GF}	0.425 (0.002)^{C}
425	0.395 (0.003)^{F}	0.403 (0.004)^{E}	0.437 (0.005)^{B}
600	0.410 (0.005)^{D}	0.412 (0.006)^{D}	0.444 (0.007)^{A}
850	0.413 (0.006)^{D}	0.423 (0.005)^{C}	0.421 (0.004)^{C}

Values in parenthesis indicate standard deviations (n= 10).
Means with the same letter are not significantly different.

B.18. Variation of angle of repose with particle size for thin-layer drying at low-air temperature of 45°C, high-air temperature at 150°C and superheated steam drying at150°C. The statistical analysis was performed in SAS using the Bartlett's Test.

Particle Size (µm)	Angle of Repose (°)		
	Thin-layer low-temperature drying at 45°C	Thin-layer high-temperature drying at 150°C	Superheated steam drying
300	50.4 (1.7)^{A}	49.4 (2.0)^{B}	50.0 (2.3)^{BA}
425	47.1 (1.8)^{C}	46.9 (1.9)^{DC}	47.2 (2.5)^{C}
850	46.7 (1.8)^{DC}	46.0 (2.3)^{D}	47.2 (2.1)^{C}

Values in parenthesis indicate standard deviations (n= 10).
Means with the same letter are not significantly different.

B.19. Variation of angle of repose as affected by different concentrations of condensed distiller's solubles (CDS). The statistical analysis was performed in SAS using the Bartlett's Test.

Particle Size (µm)	Angle of Repose (°)		
	10% CDS	20% CDS	30% CDS
300	49.5 (2.0)^{A}	49.8 (1.6)^{A}	48.9 (2.4)^{A}
425	47.9 (1.7)^{B}	47.2 (2.4)^{CB}	48.0 (2.4)^{B}
850	46.5 (2.0)^{C}	47.7 (1.8)^{B}	46.7 (2.2)^{C}

Values in parenthesis indicate standard deviations (n= 10).
Means with the same letter are not significantly different.

B.20. Compression characteristics of distiller's spent grain samples using Jones Model. The statistical analysis was performed in SAS using the Bartlett's Test. m, b are model constants.

Moisture content (%, wb)	Soluble content (%)	m (kg/N-m)	b (kg/m^3)
15	0	0.135^{AB}	6.345^{BC}
20	0	0.138^{A}	6.321^{C}
25	0	0.155^{A}	6.231^{C}
25	15	0.108^{B}	6.455^{B}
25	30	0.078^{C}	6.602^{A}

Means with the same letter are not significantly different.